ISSN 1881-7831 Online ISSN 1881-784X

DD&T

Drug Discoveries & Therapeutics

Volume 12, Number 6
December 2018

IRCA BSSA

IACMHR

www.ddtjournal.com

DD&T
Drug Discoveries & Therapeutics

ISSN: 1881-7831
Online ISSN: 1881-784X
CODEN: DDTRBX
Issues/Year: 6
Language: English
Publisher: IACMHR Co., Ltd.

Drug Discoveries & Therapeutics is one of a series of peer-reviewed journals of the International Research and Cooperation Association for Bio & Socio-Sciences Advancement (IRCA-BSSA) Group and is published bimonthly by the International Advancement Center for Medicine & Health Research Co., Ltd. (IACMHR Co., Ltd.) and supported by the IRCA-BSSA and Shandong University China-Japan Cooperation Center for Drug Discovery & Screening (SDU-DDSC).

Drug Discoveries & Therapeutics publishes contributions in all fields of pharmaceutical and therapeutic research such as medicinal chemistry, pharmacology, pharmaceutical analysis, pharmaceutics, pharmaceutical administration, and experimental and clinical studies of effects, mechanisms, or uses of various treatments. Studies in drug-related fields such as biology, biochemistry, physiology, microbiology, and immunology are also within the scope of this journal.

Drug Discoveries & Therapeutics publishes Original Articles, Brief Reports, Reviews, Policy Forum articles, Case Reports, News, and Letters on all aspects of the field of pharmaceutical research. All contributions should seek to promote international collaboration in pharmaceutical science.

Editorial Board

Editorial and Head Office:

Pearl City Koishikawa 603,
2-4-5 Kasuga, Bunkyo-ku,
Tokyo 112-0003, Japan
Tel.: +81-3-5840-9697
Fax: +81-3-5840-9698
E-mail: office@ddtjournal.com

Drug Discoveries & Therapeutics

Editorial and Head Office

Pearl City Koishikawa 603, 2-4-5 Kasuga, Bunkyo-ku,
Tokyo 112-0003, Japan

Tel: +81-3-5840-9697, Fax: +81-3-5840-9698
E-mail: office@ddtjournal.com
URL: www.ddtjournal.com

Editorial Board Members

CONTENTS

Volume 12, Number 6, 2018

Review

Original Article

Case Report

CONTENTS (*Continued*)

Review

DOI: 10.5582/ddt.2018.01066

Discovery of novel bioactive natural products driven by genome mining

Zhongyue Li[1], Deyu Zhu[2], Yuemao Shen[1,*]

[1] *Key Laboratory of Chemical Biology, School of Pharmaceutical Sciences, Shandong University, Ji'nan, Shandong, China;*
[2] *School of Basic Medical Sciences, Shandong University, Ji'nan, Shandong, China.*

Summary **Microbial natural product is an important source for drug discovery. As more and more microbial genomes are sequenced, bioinformatics analysis shows that there are huge resources of novel natural products. Genome mining is a new strategy of natural product discovery based on gene cluster sequences and biosynthetic pathways. At the same time, it can directly associate the structures of natural products with synthetic pathways, and facilitate the study of biosynthesis and combinatorial biosynthesis. In this paper, the strategies of genome mining, including bioinformatics predictions, metabolomic comparisons and genetic manipulations, are reviewed, which shows a great advantage of this strategy in exploiting the potential of microbial natural products. With the development of genome mining methodology and techniques, it will be possible to realize rational exploitation of microbial natural product resources.**

Keywords: Genome mining, natural products, gene cluster, biosynthesis; microorganisms

1. Introduction

The discovery of streptomycin from *Streptomyces* has inspired the research of antibiotics from microorganisms. The discovery rate of new antibiotics has been increasing year by year, reaching its peak in the 1970s, and experienced a golden period of nearly 30 years. However, in the 1980s, due to the repeated isolation and screening of most actinomycetes, and the repeated isolation of bioactive natural products, the probability of finding new active compounds decreased rapidly and became more and more difficult. However, according to the most conservative estimates, the number of natural products found so far from any microbial strain is only 20% of the total encoded by its genome. Therefore, the decline in the rate of discovery of new active natural products is not due to the exhaustion of the biosynthetic gene resources of microbial natural products, but is limited by the methods of microbial isolation, cultivation and bioactivity screening (*1*). More importantly, since the birth of microbial natural product chemistry, the research methodology adapted has striking randomness, blindness and contingency, is insufficient in rationality. There is a lack of rational experimental design and theoretical guidance from isolation and culture of strains to extraction and separation of active components in addition to activity screening, so we can only expect to obtain the activity specified in the screening model but can't predict the structures of bioactive components.

In recent years, with decreasing sequencing costs and continuous improvements in sequencing and longer read technologies, more and more microorganism genomes have been sequenced. The emergence of these genomic information is gradually changing the research model of the whole life sciences and related disciplines. It is found that the natural product resources of conventional microorganisms are greatly underestimated (*2*). Taking bacterial genomes as an example, bioinformatics analysis shows that each strain of bacteria has the ability to synthesize 25-30 types of natural products, of which ca. 90% is still unknown. Even if only 20% of the 25-30 types of natural products produced by each strain are new structures, the number of new natural products we obtain will increase exponentially (*3*).

**Address correspondence to:*
Dr. Yuemao Shen, Key Laboratory of Chemical Biology, School of Pharmaceutical Sciences, Shandong University, No. 44 West Wenhua Road, Ji'nan, Shandong 250012, China.
E-mail: yshen@sdu.edu.cn

The Genomes Online Database (GOLD v.6) (*https://gold.jgi.doe.gov*) shows huge genomic data (*4*), which imposes a challenging and exciting research topic how to obtain novel natural products quickly and effectively by the method of genome mining. Compared with traditional methods, novel natural product discovery strategies based on gene cluster sequences and biosynthesis pathways have the following advantages: 1. Through gene "prediction" of natural product structure, "de-duplication" can be achieved. The possibility of finding new structures would be greatly increased by excluding known compounds. 2. Combined with transcriptional analysis and genetic manipulation of regulatory genes, the secondary metabolic potential of the strain could be released to the maximal extent. 3. The structures of natural products can be directly linked with the synthetic pathways, which can facilitate the study of biosynthesis and combinatorial biosynthesis, and further expand the structural diversity of natural products. Thus far, natural product discovery has been transformed to heavily rely on bioinformatics-based structure prediction, activation of cryptic gene clusters by genetic manipulation and heterologous expression, and potential engineering of natural product analogs (*5*).

2. Discovery of novel natural products with the aid of bioinformatics prediction and comparative metabolomic analysis

Until the late 1980s, biosynthetic pathways of microbial natural products could only be inferred by feeding selectively labelled precursors, and by analyzing the MS and NMR data of the products to obtain the labelling patterns of the products. In 1984, Malpartida and Hopwood reported the cloning and heterologous expression of the biosynthetic gene cluster of actinorhodin (*6*). Katz and his colleagues from Abbott and Leadlay from Cambridge University reported independently the cloning of polyketide synthase (PKS) gene of 6-deoxyerythronolide B (6-DEB) in 1990 and 1991, respectively, which greatly changed the research mode of biosynthetic pathway of natural products. Subsequently, it was found that the nonribosomal peptides such as penicillin/cephalosporin, vancomycin, cyclosporin and daptomycin were also synthesized by the assembly lines, nonribosomal peptide synthetases (NRPSs), similar to that of 6-DEB PKS. These studies have changed our understanding of biosynthetic mechanisms of peptide natural products. With the further study of biosynthetic genes of rapamycin and FK506, it has been found that their syntheses have the compatibility of biosynthetic system with assembly line characteristic by hybrid of PKS and NRPS. This seemingly simple "assembly line enzymology" can explain the syntheses of thousands of complex and diverse natural products.

It is precisely because of the discovery of those biosynthetic pathways, the number of modules contained and the composition of the domain of each module can be determined by analyzing the sequences of PKS and NRPS genes of multiple modules, and the compound structures encoded by them can be predicted. By analyzing the predicted structures of the compounds, we can identify the assembly modules and the related physicochemical properties needed for the synthesis, so as to direct the isolation procedure and finally obtain the natural products encoded by the corresponding biosynthetic gene clusters (*7*). Specifically, the genomisotopic strategy includes discovering novel natural products on the basis of predicting structural moieties and biosynthetic precursors (*8*), which is carried out by bioinformatics analysis, subsequently, feeding isotope labelled precursors and isotope-guided isolation of the targeted natural products. E.g., orfamides A-C were isolated from *Pseudomonas fluorescens* Pf-5 by this genomisotopic approach as bioinformatics analysis indicated that these cyclopeptides contain four L-leucine residues (Figure 1) (*8*). Erythrochelin was obtained from *Saccharopolyspora erythraea* by feeding ^{14}C-L-ornithine followed by radio-LC-MS-guided isolation (Figure 1) (*9,10*). Additionally, bioinformatics analysis revealed that the *cch* gene cluster could be responsible

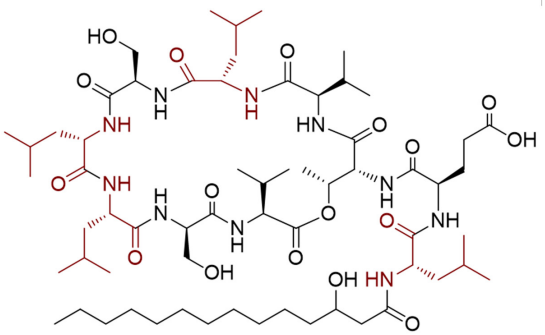

The isolation of orfamide A from *Pseudomonas fluorescens* Pf-5 represents a proof of concept example of genomisotopic approach of genome mining to obtain the natural products encoded by cryptic gene clusters through isotope-guided fractionation by NMR after the feeding of ^{13}C-L-leucine (red) (ref. 8).

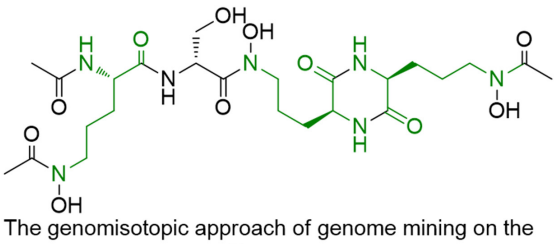

The genomisotopic approach of genome mining on the basis of the feeding of ^{14}C-L-ornithine (green) and radio-LC-MS-guided fractionation resulted in the isolation of erythrochelin (ref. 9).

Figure 1. Two example compounds, orfamides A and erythrochelin, isolated through the genomisotopic approach.

for the biosynthesis of the tetrapeptides with the presence of a hydroxamate moiety. Hydroxamate readily conjugates with ferric ion, which produces characteristic UV absorbance. Through UV comparison of the products of *Streptomyces coelicolor* M145 mutant and wild type strains, coelichelin was obtained (*11*). UV spectra-guided isolations were also successful in the discovery of many chromophore-containing natural products, *e.g*., aspoquinolones A-D from *Aspergillus nidulans* (*12*), salinilactam A from *Salinispora tropica* (*13*), thailandamide A from *Burkholderia thailandensis* (*14*). The feasibility of structural moiety-based genome mining was demonstrated in screening a collection of over 10,000 actinomycetes for the genetic potential of producing phosphonic acids. Before this study no genome mining experiments were performed on a large number of bacterial strains (*15*).

For the natural products encoded by unknown gene clusters in genomes, it is difficult to predict their structures or physiochemical properties (*16*). Usually, it is useful to obtain these natural products through the approach of gene inactivation and metabolomic comparison of the mutant and the wild type strains by HPLC or LC-MS analysis (*17-20*). HPLC profile comparison is the most straightforward method used in genome mining. However, its limitation is obvious in that low resolution and rough identities of products. Once coupled with bioassays, this method could be feasible. WAP-8294As are cyclic depsipeptides and potent anti-MRSA agents. Their biosynthetic genes were not reported before Zhang *et al*.'s study (*21*). The genome of *Lysobacter enzymogenes* OH11 contains a large number of biosynthetic gene clusters including several hybrid PKS-NRPS ones. Disrupting one of the gene clusters containing two huge open reading frames, together encoding 12 modules of NRPS, resulted in the HPLC profile change and disappearance of the antibacterial activity of the mutant. Finally, Zhang *et al*. obtained WAP-8294A2 through HPLC- and bioassay-guided fractionation, so to characterize the biosynthetic gene cluster for this type of depsipeptides (*21*).

For the discovery of peptide natural products, an improved MS-guided genome mining method called NPP (natural product peptidogenomics) was invented by iteratively matching de novo tandem MS structures to genomics-based structures. Indeed, NPP enabled the rapid characterization of diverse ribosomal and nonribosomal peptide natural products (*22*). Recently, the MS-guided genome mining method has been evolved to molecular networking, a MS/MS data organizational approach (*23*), which can be integrated with many other methods, *e.g*., bioassays (*24*) and chemical synthesis (*25*). To simultaneously assess large numbers of closely related bacterial strains and their pan-metabolomes, molecular networking should be improved to recognize the MS/MS fragmentation patterns with the availability of biosynthetic gene clusters. This newly invented method identifies molecular families rather than individual molecules thus that enables the discovery of related molecules. Duncan *et al*. invented and applied this method to thirty five *Salinispora* strains, including 30 with draft genome sequences, which successfully resulted in the isolation and characterization of a quinomycin-type depsipeptide, namely retimycin A (*26*).

3. Activating cryptic gene clusters through genetic manipulations

In the genome of actinomycetes, many secondary metabolic gene clusters are silent. If we know how to activate these clusters, we will discover huge number of new enzymes, biological pathways and natural product resources (*27,28*). Microbial secondary metabolism has a very complex transcriptional regulatory system (*29*), probably because: 1. The biosynthetic gene cluster is composed of multiple genes of different origins containing independent regulatory elements. 2. The combined biosynthetic pathway can use different primary metabolites as the starting substances for synthesis, which requires a complex regulatory system. 3. Having more than one metabolic regulation system can help the secondary metabolism process to be sensitive to the external environment changes. In particular, the responses of actinomycetes to environmental factors are more complex than other bacteria. Many regulatory factors are involved in the secondary metabolism regulation of actinomycetes and form a complex multi-level network system. These include high-level multifunctional genes and low-level pathway-specific genes.

Activating cryptic gene clusters can be carried out through manipulating global regulations including: 1. Optimization of culture conditions including the composition of culture media, aeration volume, shape of fermenter, light condition, culture temperature, adding enzyme inhibitors (*30*), elicitors (*31*), rare earth elements (*32*), and co-culture (*33*). 2. Ribosomal engineering, a breeding method of ribosomal mutant, which uses various resistant mutants of microorganisms as screening markers to obtain highly efficient ribosomal mutants with improved secondary metabolite biosynthesis (*34,35*). The methods of activating cryptic gene clusters through manipulating pathway specific regulations include: 1. Overexpression of pathway specific transcriptional factors. Structural genes such as PKS genes and NRPS genes in the secondary metabolic gene cluster of actinomycetes are usually concentrated on 1-2 operons. The wild type promoters can be replaced by gene recombination with constitutive strong promoters such as *PermE*, which bypasses the transcriptional regulations in wild-type strains and activate or partially activate the corresponding gene clusters. 2. Heterologous expression of putative cryptic

gene clusters (*14,36*). The exploitation of secondary metabolic gene clusters requires the continuous development of transgenic cluster techniques among different organisms, including the optimization of super-hosts and the improvement of the methods for constructing/expressing multiple genes in heterologous systems (*37,38*).

4. Transcriptional regulations of secondary metabolisms in actinomycetes

The transcriptional regulations are particularly complex in actinomycetes. Multifunctional global regulators not only regulate the production of multiple secondary metabolites, but also participate in the morphological differentiation of actinomycetes, such as BldA, A-factors, Sigma factor and two-component regulatory systems often cascade into complex regulatory networks. Path-specific regulatory factors are mainly involved in the biosynthesis of specific metabolites, such as members of transcription factor families such as SARP (*Streptomyces* antibiotic regulatory protein) and LuxR. These specific regulatorys are often the only way for various global regulators to regulate specific biosynthetic pathways.

Among the numerous families of transcriptional regulatory proteins of actinomycetes (*39*), TetR (Tetracycline Repressor protein) family plays an important role in coordinating the growth and development of actinomycetes and responses to environmental factors. TetR family members are mainly involved in the regulation of antibiotic biosynthesis, efflux pumps and osmotic stress, and particularly abundant in environmentally vulnerable microorganisms, *e.g*. *Streptomyces coelicolor* A3(2) and *S. avermitilis* MA-4680 have 150 and 116 TetR members, respectively (*40*). TetRs are double domain proteins, one domain binds inducer and receives signals, another domain binds promoter DNA and transduces signals. Only the DNA binding domains are conserved among the TetRs, the elicitor binding domains are not significantly conserved, indicating the fine-tuned responses of actinomycetes to the high diversity of the inducers in the environments. After the unconserved domains binding inducers, the DNA binding domains may be altered allosterically and the ability of binding to DNA be lost, thus releasing the transcriptional repressing effects of TetRs. The TetR-binding inducers, also known as self-regulatory factors, usually are small molecular compounds that initiate secondary metabolism and morphological differentiation at the concentrations of nanomolor, and act as the hormones in eukaryotes.

Presently known self-regulatory factors of actinomycetes include 2,3-disubstituted γ-butyrolactone and its analogues including A-factor, SCB1, 2 and 3, VB-A, B, C, D and E, IM-2 and Factor I, methylenomycin furans (*41*), P1 factor (*42*), peptides including SapB, goadsporin and Factor C, siderophores and certain antibiotics (*43,44*). A-factor was originally found in *S. griseus* (*45,46*). The receptor protein of A-factor is ArpA. When A-factor binds to ArpA, the transcriptional repression of ArpA is removed (*47*). The heterologous expression of *ArpA* always produces inclusion bodies. The CprB in *S. coelicolor* A3(2) is the homologous protein of ArpA, and the crystal structure is obtained. However, the small molecular ligands of CprB have not been found (*48*).

Because self-regulatory factors are similar to the "second messengers" of environmental signals (stimuli), it may be possible to integrate the regulation of secondary metabolisms and morphological differentiations of actinomycetes (integrative regulations). This mechanism is widely used in the regulation of secondary metabolism by actinomycetes, which is consistent with that secondary metabolisms are environment sensitive. Therefore, identification of elicitors and related regulatory mechanisms is another way to activate cryptic gene clusters in actinomycetes (*49*).

5. Transcriptional regulations of ansamycin biosynthesis

The ansamycin class of natural products includes the important anti-tuberculosis drug rifamycin (*50*), and the antitumor drug leads geldanamycins (*51*) and maytansinoids (*52*). These macrolactams arise from the polyketide pathway *via* multidomain modular type I PKSs using 3-amino-5-hydroxybenzoic acid (AHBA) as the starter unit. Based on the structures of AHBA-derived aromatic moieties, ansamycins are divided into benzenic and naphthalenic groups. Each group can be further classified according to the numbers and types of extender units recruited. So far, only about 200 ansamycins have been reported. By analogy to the biosynthesis of other types of type I polyketides such as macrolactones, we speculate that more ansamycin scaffolds, *e.g*. hexaketide, dodecaketide and tridecaketide backbones, are waiting for exploitation. In the existing categories, both of benzenic and naphthalenic types have been identified only in the novel ansamycins divergolides (*53,54*). Moreover, novel ansamycins with unusual extender units have been identified recently (*55*).

Although ansamycin antibiotics are important secondary metabolites of microorganisms, and rifampicin, the derivative of rifamycin, has been used for more than 50 years in clinic, we don't know much about the molecular mechanisms that regulate their biosynthesis. The current literature reports are limited to the regulation mechanism of the biosynthesis of rifamycin, ansamitocin and geldenamycin. *RifO*, *P*, *Q* in rifamycin biosynthetic gene cluster (*rif*) may be involved in the regulation of rifamycin biosynthesis,

and *rifO* may be involved in the regulation of B-factor (*56*). *RifP* encodes a transmembrane protein, a member of the DHA14 Drug:H^+ antiporter family, that pumps antibiotics out of cells using the H^+ gradient produced by respiration. The antisense gene strategy partially silenced the expression of *rifP*, which resulted in the reduction of the production of rifamycin B by 70%, confirming the proton pump function of RifP (*57*). The *rifQ* gene is highly homologous to the transcriptional suppressor gene *actII-ORF1* (*58*). The latter belongs to the TetR family of transcriptional repressor proteins, indicating that RifQ may be involved in the self-regulation of *rifPQ* operon. In addition, the protein encoded by *rif-orf3* may be involved in the negative regulation of rifamycin biosynthesis. The production of rifamycin B in *rif-orf3* knockout mutant increased by about 40% (*59*). Additionally, *gdmR1*, *gdmR2*, *orf19* and *orf20* may be involved in the regulation of geldanamycin biosynthesis, and *orf16* and *orf17* may encode resistant genes (*60*). Gene knockout and complement experiments confirmed that the LuxR family regulators GdmRI and GdmRII positively regulated the transcription of PKS genes, but did not regulate the expression of post-PKS modification genes such as *gdmN* (*61*).

Though the biosynthetic mechanism of ansamitocins has been studied extensively (*62*), much is remained elusive about the regulation of their biosynthesis. However, tremendous effort has been contributed to enhance the production of ansamitocins by optimizations of culture media and fermentation conditions (*63,64*). Indeed, there are ten possible regulatory genes in the ansamitocin biosynthetic gene cluster, which are *asm2*, *asm8*, *asm18*, *asm29*, *asm31*, *asm34*, *asm35*, *asm39*, *asm40* and *asm48*, respectively (*65*). Asm2, Asm29, and Asm34 belong to the TetR-family transcriptional regulators. Knockout of the *asm2* gene resulted in a nine-fold increase in the production of ansamitocin P3 (*66*), showing that Asm2 plays a negative regulatory role in the biosynthesis of ansamitocins. But surprisingly, overexpression of the *asm2* gene also led to 1.3-fold increase in the production of ansamitocin P3 (*67*). Asm31, Asm39, and Asm40 are sigma factor, sigma factor antagonist and anti-sigma antagonist, respectively. Specifically, Asm39 is a regulatory protein having a histidine kinase-like ATPase C-terminal domain. The constitutive overexpression of the *asm39* gene also increased the yield of ansamitocin P3, but the overexpression of either the *asm29* or the *asm34* gene did not significantly affect the yield of ansamitocin P3 (*67*). Asm8 and Asm48 belong to LuxR or LAL (Large ATP-binding regulator of the LuxR) family transcriptional regulators, depletion of the *asm8* gene resulted in the complete loss of ansamitocin production (*65*). Asm18 is homologous to the SARP family proteins. Bioinformatics analysis suggested that Asm18 is a putative transcriptional regulator, but its gene was refractory to amplification from the genomic DNA (gDNA) of *Actinosynnema pretiosum* (*67*).

Very recently, the function of the *asm18* gene was studied through overexpression in the HGF052 strain (*A. pretiosum* ATCC 31565Δ*asm19*). The results of transcription and HPLC analysis indicate that *asm18* gene encodes a positive transcriptional regulator of the *asm* gene cluster. Real-time PCR analysis showed that the overexpression of the *asm18* gene specifically increased the transcription levels of the genes involved in the biosynthesis of the starter unit 3-amino-5-hydroxybenzoic acid (AHBA) (*asm43*), polyketide assembly (*asmA*), post-PKS modification (*asm21*), as well as the transcription levels of the regulatory gene (*asm8*). Asm8 is a pathway specific LAL-type activator in ansamitocin biosynthesis. Previous study revealed its positive regulatory role in ansamitocin biosynthesis (*65*). Further investigation of the chemical constituents of *asm18*-overexpressed HGF052 strain (HGF052+pJTU824-asm18) led to the isolation of seven ansamitocin derivatives (*68*). Interestingly, these ansamitocin derivatives include maytansinol, which is an important component for the production of antibody-maytansinoid conjugates (*69*).

6. Activation of cryptic ansamycin gene clusters

Previously, through PCR screening of the AHBA synthase genes, we obtained dozens of AHBA synthase gene-positive strains. However, the corresponding ansamycins of most strains were refractory to identification under the conventional laboratory experimental conditions, indicating that the gene clusters containing the AHBA synthase gene were not expressed or just expressed at very low levels (*70*). *S.* sp. LZ35 is one of such AHBA-positive strains, and produces two different types of ansamycins, geldanamycins and hygrocins, under the conventional laboratory conditions (*71-73*). Genome sequence analysis of the LZ35 strain revealed the presence of one more ansamycin gene cluster, namely *nam* gene cluster, besides these two ones responsible for the biosynthesis of geldanamycins and hygrocins. The *pks* genes, *namA-E* within the *nam* gene cluster, contain eight modules, implying that the *nam* cluster encodes the biosynthesis of octaketide ansamycins. Bioinformatics analysis of the eight acyltransferase (AT) domains in NamA-E revealed that the possible extender units for the assembly of polyketide chain could be different from those in known octaketide ansamycins, *i.e.* geldanamycins and ansamitocins, and that the products of this gene cluster could contain a novel scaffold. However, no predicted ansamycins were obtained by large scale fermentation under various conditions. Moreover, reverse transcription (RT) PCR analysis indicated that all the genes examined were expressed poorly in the SR101 strain, a geldanamycin-

nonproducing mutant of the strain LZ35 (*73*), indicating that the *nam* gene cluster was cryptic or weakly expressed under the conventional laboratory conditions.

To induce the expression of the *nam* gene cluster, firstly promoter replacement was carried out by introducing the strong constitutive promoter *ermE** at upstream of the *pks* and amide synthase gene operon in the SR101 strain to generate the SR101*namA-ermE** strain. Fermentation and isolation of the SR101*namA-ermE** strain resulted in the identification of a tetraketide, a derivative of SY4B under usual conditions. SY4b is one of the major tetraketides accumulated in Δ*rifF* mutant (rifamycin amide synthase gene deletion) of *Amycolatopsis mediterranei* S699 (*74*). These results indicated that promoter replacement only partially activated the *nam* gene cluster. Further analysis of the *nam* gene cluster identified *nam1* gene encoding a putative positive regulator of the LuxR family proteins. Members of the LuxR family have been previously reported as the activators of polyketide biosynthesis (*75,76*). Constitutive overexpression of the *nam1* gene was carried out by being cloned into the conjugative and integrative vector pJTU824, placed under the control of the *ermE** promoter. The resulting construct was integrated into the chromosome of the SR201 strain (*73*), which is a mutant derived from the SR101 strain with the deletion of hygrocin biosynthetic genes to create the SR201*nam1*OE strain. Fermentation and isolation of the SR201*nam1*OE strain led to the isolation of three novel ansamycins, namely neoansamycins A-C (Figure 2) (*77*), which represents the first successful example of genome mining of ansamycins and illustrates the great potential for exploration of the huge reservoir of cryptic ansamycin biosynthetic gene clusters to obtain novel ansamycins (*70,78*).

Phylogenetic analyses showed that most ansamycin biosynthesis gene clusters are flanked by LuxR-type regulators, *e.g.* geldanamycins (GdmRI, GdmRII) (*61*), hygrocins (Hgc1) (*73*), divegolides (Div8) (*79*) and ansamitocins (Asm8) (*80*). LuxR-type regulators usually contain a DNA-binding helix-turn-helix domain but lack γ-butyrolactone-binding or response regulatory domains. These LuxR-type regulators are activators of ansamycin biosynthesis. However, the mechanism of action of these LuxR-type regulators is still poorly explored. The constitutive overexpression of *nam1* induced the activation of the cryptic ansamycin gene cluster *nam* in *S.* sp. LZ35, further supporting the critical role of LuxR-type regulators in positive regulation of ansamycin biosynthesis. Comparative transcriptional analysis with quantitative RT-PCR (qRT-PCR) showed that five genes *namA*, *namK*, *nam2*, *nam7* and *nam8* involved in the biosynthesis of neoansamycins were upregulated under *nam1*-overexpressing condition in comparison to the control. The upregulation of transcription of the *nam* gene cluster, coupled with the isolation of neoansamycins in the SR201*nam1*OE strain, further confirmed that Nam1 acts as a direct activator of the *nam* gene cluster. The interaction of Nam1 with the promoter regions of these genes was verified by electrophoretic mobility shift assays (EMSA) performed using purified N-terminal truncated Nam1 protein ($Nam1^{DBD}$) and the PCR-generated promoter fragments of these *nam* genes, respectively. $Nam1^{DBD}$ retarded the mobility of all these fragments, suggesting that Nam1 binds specifically to these promoter regions. In order to identify the Nam1 binding site, the promoter region fragments shown to be retarded in EMSAs were studied by DNase I footprinting analysis. Footprinting analyses revealed protected sequences of approximately 20 to 30 nucleotides in target promoters. The comparison of the protected sequences identified the consensus binding sequence and a sequence logo (*81*) that depicts the binding site. The presence of highly conserved binding sites in these *nam* genes suggested a strong relevance of this class of transcriptional regulator in the regulation of *nam* gene expression. Moreover, the knowledge of the LuxR regulators may set the stage for understanding the genetic control of ansamycin antibiotic biosynthesis regulation and provide an effective strategy to discover and improve the yields of these antibiotics.

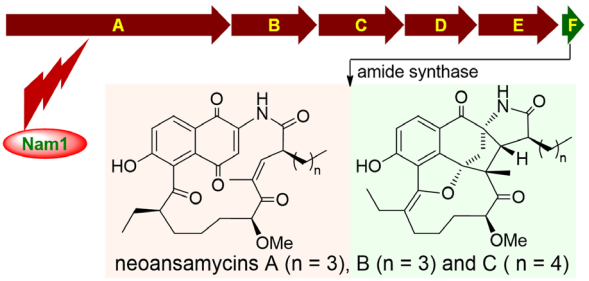

Figure 2. The first example of obtaining new ansamycins through genome mining of transcriptionally activating cryptic gene clusters.

Additionally, another AHBA synthase gene-positive strain *S.* sp. XZQH13 contains a cryptic ansamycin biosynthetic gene cluster *ast* as well. The constitutive overexpression of the *astG1* gene, encoding a Large-ATP-binding regulator of the LuxR family, induced the expression of the *ast* gene cluster including these key biosynthetic genes *astB4*, *astD1* and *astF1*. This led to the isolation of two ansatrienins hydroxymycotrienin A and thiazinotrienomycin G, further supporting that LuxR-type regulators are pathway-specific positive regulators for the biosynthesis of ansamycins (*82*). Moreover, overexpression of the LuxR-type regulator gene *div8* increases the production of divergolides in the *S.* sp. W112 strain (*79*), which further facilitates the isolation of five new ansamycins, namely divergolides O-S (*83*).

7. Perspectives

With the aid of whole genome sequences of thousands

of bacterial genomes and metagenomes, the fast development of genome mining has dramastically facilitated the automated discovery of promising new natural products, however, mostly ignored their roles in the environments. Though this development has been avoid of duplications in the discovery of natural products incurred by bioactivity-guided fractionation, it is insufficient in function predictions. This gap can be amended by adding bio-filters during genome mining (*21*). Specifically, microbial libraries for producers of both glycopeptide and ansamycin antibacterial compounds were enriched by screening the self-resistance mechanism of antibiotic producers. Together with screenings for biosynthetic genes resulted in the discovery of a new glycopeptide antibiotic, pekiskomycin (*84*). The self-resistance guided genome mining approach can be also applied in the discovery of inhibitors of target proteins beyond microorganisms. Panter *et al*. utilized the pentapeptide repeat protein (PRP)-mediated self-resistance mechanism against topoisomerase inhibitors to search the genome of *Pyxidicoccus fallax*. A gene cluster was identified adjacent to a predicted PRP (co-clustering), however, no corresponding compounds were reported before their study. Activation in the native host and heterologous expression of this gene cluster resulted in the isolation of pyxidicyclines, a group of new in inhibitors of *E. coli* DNA topoisomerase IV and human DNA topoisomerase I (*85*). Similarly, the fungal sesquiterpenoid aspterric acid, a potent herbicide, was obtained by the approach of co-clustering self-resistance gene and biosynthetic gene cluster as well (*86*). Indeed, the self-resistance mechanisms of microorganisms against natural products are diverse (*50,87-89*) thus that the self-resistance-directed genome mining would be fruitful in the focused discovery of novel bioactive natural products (*90,91*).

Some natural products are produced by microorganisms evolved from natural selection for acquisition of improved defence against competing deleterious organisms. The production of these defensive secondary metabolites is inducible because they originally serve as responses to environmental challenges. Therefore, the combination of chemical ecology and genome mining can be an integrative approach to the discovery of novel bioactive natural products (*92*). Much more ambitious, Medema and Fischbach suggested to use globe-wide metagenomes to footprint microbial ecosystems, and then to target these for exhaustive single-cell sequencing, which would facilitate our understanding the ecological roles, and even further the natural roles, of natural products. Ideally, computational analysis can predict the action targets of natural products with the availability of ecological distribution and evolution of biosynthetic gene clusters (*93*).

Besides ecology, evolution is another critical issue of natural products that should be considered during genome mining. Natural products are produced by secondary metabolism. Secondary metabolism is the response and adaptation mechanisms of organisms to environmental biotic and abiotic stresses, and natural products are the executors of these mechanisms. Based on the evolutionary theory of natural selection, biological traits are derived from the selection of variations in a population. It is beneficial to improve the fitness of organisms to their environments. The mutations that reduce fitness are directly harmful or irreparable, and will disappear from the population. Some of the new properties of variations have no profit or loss, so they belong to neutral variations. Applying these ideas to natural products, it is generally believed that the cost will increase in producing new natural products. If these costs are accompanied by benefits, organisms will be more adaptable. Moreover, mutations of biosynthetic gene clusters are beneficial to fitness but are not lethal to organisms, which exactly fits the nearly neutral theory that the adaptation may be due not to strong selection of rare variants with large effects, but to weak selection of common variants (*94-96*). Thus, computational analysis of the evolution of the biosynthetic gene clusters in sequences and organizations could help in simulating the evolution of pathways to facilitate genome mining (*97*).

The phylogeny-guided genome mining represents an approach on the basis of evolutionary biology to the discovery of natural products. This approach was established on the assumption that "a single biosynthetic gene that must have co-evolved with its respective biosynthetic gene cluster could be used as a phylogenetic marker that might represent an evolutionary path of its entire biosynthetic gene cluster" (*98*). This approach provides a very straightforward means to screen a large number of microbial genomes or metagenomes attributed to the use of a single gene as a molecular marker in search for new biosynthetic gene clusters of interest, which has already resulted in some fruitful findings (*98*). In particular, with the advance of natural product phylogeny, *e.g*. the Bayesian analysis of biosynthetic modules and/or domains rather than the sequence of a single gene (*99*), novel algorithms-promoted integrative pan-genome mining approach will play an important role in both the mining and the synthetic biology of natural products (*100*).

8. Conclusion

In conclusion, genome mining has brought revolutionary influence on the discovery of novel natural products and the characterization of biosynthetic pathways. The future genome mining would evolve to an integrative approach by the involvement of multiple disciplines to bioactivity-targeted mining of novel natural products.

Acknowledgement

This work was supported in part by the National Natural Science Foundation of China (81530091), and and Program for Changjiang Scholars and Innovative Research Team in University (IRT_17R68).

References

1. Harvey AL, Edrada-Ebel R, Quinn RJ. The re-emergence of natural products for drug discovery in the genomics era. Nat Rev Drug Discov. 2015; 14:111-129.
2. Ikeda H. Natural products discovery from micro-organisms in the post-genome era. Biosci Biotechnol Biochem. 2017; 81:13-22.
3. Winter JM, Behnken S, Hertweck C. Genomics-inspired discovery of natural products. Curr Opin Chem Biol. 2011; 15:22-31.
4. Mukherjee S, Stamatis D, Bertsch J, Ovchinnikova G, Verezemska O, Isbandi M, Thomas AD, Ali R, Sharma K, Kyrpides NC, Reddy TB. Genomes OnLine Database (GOLD) v.6: Data updates and feature enhancements. Nucleic Acids Res. 2017; 45:D446-D456.
5. Choi S-S, Katsuyama Y, Bai L, Deng Z, Ohnishi Y, Kim E-S. Genome engineering for microbial natural product discovery. Curr Opin Microbiol. 2018; 45:53-60.
6. Malpartida F, Hopwood DA. Molecular cloning of the whole biosynthetic pathway of a *Streptomyces* antibiotic and its expression in a heterologous host. Nature. 1984; 309:462-464.
7. Tremblay N, Hill P, Conway KR, Boddy CN. The use of ClusterMine360 for the analysis of polyketide and nonribosomal peptide biosynthetic pathways. In: Nonribosomal peptide and polyketide biosynthesis: Methods and Protocols (Evans BS, ed.). Springer New York, New York, NY, 2016; pp. 233-252.
8. Gross H, Stockwell VO, Henkels MD, Nowak-Thompson B, Loper JE, Gerwick WH. The genomisotopic approach: A systematic method to isolate products of orphan biosynthetic gene clusters. Chem Biol. 2007; 14:53-63.
9. Robbel L, Knappe TA, Linne U, Xie X, Marahiel MA. Erythrochelin − a hydroxamate-type siderophore predicted from the genome of *Saccharopolyspora erythraea*. FEBS J. 2010; 277:663-676.
10. Peano C, Bicciato S, Corti G, Ferrari F, Rizzi E, Bonnal RJ, Bordoni R, Albertini A, Bernardi LR, Donadio S, De Bellis G. Complete gene expression profiling of *Saccharopolyspora erythraea* using GeneChip DNA microarrays. Microb Cell Fact. 2007; 6:37.
11. Lautru S, Deeth RJ, Bailey LM, Challis GL. Discovery of a new peptide natural product by *Streptomyces coelicolor* genome mining. Nat Chem Biol. 2005; 1:265-269.
12. Scherlach K, Hertweck C. Discovery of aspoquinolones A-D, prenylated quinoline-2-one alkaloids from *Aspergillus nidulans*, motivated by genome mining. Org Biomol Chem. 2006; 4:3517-3520.
13. Udwary DW, Zeigler L, Asolkar RN, Singan V, Lapidus A, Fenical W, Jensen PR, Moore BS. Genome sequencing reveals complex secondary metabolome in the marine actinomycete *Salinispora tropica*. Proc Natl Acad Sci U S A. 2007; 104:10376-10381.
14. Nguyen T, Ishida K, Jenke-Kodama H, Dittmann E, Gurgui C, Hochmuth T, Taudien S, Platzer M, Hertweck C, Piel J. Exploiting the mosaic structure of trans-acyltransferase polyketide synthases for natural product discovery and pathway dissection. Nat Biotechnol. 2008; 26:225-233.
15. Ju K-S, Gao J, Doroghazi JR, *et al*. Discovery of phosphonic acid natural products by mining the genomes of 10,000 actinomycetes. Proc Natl Acad Sci U S A. 2015; 112:12175-12180.
16. Owen JG, Reddy BVB, Ternei MA, Charlop-Powers Z, Calle PY, Kim JH, Brady SF. Mapping gene clusters within arrayed metagenomic libraries to expand the structural diversity of biomedically relevant natural products. Proc Natl Acad Sci U S A. 2013; 110:11797-11802.
17. Chen LY, Wang XQ, Wang YM, Geng X, Xu XN, Su C, Yang YL, Tang YJ, Bai FW, Zhao XQ. Genome mining of *Streptomyces xinghaiensis* NRRL B-24674(T) for the discovery of the gene cluster involved in anticomplement activities and detection of novel xiamycin analogs. Appl Microbiol Biotechnol. 2018; 102:9549-9562.
18. Krug D, Müller R. Secondary metabolomics: The impact of mass spectrometry-based approaches on the discovery and characterization of microbial natural products. Nat Prod Rep. 2014; 31:768-783.
19. Surup F, Viehrig K, Rachid S, Plaza A, Maurer CK, Hartmann RW, Muller R. Crocadepsins-depsipeptides from the myxobacterium *Chondromyces crocatus* found by a genome mining approach. ACS Chem Biol. 2018; 13:267-272.
20. Doroghazi JR, Albright JC, Goering AW, Ju K-S, Haines RR, Tchalukov KA, Labeda DP, Kelleher NL, Metcalf WW. A roadmap for natural product discovery based on large-scale genomics and metabolomics. Nat Chem Biol. 2014; 10:963.
21. Zhang W, Li Y, Qian G, Wang Y, Chen H, Li Y, Liu F, Shen Y, Du L. Identification and characterization of the anti-methicillin-resistant *Staphylococcus aureus* WAP-8294A2 biosynthetic gene cluster from *Lysobacter enzymogenes* OH11. Antimicrob Agents Chemother. 2011; 55:5581-5589.
22. Kersten RD, Yang Y-L, Xu Y, Cimermancic P, Nam S-J, Fenical W, Fischbach MA, Moore BS, Dorrestein PC. A mass spectrometry-guided genome mining approach for natural product peptidogenomics. Nat Chem Biol. 2011; 7:794-802.
23. Quinn RA, Nothias LF, Vining O, Meehan M, Esquenazi E, Dorrestein PC. Molecular networking as a drug discovery, drug metabolism, and precision medicine strategy. Trends Pharmacol Sci. 2017; 38:143-154.
24. Nothias LF, Nothias-Esposito M, da Silva R, Wang M, Protsyuk I, Zhang Z, Sarvepalli A, Leyssen P, Touboul D, Costa J, Paolini J, Alexandrov T, Litaudon M, Dorrestein PC. Bioactivity-based molecular networking for the discovery of drug leads in natural product bioassay-guided fractionation. J Nat Prod. 2018; 81:758-767.
25. Bonneau N, Chen G, Lachkar D, Boufridi A, Gallard JF, Retailleau P, Petek S, Debitus C, Evanno L, Beniddir MA, Poupon E. An unprecedented blue chromophore found in nature using a "chemistry first" and molecular networking approach: Discovery of dactylocyanines A-H. Chemistry. 2017; 23:14454-14461.
26. Duncan K, Crüsemann M, Lechner A, Sarkar A, Li J, Ziemert N, Wang M, Bandeira N, Moore B, Dorrestein P, Jensen P. Molecular networking and pattern-based genome mining improves discovery of biosynthetic gene

clusters and their products from *Salinispora* species. Chem Biol. 2015; 22:460-471.
27. Chiang YM, Chang SL, Oakley BR, Wang CCC. Recent advances in awakening silent biosynthetic gene clusters and linking orphan clusters to natural products in microorganisms. Curr Opin Chem Biol. 2011; 15:137-143.
28. Niu G. Genomics-driven natural product discovery in actinomycetes. Trends Biotechnol. 2018; 36:238-241.
29. Ishihama A. Prokaryotic genome regulation: Multifactor promoters, multitarget regulators and hierarchic networks. FEMS Microbiol Rev. 2010; 34:628-645.
30. Bode HB, Bethe B, Hofs R, Zeeck A. Big effects from small changes: Possible ways to explore nature's chemical diversity. Chembiochem. 2002; 3:619-627.
31. Yoon V, Nodwell JR. Activating secondary metabolism with stress and chemicals. J Ind Microbiol Biotechnol. 2014; 41:415-424.
32. Ochi K, Tanaka Y, Tojo S. Activating the expression of bacterial cryptic genes by *rpoB* mutations in RNA polymerase or by rare earth elements. J Ind Microbiol Biotechnol. 2014; 41:403-414.
33. Lu C, Shen Y. Harnessing the potential of chemical defenses from antimicrobial activities. Bioessays. 2004; 26:808-813.
34. Hosaka T, Ohnishi-Kameyama M, Muramatsu H, Murakami K, Tsurumi Y, Kodani S, Yoshida M, Fujie A, Ochi K. Antibacterial discovery in actinomycete strains with mutations in RNA polymerase or ribosomal protein S12. Nat Biotechnol. 2009; 27:462-464.
35. Ochi K, Okamoto S, Tozawa Y, Inaoka T, Hosaka T, Xu J, Kurosawa K. Ribosome engineering and secondary metabolite production. Adv Appl Microbiol. 2004; 56:155-184.
36. Hrvatin S, Piel J. Rapid isolation of rare clones from highly complex DNA libraries by PCR analysis of liquid gel pools. J Microbiol Methods. 2007; 68:434-436.
37. Bian X, Tang B, Yu Y, *et al*. Heterologous production and yield improvement of epothilones in *Burkholderiales* strain DSM 7029. ACS Chem Biol. 2017; 12:1805-1812.
38. Wang X, Zhou H, Chen H, *et al*. Discovery of recombinases enables genome mining of cryptic biosynthetic gene clusters in *Burkholderiales* species. Proc Natl Acad Sci U S A. 2018; 115:E4255-E4263.
39. Bentley SD, Chater KF, Cerdeno-Tarraga AM, *et al*. Complete genome sequence of the model actinomycete *Streptomyces coelicolor* A3(2). Nature. 2002; 417:141-147.
40. Ramos JL, Martinez-Bueno M, Molina-Henares AJ, Teran W, Watanabe K, Zhang X, Gallegos MT, Brennan R, Tobes R. The TetR family of transcriptional repressors. Microbiol Mol Biol Rev. 2005; 69:326-356.
41. Corre C, Song L, O'Rourke S, Chater KF, Challis GL. 2-Alkyl-4-hydroxymethylfuran-3-carboxylic acids, antibiotic production inducers discovered by *Streptomyces coelicolor* genome mining. Proc Natl Acad Sci U S A. 2008; 105:17510-17515.
42. Recio E, Colinas A, Rumbero A, Aparicio JF, Martin JF. PI factor, a novel type quorum-sensing inducer elicits pimaricin production in *Streptomyces natalensis*. J Biol Chem. 2004; 279:41586-41593.
43. Willey JM, Gaskell AA. Morphogenetic signaling molecules of the streptomycetes. Chem Rev. 2011; 111:174-187.
44. Mlot C. Antibiotics in nature: Beyond biological warfare. Science. 2009; 324:1637-1639.
45. Khokhlov AS, Tovarova I, Borisova LN, Pliner SA, Shevchenko LN, Kornitskaia E, Ivkina NS, Rapoport IA. A-factor responsible for the biosynthesis of streptomycin by a mutant strain of *Actinomyces streptomycini*. Dokl Akad Nauk SSSR. 1967; 177:232-235.
46. Kato JY, Funa N, Watanabe H, Ohnishi Y, Horinouchi S. Biosynthesis of gamma-butyrolactone autoregulators that switch on secondary metabolism and morphological development in *Streptomyces*. Proc Natl Acad Sci U S A. 2007; 104:2378-2383.
47. Nishida H, Ohnishi Y, Beppu T, Horinouchi S. Evolution of gamma-butyrolactone synthases and receptors in *Streptomyces*. Environ Microbiol. 2007; 9:1986-1994.
48. Natsume R, Ohnishi Y, Senda T, Horinouchi S. Crystal structure of a gamma-butyrolactone autoregulator receptor protein in *Streptomyces coelicolor* A3(2). J Mol Biol. 2004; 336:409-419.
49. Osbourn A. Secondary metabolic gene clusters: Evolutionary toolkits for chemical innovation. Trends Gene. 2010; 26:449-457.
50. Floss HG, Yu TW. Rifamycin-mode of action, resistance, and biosynthesis. Chem Rev. 2005; 105:621-632.
51. Fukuyo Y, Hunt CR, Horikoshi N. Geldanamycin and its anti-cancer activities. Cancer Lett. 2010; 290:24-35.
52. Cassady JM, Chan KK, Floss HG, Leistner E. Recent developments in the maytansinoid antitumor agents. Chem Pharm Bull. 2004; 52:1-26.
53. Ding L, Maier A, Fiebig HH, Gorls H, Lin WH, Peschel G, Hertweck C. Divergolides A-D from a mangrove endophyte reveal an unparalleled plasticity in ansa-macrolide biosynthesis. Angew Chem Int Ed Engl. 2011; 50:1630-1634.
54. Xu Z, Baunach M, Ding L, Peng H, Franke J, Hertweck C. Biosynthetic code for divergolide assembly in a bacterial mangrove endophyte. Chembiochem. 2014; 15:1274-1279.
55. Wilson MC, Nam SJ, Gulder TA, Kauffman CA, Jensen PR, Fenical W, Moore BS. Structure and biosynthesis of the marine streptomycete ansamycin ansalactam A and its distinctive branched chain polyketide extender unit. J Am Chem Soc. 2011; 133:1971-1977.
56. August PR, Tang L, Yoon YJ, Ning S, Muller R, Yu TW, Taylor M, Hoffmann D, Kim CG, Zhang X, Hutchinson CR, Floss HG. Biosynthesis of the ansamycin antibiotic rifamycin: Deductions from the molecular analysis of the rif biosynthetic gene cluster of *Amycolatopsis mediterranei* S699. Chem Biol. 1998; 5:69-79.
57. Absalon AE, Fernandez FJ, Olivares PX, Barrios-Gonzalez J, Campos C, Mejia A. RifP; a membrane protein involved in rifamycin export in *Amycolatopsis mediterranei*. Biotechnol Lett. 2007; 29:951-958.
58. Fernández-Moreno MA, Caballero J, Hopwood DA, Malpartida F. The act cluster contains regulatory and antibiotic export genes, direct targets for translational control by the *bldA* tRNA gene of *Streptomyces*. Cell. 1991; 66:769-780.
59. Xu J, Wan E, Kim CJ, Floss HG, Mahmud T. Identification of tailoring genes involved in the modification of the polyketide backbone of rifamycin B by *Amycolatopsis mediterranei* S699. Microbiology. 2005; 151:2515-2528.
60. Rascher A, Hu Z, Viswanathan N, Schirmer A, Reid R, Nierman WC, Lewis M, Hutchinson CR. Cloning and characterization of a gene cluster for geldanamycin

production in *Streptomyces hygroscopicus* NRRL 3602. FEMS Microbiol Lett. 2003; 218:223-230.
61. He W, Lei J, Liu Y, Wang Y. The LuxR family members GdmRI and GdmRII are positive regulators of geldanamycin biosynthesis in *Streptomyces hygroscopicus* 17997. Arch Microbiol. 2008; 189:501-510.
62. Li Y, Zhao P, Kang Q, Ma J, Bai L, Deng Z. Dual carbamoylations on the polyketide and glycosyl moiety by Asm21 result in extended ansamitocin biosynthesis. Chem Biol. 2011; 18:1571-1580.
63. Gao Y, Fan Y, Nambou K, Wei L, Liu Z, Imanaka T, Hua Q. Enhancement of ansamitocin P-3 production in *Actinosynnema pretiosum* by a synergistic effect of glycerol and glucose. J Ind Microbiol Biotechnol. 2014; 41:143-152.
64. Lin J, Bai L, Deng Z, Zhong JJ. Effect of ammonium in medium on ansamitocin P-3 production by *Actinosynnema pretiosum*. Biotechnol Bioproc Eng. 2010; 15:119-125.
65. Yu TW, Bai L, Clade D, Hoffmann D, Toelzer S, Trinh KQ, Xu J, Moss SJ, Leistner E, Floss HG. The biosynthetic gene cluster of the maytansinoid antitumor agent ansamitocin from *Actinosynnema pretiosum*. Proc Natl Acad Sci U S A. 2002; 99:7968-7973.
66. Bandi S, Kim Y, Chang YK, Shang GD, Yu TW, Floss HG. Construction of asm2 deletion mutant of *Actinosynnema pretiosum* and medium optimization for ansamitocin P-3 production using statistical approach. J Ind Microbiol Biotechnol. 2006; 16:1338-1346.
67. Ng D, Chin HK, Wong VV. Constitutive overexpression of asm2 and asm39 increases AP-3 production in the actinomycete *Actinosynnema pretiosum*. J Ind Microbiol Biotechnol. 2009; 36:1345-1351.
68. Li S, Lu C, Chang X, Shen Y. Constitutive overexpression of asm18 increases the production and diversity of maytansinoids in *Actinosynnema pretiosum*. Appl Microbiol Biotechnol. 2016; 100:2641-2649.
69. Amiri-Kordestani L, Blumenthal GM, Xu QC, *et al*. FDA approval: Ado-trastuzumab emtansine for the treatment of patients with HER2-positive metastatic breast cancer. Clin Cancer Res. 2014; 20:4436-4441.
70. Wang H, Chen Y, Ge L, *et al*. PCR screening reveals considerable unexploited biosynthetic potential of ansamycins and a mysterious family of AHBA-containing natural products in actinomycetes. J Appl Microbiol. 2013; 115:77-85.
71. Lu C, Li Y, Deng J, Li S, Wang H, Shen Y. Hygrocins C-G, cytotoxic naphthoquinone ansamycins from *gdmAI*-disrupted *Streptomyces* sp. LZ35. J Nat Prod. 2013; 76:2175-2179.
72. Shi N, Wang H, Lu C, Liu Z, Shen Y. Ansamycins produced by *Streptomyces* sp. LZ35. Chin Pharm J. 2011; 46:1317-1320.
73. Li S, Wang H, Li Y, Deng J, Lu C, Shen Y, Shen Y. Biosynthesis of hygrocins, antitumor naphthoquinone ansamycins produced by *Streptomyces* sp. LZ35. Chembiochem. 2014; 15:94-102.
74. Yu TW, Shen Y, Doi-Katayama Y, Tang L, Park C, Moore BS, Richard Hutchinson C, Floss HG. Direct evidence that the rifamycin polyketide synthase assembles polyketide chains processively. Proc Natl Acad Sci U S A. 1999; 96:9051-9056.
75. Laureti L, Song L, Huang S, Corre C, Leblond P, Challis GL, Aigle B. Identification of a bioactive 51-membered macrolide complex by activation of a silent polyketide synthase in *Streptomyces ambofaciens*. Proc Natl Acad Sci U S A. 2011; 108:6258-6263.
76. Kuscer E, Coates N, Challis I, Gregory M, Wilkinson B, Sheridan R, Petkovic H. Roles of rapH and rapG in positive regulation of rapamycin biosynthesis in *Streptomyces hygroscopicus*. J Bacteriol. 2007; 189:4756-4763.
77. Li S, Li Y, Lu C, Zhang J, Zhu J, Wang H, Shen Y. Activating a cryptic ansamycin biosynthetic gene cluster to produce three new naphthalenic octaketide ansamycins with *n*-pentyl and n-butyl side chains. Org Lett. 2015; 17:3706-3709.
78. Huitu Z, Linzhuan W, Aiming L, Guizhi S, Feng H, Qiuping L, Yuzhen W, Huanzhang X, Qunjie G, Yiguang W. PCR screening of 3-amino-5-hydroxybenzoic acid synthase gene leads to identification of ansamycins and AHBA-related antibiotic producers in actinomycetes. J Appl Microbiol. 2009; 106:755-763.
79. Li SR, Zhao GS, Sun MW, He HG, Wang HX, Li YY, Lu CH, Shen YM. Identification and characterization of the biosynthetic gene cluster of divergolides from *Streptomyces* sp. W112. Gene. 2014; 544:93-99.
80. Pan W, Kang Q, Wang L, Bai L, Deng Z. Asm8, a specific LAL-type activator of 3-amino-5-hydroxybenzoate biosynthesis in ansamitocin production. Sci China Life Sci. 2013; 56:601-608.
81. Crooks GE, Hon G, Chandonia JM, Brenner SE. WebLogo: A sequence logo generator. Genome Res. 2004; 14:1188-1190.
82. Xie C, Deng JJ, Wang HX. Identification of AstG1, a LAL family regulator that positively controls ansatrienins production in *Streptomyces* sp. XZQH13. Curr Microbiol. 2015; 70:859-864.
83. Zhao G, Li S, Guo Z, Sun M, Lu C. Overexpression of div8 increases the production and diversity of divergolides in *Streptomyces* sp. W112. RSC Advances. 2015; 5:98209-98214.
84. Thaker MN, Wang W, Spanogiannopoulos P, Waglechner N, King AM, Medina R, Wright GD. Identifying producers of antibacterial compounds by screening for antibiotic resistance. Nat Biotechnol. 2013; 31:922-927.
85. Panter F, Krug D, Baumann S, Muller R. Self-resistance guided genome mining uncovers new topoisomerase inhibitors from myxobacteria. Chem Sci. 2018; 9:4898-4908.
86. Yan Y, Liu Q, Zang X, Yuan S, Bat-Erdene U, Nguyen C, Gan J, Zhou J, Jacobsen SE, Tang Y. Resistance-gene-directed discovery of a natural-product herbicide with a new mode of action. Nature. 2018; 559:415-418.
87. Gomi S, Ikeda D, Nakamura H, Naganawa H, Yamashita F, Hotta K, Kondo S, Okami Y, Umezawa H, Iitaka Y. Isolation and structure of a new antibiotic, indolizomycin, produced by a strain SK2-52 obtained by interspecies fusion treatment. J Antibiot. 1984; 37:1491-1494.
88. Hopwood DA. How do antibiotic-producing bacteria ensure their self-resistance before antibiotic biosynthesis incapacitates them? Mol Microbiol. 2007; 63:937-940.
89. Xu H, Huang W, He QL, Zhao ZX, Zhang F, Wang R, Kang J, Tang GL. Self-resistance to an antitumor antibiotic: A DNA glycosylase triggers the base-excision repair system in yatakemycin biosynthesis. Angew Chem Int Ed Engl. 2012; 51:10532-10536.
90. Ziemert N, Alanjary M, Weber T. The evolution of genome mining in microbes – a review. Nat Prod Rep. 2016; 33:988-1005.

91. Machado H, Tuttle RN, Jensen PR. Omics-based natural product discovery and the lexicon of genome mining. Curr Opin Microbiol. 2017; 39:136-142.
92. Vizcaino MI, Guo X, Crawford JM. Merging chemical ecology with bacterial genome mining for secondary metabolite discovery. J Ind Microbiol Biotechnol. 2014; 41:285-299.
93. Medema MH, Fischbach MA. Computational approaches to natural product discovery. Nat Chem Biol. 2015; 11:639-648.
94. Hurst LD. Fundamental concepts in genetics: Genetics and the understanding of selection. Nat Rev Genet. 2009; 10:83-93.
95. Kimura M. The neutral theory of molecular evolution and the world view of the neutralists. Genome. 1989; 31:24-31.
96. Valenzuela CY. Foundational errors in the Neutral and Nearly-Neutral theories of evolution in relation to the Synthetic Theory: Is a new evolutionary paradigm necessary? Biol Res. 2013; 46:101-119.
97. Rudolf JD, Yan X, Shen B. Genome neighborhood network reveals insights into enediyne biosynthesis and facilitates prediction and prioritization for discovery. J Ind Microbiol Biotechnol. 2016; 43:261-276.
98. Kang HS. Phylogeny-guided (meta)genome mining approach for the targeted discovery of new microbial natural products. J Ind Microbiol Biotechnol. 2017; 44:285-293.
99. Schmitt I, Barker FK. Phylogenetic methods in natural product research. Nat Prod Rep. 2009; 26:1585-1602.
100. van der Lee TAJ, Medema MH. Computational strategies for genome-based natural product discovery and engineering in fungi. Fungal Genet Biol. 2016; 89:29-36.

(Received November 1, 2018; Revised December 25, 2018; Accepted December 28, 2018)

Review

DOI: 10.5582/ddt.2018.01079

Models for acne: A comprehensive study

Indu Lata Kanwar, Tanweer Haider, Anju Kumari, Sandeep Dubey, Priyanka Jain, Vandana Soni*

Department of Pharmaceutical Sciences, Dr. Harisingh Gour University, Sagar, Madhya Pradesh, India.

Summary **Acne vulgaris (AV) is the familiar chronic skin ailment affecting most of the individuals. This multifarious, disease involves the bacterium gram-positive, anaerobic *Propionibacterium acnes* (*P. acnes*) which resides on skin microflora, and participated in acne inflammation and acne lesions. The object of this review is to discuss presently available *in vitro*, *ex vivo*, and *in vivo* models to evaluate the cosmetic formulations that are developed for dealing and prevention of acne formation. These various available models offer new chances for further research on biologically active materials, drugs & pharmaceutical as well as cosmetics for acne treatment.**

Keywords: Acne, *Propionibacterium acnes*, pilosebaceous unit, sebaceous gland, animal models

1. Introduction

Acne, a multifarious chronic inflammatory state, is said to be happening within a pilosebaceous unit (PSU) including hair, hair follicles, sebaceous gland (SG) of the skin, characterized by non-inflammatory lesions-blackheads, whiteheads and inflammatory lesions-papules, pustul, nobless, nodules, and cysts (*1-3*). Acne is associated mostly with *P. acnes* which produces inflammation *via* release of extracellular enzymatic products like proteases, lipases, and hyaluronidases. About 94-95% of the pubertal population, 20-40% of adults and < 25% of women suffered from acne. Even after 25 years of age, women can suffer from is termed as adult female acne (*4-6*). Primarily four causes are critically responsible for the growth of acne lesion as shown in Figure 1 (*7*).

Some other factors are also responsible either alone or in combination for the formation of acne such as heredity, hormones, diet, and other bacterial species. This is well known that there are more chances for the children to have acne if their parents had acne in their young age, some heredity characters and genes which carry the similar information from parents to children. In another case, the various sex hormones like estrogens, androgens and tyrosine kinase hormones, corticotropin-releasing hormone, adrenocorticotropic hormone, glucocorticoid, and melanocortins are required to regulate SG activity. The androgen hormones produced during the adulthood activate the secretion of the oil glands and creates an obstacle in the pores resulting in the progression of blackhead and acne (*8-10*). In general, SG is major responsible part causing disease due to the existence of the enzyme necessary for the formation of various hormones, cytokines and unique lipid mixture of squalene, wax esters, triglycerides and sebum (by the holocrine process) (*11-13*). The structure of all SG found on different skin parts are similar but their nature and the regulation of secretions and secretory process are different (*14,15*). The larger part of SG in hair-covered areas is connected with hair follicles are known as pilosebaceous (PS) glands. The SG of the mucosal margin and modified skin are sovereign of hair follicles (*16*). Excess sebum secretion, abnormal differentiation and desquamation (the shedding) of follicular keratinocyte are some other responsible factors for acne (*17*). The upsurge of the microcomedo as a result of free fatty acid production is primary lesion which has been further developed as inflammatory along with non-inflammatory lesions (*18,19*). In other cases, the various species of bacteria *P. acnes*, *Staphylococcus epidermidis* (*S. epidermidis*), *Staphylococcus aureus* (*S. aureus*), *Streptococcus agalactiae* (*S. agalactiae*), *Klebsiella pneumoniae* (*K. pneumoniae*) *etc*. has also been for the hyperactivity of the SG and ultimately acne (*20*). *P. acnes* are the major causative bacteria which by stimulating androgen receptor to increase the androgen

**Address correspondence to:*
Dr. Vandana Soni, Department of Pharmaceutical Sciences, Dr. Harisingh Gour University, Sagar, Madhya Pradesh-470003, India.
E-mail: drvandanasoni@gmail.com

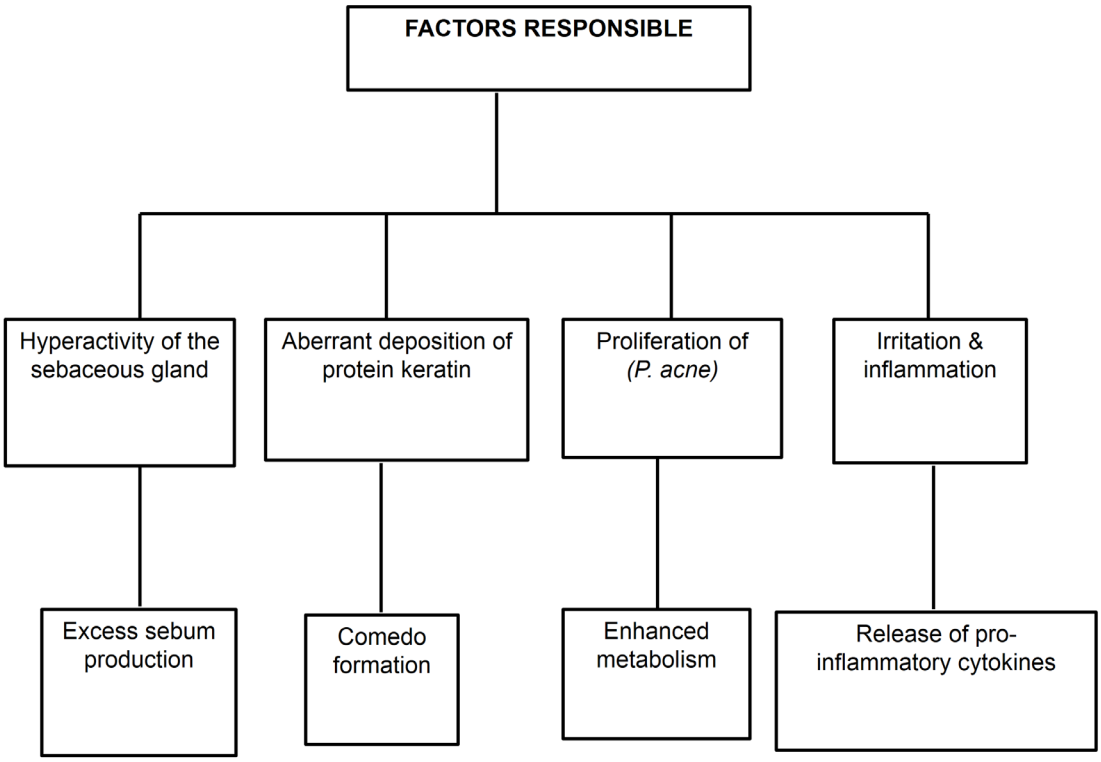

Figure 1. Factors responsible for acne.

secretion *via* androgenic hormone which induces the sebum production, keratinization, and colonization and finally induction of the inborn immune responses which cause inflammation (*21-26*). *P. acnes* also contribute to inflammation *via* activating various chemotactic factors and activate the inflammatory cascade through Toll-like receptors (*27*).

2. Mechanism of acne formation

The acne formation initiates with the overactive SG, follicular hyperkeratinization, immunological changes, and plugging of the infundibulum facilitating *P. acnes*, bacteria colonization, and inflammation (*28*). Increased sebum that is the major source of nutrients for *P. acnes* production is an important participating cause of the acne formation (*29-31*). The mechanism of acne formation should be understood for the design and estimation of the formulation for the effective treatment of acne. Hence, the detail pathogenic factors and process of acne formation is elucidated in Figure 2 and 3.

The various pathogenic factors blamed for the development of acne include the PSU, hyperkeratinization and undue sebum production, discharge inflammatory mediators, and inflammatory infiltrates (causes the progress of growing steps resulting in severity). *P. acnes* bacteria initiate the formation of propionic and acetic acid, thus resulting in the metabolism of sebaceous triglycerides into fatty acids. This results in the irritation of the follicular wall and surrounding dermis (*2,32*). *S. epidermidis*, an anaerobic microorganism, is another causative microorganism involved in acne pathogenesis and produces fatty acid modifying enzyme that forms cholesterol by the fatty acid esterification in the skin (*33,34*). *S. Aureus*, gram-positive rod-shaped bacteria, invade the skin and start producing extracellular enzymes such as lipases, proteases, hyaluronidases, and collagenase. These enzymes cause tissue injury and spread the pathogen into the deeper tissues (*35,36*). *S. agalactiae*, gram-positive coccus bacteria, is also involved in the development of *P. acnes*. The capsular polysaccharides and the pore-forming toxins of *S. agalactiae* are the key factors of *S. agalactiae* (*37*). *K. pneumoniae*, gram-negative bacteria present on the skin flora, causes infection in acne patients undergoing long-term antibiotic therapy. The malicious factors of *K. Pneumoniae* is capsular polysaccharides, siderophores, and adhesins, this virulence produces seditious acne lesions papules, pustules (*38*).

Various models for the antiacne analyze of the drugs and drug carrier are available, but not a single article available which is fully devoted to models for antiacne activities (*39*). Therefore, with the present review article, the authors try to gather and compile the information regarding *in vitro*, *ex vivo*, and *in vivo* models applicable to study acne and are reviewed in the subsequent section (Figure 4).

3. *In vitro* models for acne

In vitro acne models used for the study are organ culture, monolayer culture, follicle model and testosterone-

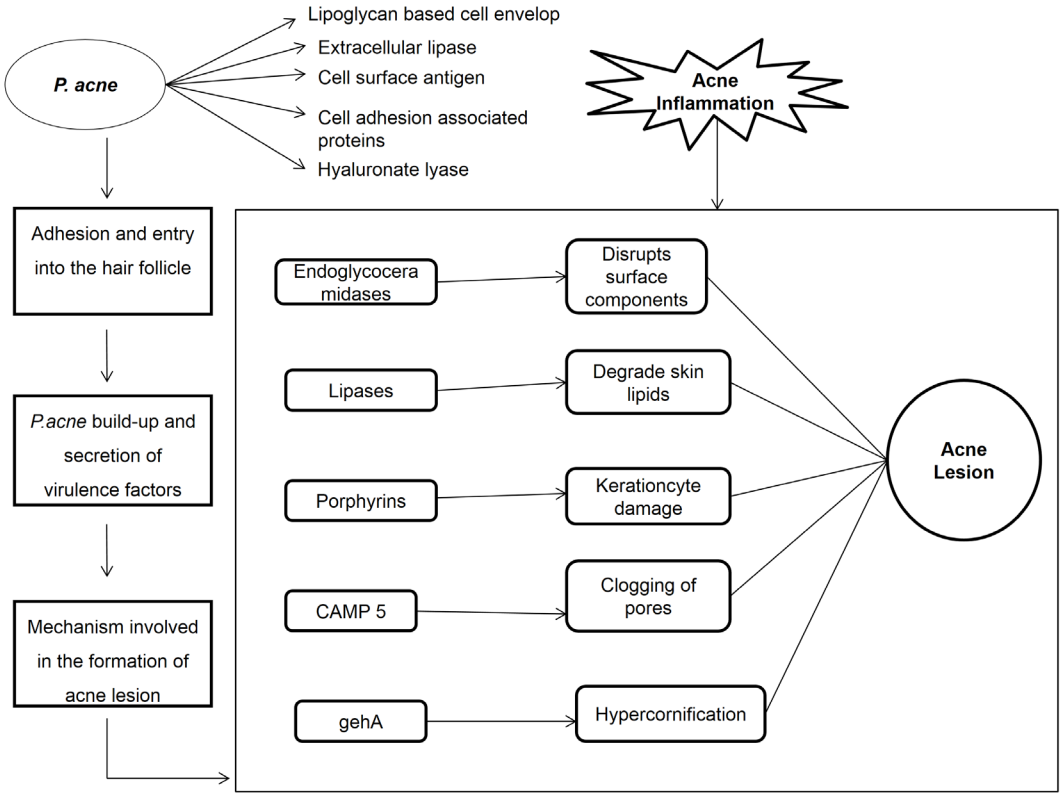

Figure 2. Mechanism of acne formation.

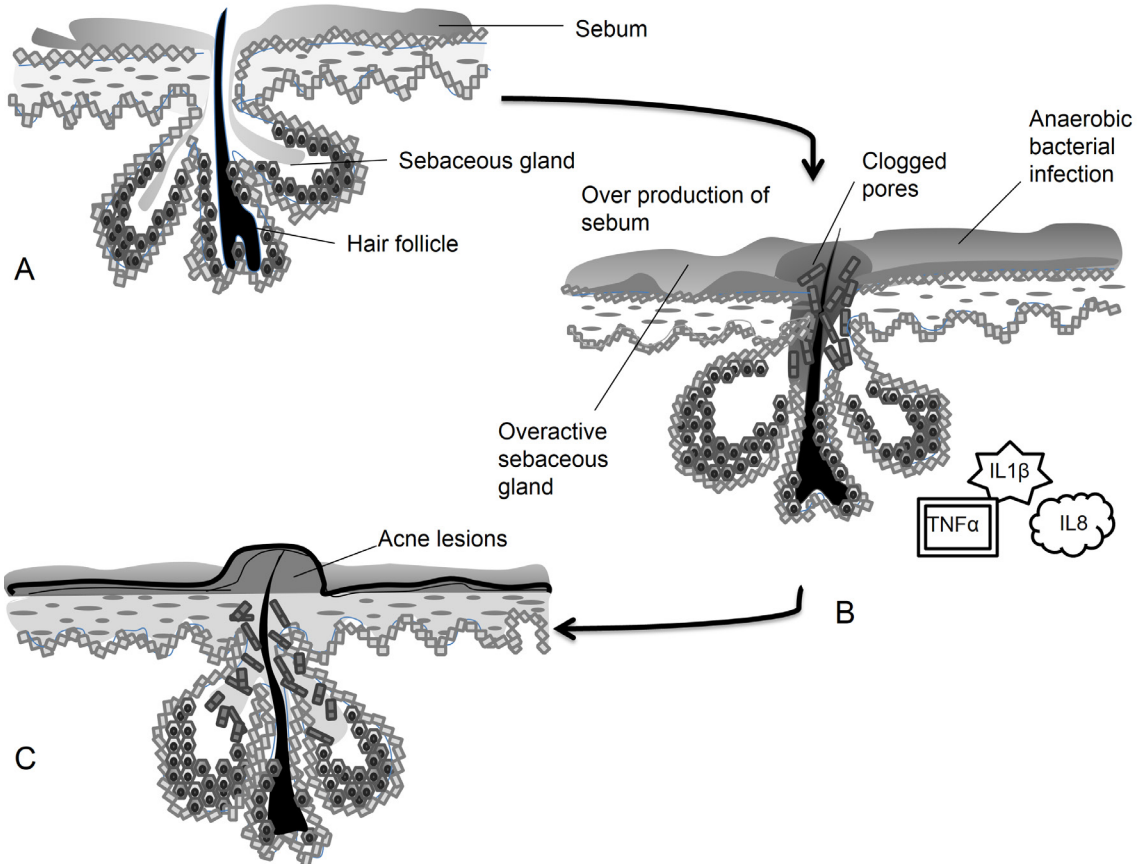

Figure 3. Causative pathogenic factors in acne: (1) Pilosebaceous unit. (2) Mechanism and effects of clogging pore. (3) Inflammatory infiltrates in acne formation.

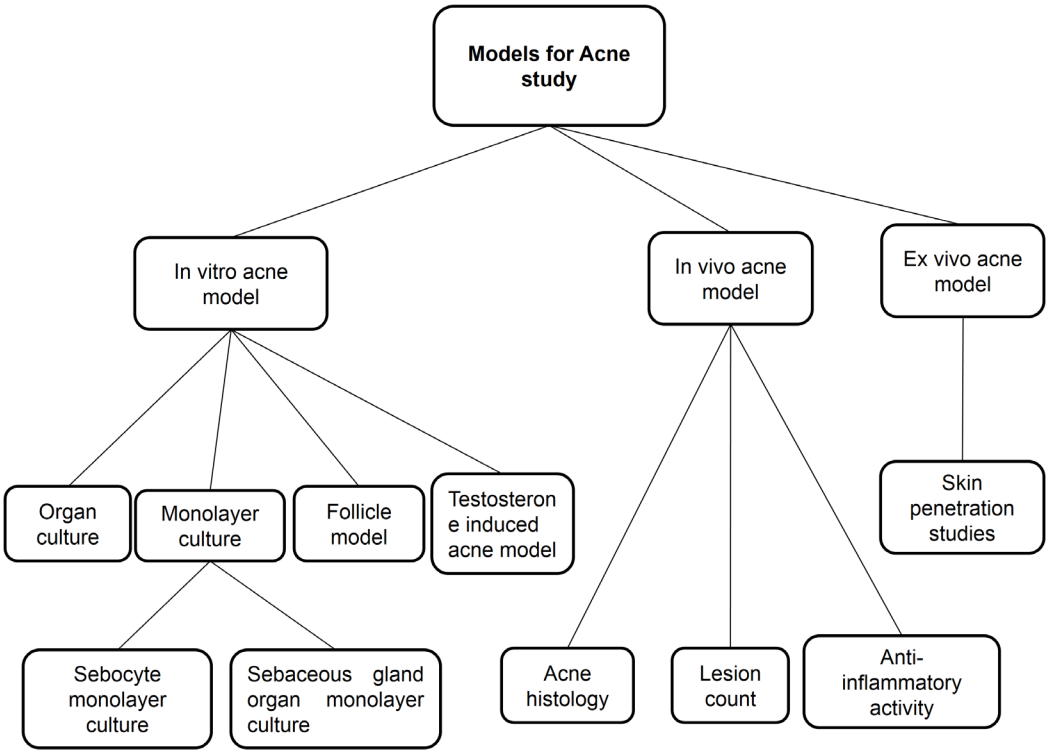

Figure 4. Models for acne study.

induced model. Though, no *in vitro* model is presented which can be used to study the complete perplexity of lesion formation. In *in vitro* organ culture model, the growth and preservation of any tissue, organ, and parts of organ allow the demarcation of that tissue and organ (*40*). In monolayer culture, cells are grown in a single layer on a culture medium in a Petri dish and prepared by the enzymatic separation of organ fragments. Cells in the monolayer culture need a substrate, which should be biologically inert, nontoxic and both the substrate and cells should be compatible with each other, otherwise, the culture will not endure and causes anomalous morphological changes (*41*). While in sebocytes (specialized epithelial cells) monolayer culture the sebocytes are used. These cells release their cellular content by degradation and by rupturing the cell membrane. The lipid synthesis in sebocytes is characterized by the rapid cell multiplication and differentiation of sebocytes. Cultured sebocytes are producing fewer amounts of wax esters and Squalene than the freshly isolated and *in vivo* SG (*42*).

3.1. *SG organ culture*

These models are important to explore the pathophysiology of human skin disorders which involves the SG, *i.e.* sebostasis, seborrhea, and acne. These models are a valuable means to develop and evaluate cosmetics and drug products. Human SG organ culture models highlight the role of SG and explain their functions in skin homeostasis. This model offers numerous benefits in comparison to sebocytes monolayer culture (*40*). These models are developed in isolation of SG by dissection of human skin (surgical waste, donor, cadaver, *etc*.) or by micro-dissection and shearing. The isolated specimens are transferred quickly into Dulbecco's modified Eagle's medium. The epidermal layers of the isolated specimen are separated and remaining dermis parts are directly placed in the growth medium. Intact SGs with/without dermal/epidermal components are utilized to measure lipogenesis rate in subjects with acne and the effect of substrates on lipid rates. To cultivate SG-derived cells, the isolated SGs were seeded in Petri dishes on a 3T3-cell feeder layer and complete culture medium. The cultures were incubated. The proliferation and lipid formation can be simultaneously examined in the basal and differentiated cell layer (*43*). An additional advantage lies over animal model in the fact that delivery of potential sebum suppression compound to the gland is not hindered, so absolute biological efficacy can be evaluated. The advantages of SG organ culture are distinct, although they involve the procedure which is time-consuming.

The SG *in situ* model is applicable for the antiacne studies using the culture of SGs isolated from animals. Toyoda and Morohashi performed organ culture on SG obtained from mice to compute the effects of neuropeptides (calcitonin gene-related peptide, substance P, vasoactive intestinal polypeptide, and neuropeptide Y) along with nerve growth factor. SG treated with substance P resulted in the accelerated lipid synthesis over the control glands by escalating the rate of

Table 1. Reported SG experimental models

Experimental model	*Ref.*
Isolation of SGs after enzymatic dissociation for the cultivation of human sebocytes (HSs).	*45*
Introduced the condition to maintain SG ex vivo.	*46*
A modified version of the technique reported by Karasek, 1986. In this experiment the second 0.4-mm dermal section is used as a source of HSs after removal of epidermis and dermis layer (about 0.4 mm thick) of facial skin.	*47*
In vitro cultivation of human SG-derived cells. HS monolayer cultures as growth from the periphery of SG organ cultures were obtained.	*48*
Xia *et al*. 2009 developed the 1° sebocyte cultures by omitting the 3 T3 fibroblast layer, and 2° culture medium supplemented with delipidized serum and serum-free keratinocyte basal medium.	*49*
Zouboulis *et al*. 2009 described the method for generation of an immortalized sebocyte cell line "SZ95" by transfecting human facial sebocytes with Simian virus-40 large T antigen. This cell showed similar morphologic, phenotypic and functional characteristics of normal HSs. Thiboutot *et al.* Immortalized human SG cell line (SEB-1) by applying the transfection system and Zouboulis *et al*. immortalized SG cell line (Seb-E6E7) by the introduction of HPV16 E6 and E7 genes.	*50-52*

differentiation and proliferation postulating that stress which leads to acne (*44*). SG experimental models are reported in Table 1.

3.2. *Sebocyte monolayer culture*

Although the advantages of SG organ culture are evident, the procedure is time-consuming and depends on continued sources of viable tissue for additional glands. Cell culture offers an alternative over organ culture maintenance, a massive amount of cells can be processed and frozen, allowing multiple experiments to be performed on a similar cell lineage. Several laboratories have productively cultured HS cultures, in the presence of fibroblast support and in serum-free medium. This allows observing the effects of serum and growth factors. HS culture is a well-formed model to change local environmental growth conditions, evaluate lipogenesis inhibitors in a higher throughput mode than that which would normally be obtained through the utilization of organ culture and facilitate the study of cell metabolism, specifically to the androgen metabolism and lipid synthesis. In sebocytes, the synthesis of lipid is dose-dependent (*7*). Sebocytes monolayer culture offers an advantage that maximum cells can be processed and frozen which is used for performing multiple experiments on a similar cell lineage. There are two procedures for generating sebocytes monolayer cultures: (a) first one is explant outgrowth method where isolated SG are attached to culture plates followed by addition of growth medium, following incubation for several days, visible outgrowths (proliferative basal sebocytes) are seen from the glands; (b) second one is SG digestion method which involves digestion of SGs by limited trypsin proteolysis and released cells are plated in mass culture upon a fibroblast feeder layer. After a few days, there is a replication of attached cells into small colonies that can be further used as cloned cells.

3.2.1. *Rat preputial sebocyte monolayer culture*

The preputial gland of rodent possibly is employed as a model for the human SG. These specialized glands open to the surface with a surface of the urethral meatus, and secretions are included in territorial marking and mating behavior. Rat preputial glands are utilized to produce monolayer cultures that can be isolated, digested, and cultured upon a fibroblast nutritive layer (*53,54*). The preputial monolayer cultures of these cells are a suitable model for evaluating the hormone effects on sebaceous development and growth. The effects of estrogen on preputial cell behavior and determination of the cultured cells along with the action of androgen and effect of peroxisome proliferator-activated receptor (PPAR) has been reported (*55,56*). Preputial cells differentiate in a similar process, but to an overall lesser extent than human sebocytes (*57*). Preputial cells cultured *in vitro* lack the existence of PPAR ligands that will induce the formation of the oily or lipid droplet (*58*).

3.3. *Follicle model*

The follicle model is used to appraise the context among sebocytes, keratinocytes and *P. acnes*. *P. acnes* colonizes on superficial skin and PSU. For determining the connection between sebocytes, keratinocytes and *P. acnes*, preserved sebocytes (SZ95) and keratinocytes (HPV-KER) were cultured in the same chamber which is divided by a permeable polyester membrane. The permeable polyester membrane avoids the dispersion of soluble molecules among the chambers. In the healthy PSU, *P. acnes* can only be found in the hair follicular cells (*59*).

3.4. *Squalene oxidation model*

Squalene oxidation models have been developed as the skin tissue engineering models for the *in vitro* testing of acne. These models are utilized for determining the sebum composition as well as the role of oxidative derivatives of squalene (*60*). These models are developed

by the squalene oxidation under controlled atmosphere *i.e*., by oxygen, ultraviolet irradiation and controlled incubation at prescribed conditions. The oxidized squalene derivatives have been analyzed and measured by GCMS and NMR at the predecided condition. The reconstructed human epidermis (RHE) models are also developed which are depended on the use of oxidative derivatives of squalene. On this morphology of the RHE were studied and specific markers such as inflammatory cytokines were measured. This model is used to calculate the drug *in vitro* activity and their formulations to inhibit acne development (*61*).

3.5. *Testosterone-induced acne model (TIAM)*

Testosterone is, a steroidal hormone, accountable for different forms of acne. The conversion of testosterone to dihydrotestosterone, stimulate keratin through its follicular receptor (*62*). Both the dihydrotestosterone and testosterone are the causes of acne because of the increased activity and size of SG. The TIAM is prominent for determining the efficacy and biocompatibility of the various components (*4*) (Figure 5).

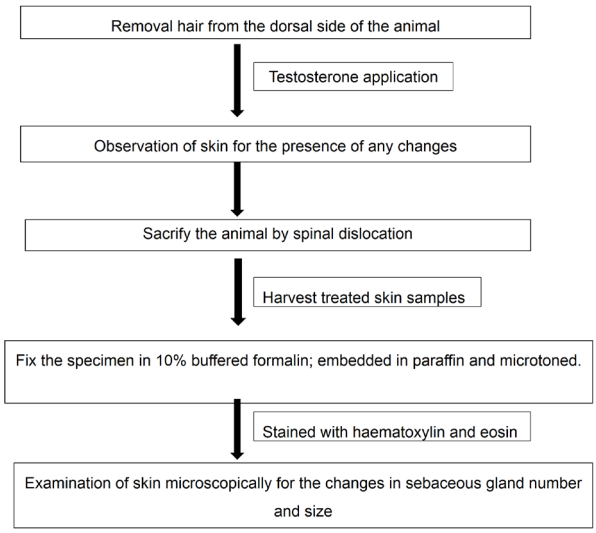

Figure 5. In-vitro testosterone acne induced model.

4. *In vivo* models for acne

These models have been utilized to predict the efficacy of the drug in the treatment of that particular disease (*63*). Recently, animal models have been used for drug development in an exponential manner. The *in-vivo* model has the same physiology as the events of human anagenesis and advantageous to appraise the anti-acnegenic nature of the formulation. These models imitate both human skin diseases and conditions. There are different human and animal models are available for acnegenesis, such as the Mexican hairless dog, rabbit ear assay and Rhino mouse model that closely resembles comedogenesis (*64*).

Skin irritation is the culmination of a complex inflammatory process involving epidermal keratinocytes, dermal fibroblasts, endothelial cells, and annexing leukocytes in which early symptoms may consist of swelling, redness, and itching continuing to scaling and erythema (*7*). Histologically, irritation involves both the epidermis and dermis with inflammatory infiltrates entering from the microvasculature and chemical mediators being released from the different types of cells. The important task of the keratinocytes is not only to provide a barrier and integral structure of the PS follicle but also to participate as the essential task in the inflammatory process through the release/response to surrounding cytokines. Alternatively, the incite inflammation is the key role of bacteria in acne. *In vivo* acne models allow studying and determining the lesion count, the effect of the drug on bacteria, comedogenicity, histology study, and other anti-acne activity.

Two types of inflammatory animal models used for ascertaining the immunostimulatory, pathogenic and pro-inflammatory properties. These models included; 1) an acute inflammation model, induced by drug topically and 2) a chronic skin inflammation model partially relevant to AV, which is developed with the bacterial intradermal injection into the mouse's ear. The detailed procedure for the estimation of anti-acne inflammatory activity and ear thickness as well as acne histology and lesion count shown in Figure 6 and 7, respectively (*65-68*).

Cytotoxins are compounds that stimulate chemotactic activity and are produced by *P. acnes* and other microorganisms in the follicle, which attract neutrophils (*69*). These chemical mediators can then go on to activate macrophages, neutrophils, natural killer cells and other cells inducing the production of additional cytokines. Major inflammation mediators include; histamine, leukotrienes, interleukins, prostaglandins, and neuropeptides. Neutrophils then produce enzymes and generate free oxygen radicals that will result in the disruption of the follicle. Inflamed parts such as pustules, papules, and nodules are developed when comedones rupture and their contents extruded into the dermis rather than above the skin surface. For analysis purposes, the live *P. acnes* (ATCC 6919) will be injected into the mouse's ear. The ear is then cut out on day 1 to day 5 after bacterial injection, and homogenized with the tissue grinder, in 0.9% saline solution. Then supernatant centrifuged for 10 min at 2000 × g to separate out the clear liquid and then cytokine is measured. The TNF-α and IL-1β concentrations are determined with the help of ELISA kits (*70,71*).

5. Skin penetration studies

Ex vivo conditions permit examination on an organism's cells or tissues under more controlled conditions than is attainable *in vivo* testing, to the detriment of modifying the "natural" environment. These studies help to observe

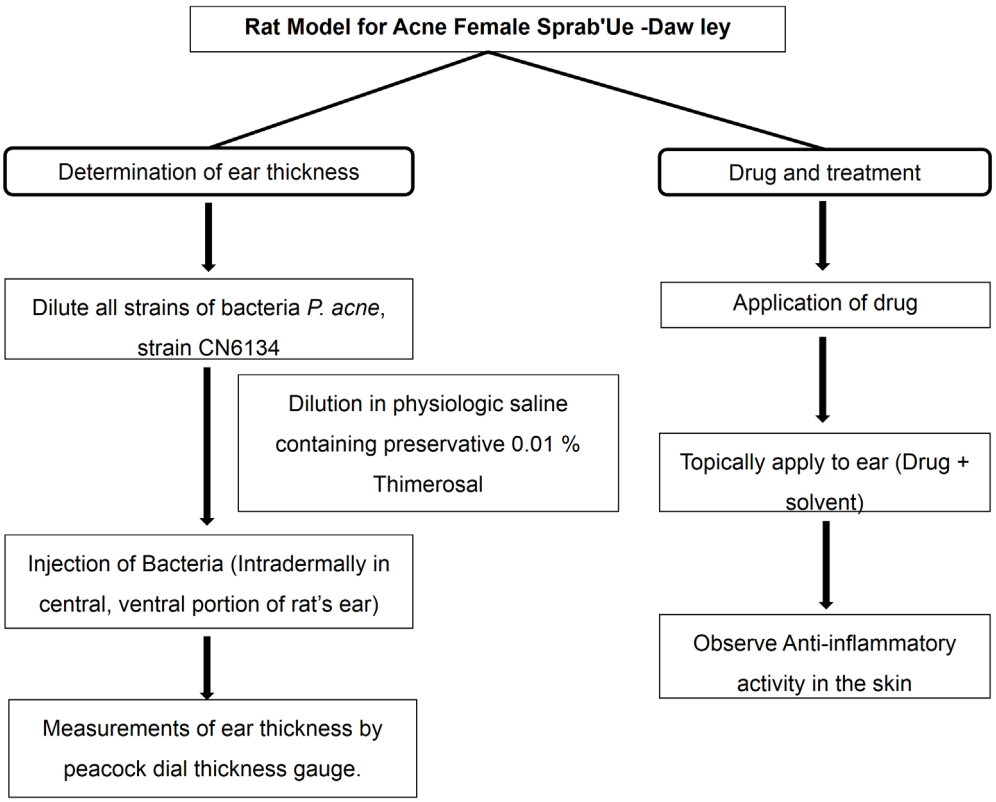

Figure 6. Rat model for acne for determination of anti-inflammatory activity and ear thickness.

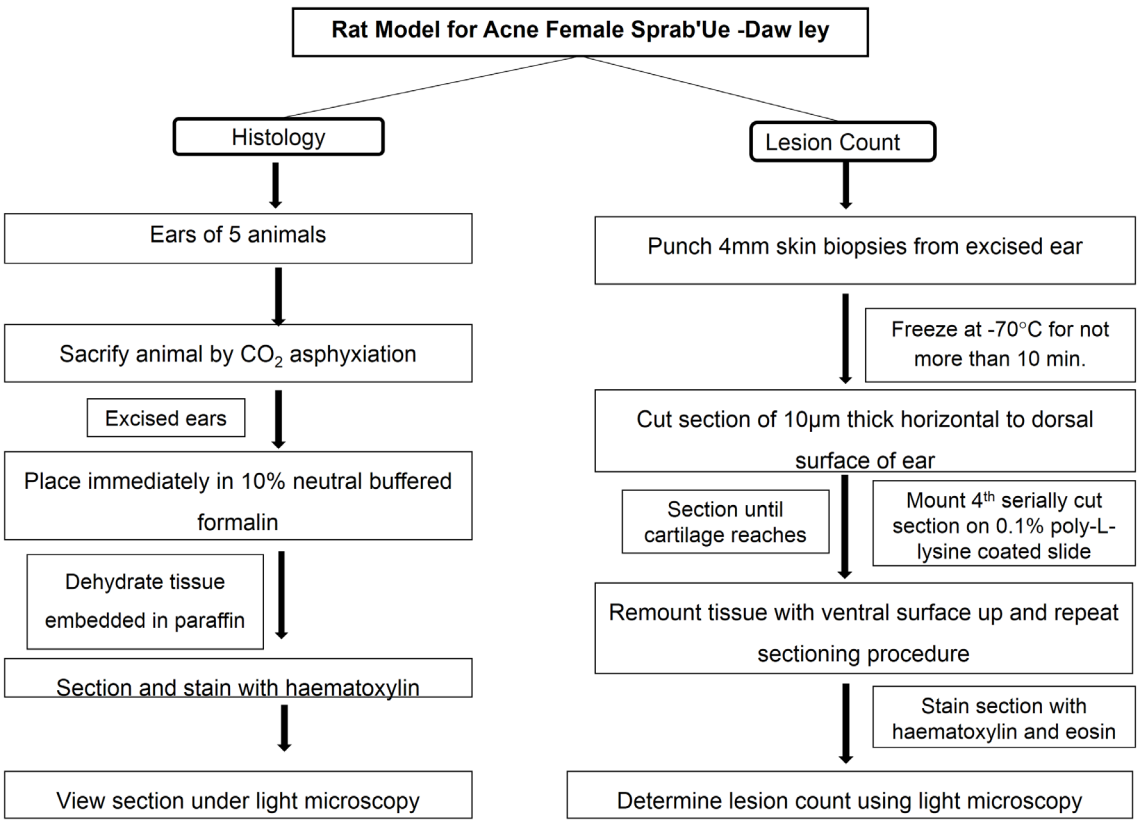

Figure 7. Rat Model for acne histology and lesion count.

the permeation rate of specific compounds through the animal skin (*72*). *Ex vivo* models are economical, effortlessly obtained, but not suitable to determine the long-term experiments or the heat sink effect. The studies can be summarized with the help of Figure 8. For *in vitro* permeation study, the permeation rate of the carrier through the skin, along with drug entrapped will determine by using egg membrane (Figure 9) (*73*).

6. Estimation of antimicrobial (ATM) activity

The activity of ATM component is measured by

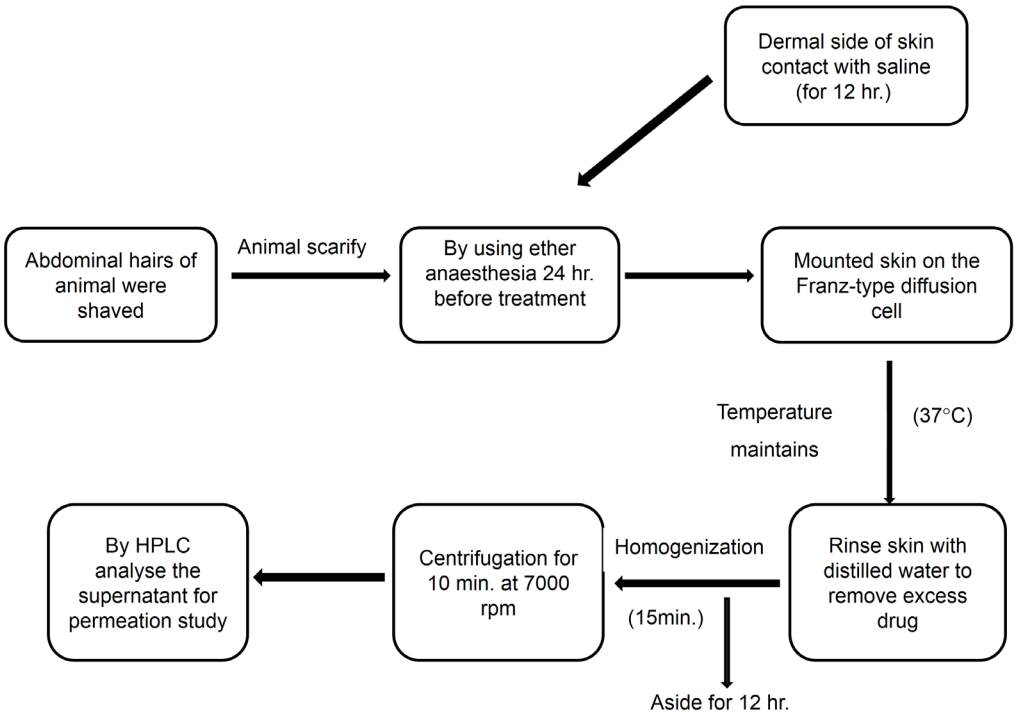

Figure 8. *Ex-vivo* skin penetration studies.

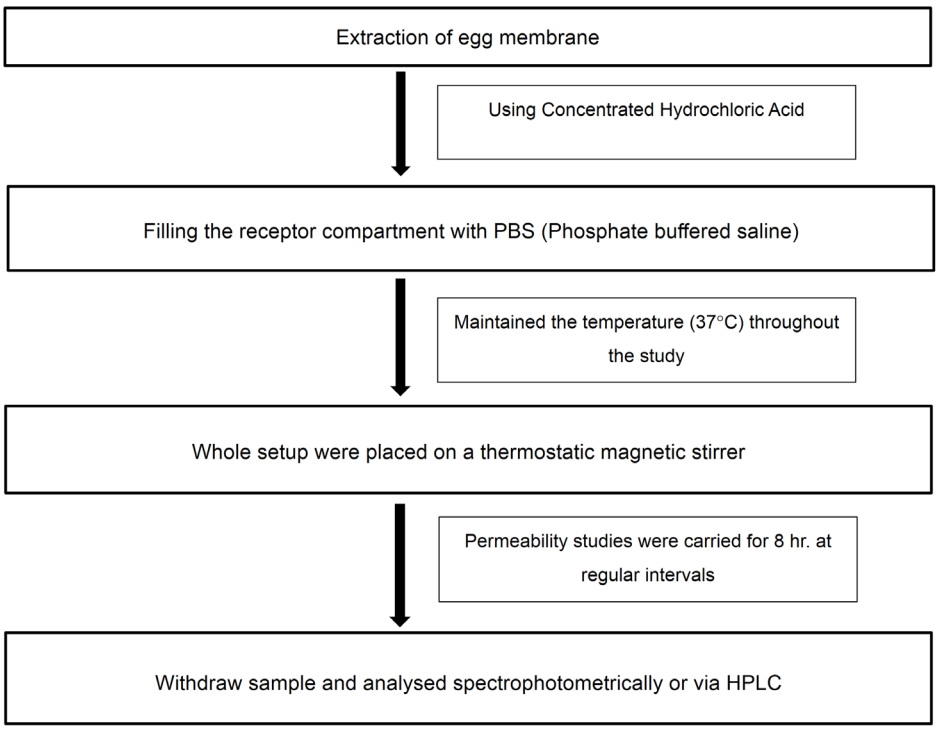

Figure 9. *In-vitro* model for skin permeation study using egg membrane.

determining the minimum inhibitory concentration (MIC). The MIC is the smallest concentration of an ATM agent that will reduce the growth and development of a definite type of organism after sub-culture on antibiotic-free medium. MIC is employed to confirm organism resistance and *in vitro* potency of the new ATMs and it is regarded as the 'gold standard' for the determination of susceptibility of the organism to ATMs. The methods used for determining the MIC of the therapeutic agent are discussed below (*4,74*).

6.1. *ATM assay*

For ATM assay, two microbial varieties *S. aureus* (MTCC 96) and *P. acnes* (MTCC 1951) is usually used. The activities of compound and formulations have been evaluated against *P. acnes* in agar and *S. aureus* in pre-warmed agar plates (APLs). For this microbial cultures should preserve in their suitable agar slants at 4°C. This is used as stock cultures (*75*). About 60 µL of each component is placed on sterile paper discs (8mm diameter) kept above the APL surface. Plates were cultured at 37°C for 48 h (*72*). The ATM potential of the test compound is determined by the measurement of the zone of inhibition (ZOI) diameter (*2,76*).

6.2. *Tube dilution technique (test tube method)*

The tube dilution method is referred to as the standard method for the assessment of microbial resistance against a specific ATM agent. In test tube method, antibiotic dilutions are prepared in a liquid medium. In the series of culture tube (filled with microbial growth medium) (*67*) the test compound (variation in concentrations of test compound) is added. Incubate the culture tube. If there is no turbidity found it represents inhibition in the tube (*7,77*).

6.3. *Agar diffusion method*

It is applied for the assessment of the ATM MIC. Both the nutrient agar and nutrient broth medium have been used for the bacterial culture and for the assessment of ATM potency (*78*). To the Petri plates containing an agar medium, ATM agent is added to filter paper disc and places it in contact with the agar surface (*46*). During the incubation period, the ZOI will be formed, after the diffusion of the test compound onto the APL from the filter paper. The effectiveness of the therapeutic agent is determined by the diameter of ZOI (*5,47,75*).

6.4. *Anti-androgen hypersecretion of sebum*

The fuzzy rat model is selected to study the assessment of hyperplastic SG and sebum hypersecretion. This model is a genetic mutant variety between hairy albino and hairless rats. It is used to determine the effects of molecules or drugs on the reduction of glandular and ductal hyperplasia in human acne. For this, a sample has been diminished into the appropriate vehicles (*i.e*. water, alcohol) *etc*. and applied on the back of all male rats for 2 months, except the control and the vehicle receiving groups of rats. The size of the sebaceous glandular lobes (GLs) and ducts will be quantified in both the fragmented epidermal preparations and frozen sections of skin. After 8 weeks it is evaluated by staining with osmium-potassium dichromate solution. The calculation can be done by the number of bromodeoxyuridine (BdU) positive cells in the GLs in split-skin tissues stained with BdU immunochemistry (*48*).

6.5. *Ex vivo pig skin colonization*

The segment of hair free pigskin has been sterilized in 70% alcohol were clipped and infect with bacterial or fungal inoculum. Then the skin pieces (10 per group) are treated with 100 µL of ATM agent. The treated skin has been incubated for 24h at 35 ± 2°C under humidified conditions. Colonies were counted by swabbing the skin surface with a sterile cotton-tipped applicator soaked in 1mL of sterile saline supplemented with ATM inhibitor. Then after the sampling solutions is diluted and poured into the plates for colony counts. If there were no viable colonies observed, this is assigned as low detection value (*49,79*).

7. Conclusion

Recently, a remarkable headway has been attained in delineating the models available for the acne. In conclusion, the culture of the human SG cell model offers unique possibilities for further fascinating investigations into the role and importance of the SG in the acne development. Moreover, these models which are an adequate tool for evaluation of the pharmacological properties of new anti-acne compounds. The sebum model sustains *P. acnes* progresses and biofilm formation and mimics some important phases of the PSU. Multiple models are available for the identification of technologies for effective acne treatment. By using these models, it is possible to estimate the mechanism of action of lead compounds. More complex culture systems, including three-dimensional models, are under development. The above-discussed approaches are very useful in further advancement in the selection of efficacious drug to the development of drug delivery systems for the acne treatment.

References

1. Feuillolay C, Pecastaings S, Le Gac C, Fiorini-Puybaret C, Luc J, Joulia P, Roques C. A Myrtus communis extract enriched in myrtucummulones and ursolic acid

reduces resistance of *Propionibacterium acnes* biofilms to antibiotics used in acne vulgaris. Phytomedicine. 2016; 23:307-315.
2. Han R, Blencke HM, Cheng H, Li C. The antimicrobial effect of CEN1HC-Br against *Propionibacterium acnes* and its therapeutic and anti-inflammatory effects on acne vulgaris. Peptides. 2018; 99:36-43.
3. Dessinioti C, Katsambas A. Difficult and rare forms of acne. Clin Dermatol. 2017; 35:138-146.
4. Raza K, Singh B, Singal P, Wadhwa S, Katare OP. Systematically optimized biocompatible isotretinoin-loaded solid lipid nanoparticles (SLNs) for topical treatment of acne. Colloids Surf B. 2013; 105:67-74.
5. Maroñas-Jiménez L, Krakowski AC. Pediatric acne: Clinical patterns and pearls. Dermatol Clin. 2016; 34:195-202.
6. Di Landro A, Cazzaniga S, Cusano F, Bonci A, Carla C, Musumeci ML, Patrizi A, Bettoli V, Pezzarossa E, Caproni M, Fortina AB, Campione E, Ingordo V, Naldi L, Group for Epidemiologic Research in Dermatology Acne Study Group. Adult female acne and associated risk factors: Results of a multicenter case-control study in Italy. J Am Acad Dermatol. 2016; 75:1134-1141.
7. Bajor J. B18 *In Vitro* Models for the Evaluation of Anti-acne Technologies. In: Acne and Its Therapy (Webster GF, Rawlings AV, eds.). CRC Press, 2007; pp. 275.
8. Thiboutot DM. Overview of acne and its treatment. Cutis. 2008; 81:3-7.
9. Arora MK, Yadav A, Saini V. Role of hormones in acne vulgaris. Clin Biochem. 2011; 44:1035-1040.
10. Melnik BC. Acne vulgaris: The metabolic syndrome of the pilosebaceous follicle. Clin Dermatol. 2018; 36:29-40.
11. Miyake K, Ciletti N, Liao S, Rosenfield RL. Androgen receptor expression in the preputial gland and its sebocytes. J Invest Dermatol. 1994; 103:721-725.
12. Muise ES, Zhu Y, Verras A, Karanam BV, Gorski J, Weingarth D, Lin HV, Hwa J, Thompson JR, Hu G, Liu J, He S, DeVita RJ, Shen DM, Pinto S. Identification and characterization of sebaceous gland atrophy-sparing DGAT1 inhibitors. PLoS One. 2014; 9:e88908.
13. Hinde E, Haslam IS, Schneider MR, Langan EA, Kloepper JE, Schramm C, Zouboulis CC, Paus R. A practical guide for the study of human and murine sebaceous glands *in situ*. Exp Dermatol. 2013; 22:631-637.
14. Tsatsou F, Zouboulis CC. Anatomy of the sebaceous gland. In: Pathogenesis and Treatment of Acne and Rosacea (Zouboulis C, Katsambas A, Kligman A, eds.). Springer, Berlin, Heidelberg, 2014; pp. 27-31.
15. Shi VY, Leo M, Hassoun L, Chahal DS, Maibach HI, Sivamani RK. Role of sebaceous glands in inflammatory dermatoses. J Am Acad Dermatol. 2015; 73:856-863.
16. Zouboulis CC, Makrantonaki E. The Role of the Sebaceous Gland. In: Pathogenesis and treatment of acne and rosacea (Zouboulis CC, Katsambas AD, Kligman AM, eds.). Springer, Berlin, Heidelberg, 2014; pp. 77-90.
17. Jahns AC, Eilers H, Ganceviciene R, Alexeyev OA. Propionibacterium species and follicular keratinocyte activation in acneic and normal skin. Br J Dermatol. 2015; 172:981-987.
18. Davidovici BB, Wolf R. The role of diet in acne: Facts and controversies. Clin Dermatol. 2010; 28:12-16.
19. Adebamowo CA, Spiegelman D, Danby FW, Frazier AL, Willett WC, Holmes MD. High school dietary dairy intake and teenage acne. J Am Acad Dermatol. 2005; 52:207-214.
20. Owen L, Grootveld M, Arroo R, Ruiz-Rodado V, Price P, Laird K. A multifactorial comparison of ternary combinations of essential oils in topical preparations to current antibiotic prescription therapies for the control of acne vulgaris-associated bacteria. Phytother Res. 2017; 31:410-417.
21. Charny JW, Choi JK, James WD. Spironolactone for the treatment of acne in women, a retrospective study of 110 patients. Int J Womens Dermatol. 2017; 3:111-115.
22. Azmahani A, Nakamura Y, McNamara KM, Sasano H. The role of androgen under normal and pathological conditions in sebaceous glands: The possibility of target therapy. Curr Mol Pharmacol. 2016; 9:311-319.
23. Dessinioti C, Katsambas A. *Propionibacterium acnes* and antimicrobial resistance in acne. Clin Dermatol. 2017; 35:163-167.
24. Tahir CM. Pathogenesis of acne vulgaris: Simplified. J Pak Assoc Dermatol. 2016; 20:93-97.
25. Rosenfield RL, Deplewski D. Role of androgens in the developmental biology of the pilosebaceous unit. Am J Med. 1995; 98:S80-S88.
26. Barrault C, Garnier J, Pedretti N, Cordier-Dirikoc S, Ratineau E, Deguercy A, Bernard FX. Androgens induce sebaceous differentiation in sebocyte cells expressing a stable functional androgen receptor. J Steroid Biochem Mol Biol. 2015; 152:34-44.
27. Zouboulis CC. Acne and sebaceous gland function. Clin Dermatol. 2004; 22:360-366.
28. Paithankar DY, Sakamoto FH, Farinelli WA, *et al*. Acne treatment based on selective photothermolysis of sebaceous follicles with topically delivered light-absorbing gold microparticles. J Invest Dermatol. 2015; 135:1727-1734.
29. Bissonnette R, Poulin Y, Drew J, Hofland H, Tan J. Olumacostat glasaretil, a novel topical sebum inhibitor, in the treatment of acne vulgaris: A phase IIa, multicenter, randomized, vehicle-controlled study. J Am Acad Dermatol. 2017; 76:33-39.
30. Appiah S, Lawley B, Vu M, Bell C, Jones H. Evaluation of the effectiveness of Eladi Keram for the treatment of acne vulgaris: A randomised controlled pilot study. Eur J Integr Med. 2017; 12:38-43.
31. Fox L, Csongradi C, Aucamp M, du Plessis J, Gerber M. Treatment modalities for acne. Molecules. 2016; 21:1063.
32. Tax G, Urbán E, Palotás Z, Puskás R, Kónya Z, Bíró T, Kemény L, Szabó K. Propionic acid produced by *Propionibacterium acnes* strains contributes to their pathogenicity. Acta Derm Venereol. 2016; 96:43-49.
33. Chessa D, Ganau G, Spiga L, Bulla A, Mazzarello V, Campus GV, Rubino S. *Staphylococcus aureus* and *Staphylococcus epidermidis* virulence strains as causative agents of persistent infections in breast implants. PLoS One. 2016; 11:e0146668.
34. Oliveira WF, Silva PMS, Silva RCS, Silva GMM, Machado G, Coelho L, Correia MTS. *Staphylococcus aureus* and *Staphylococcus epidermidis* infections on implants. J Hosp Infect. 2018; 98:111-117.
35. Khorvash F, Abdi F, Kashani HH, Naeini FF, Narimani T. *Staphylococcus aureus* in acne pathogenesis: A case-control study. N Am J Med Sci. 2012; 4:573-576.

36. Ibberson CB. Hyaluronidase in *Staphylococcus aureus* physiology and pathogenesis. University of Lowa, 2015.
37. Moreno AMS. An Attempt to Elucidate the Genes Encoding the Surface Exposed Proteins R3, Z1 and Z2 in Two Strains of Streptococcus agalactiae from Zimbabwe. Norwegian University of Science and Technology, 2014.
38. Kumar B, Pathak R, Mary PB, Jha D, Sardana K, Gautam HK. New insights into acne pathogenesis: Exploring the role of acne-associated microbial populations. Dermatol Sin. 2016; 34:67-73.
39. Verkalk N, Schurink C, Melles D. Antibiotic treatment of *Propionibacterium acnes* endocarditis. Clin Microbiol Infect. 2018; 24:171-174.
40. Ridden J, Ferguson D, Kealey T. Organ maintenance of human sebaceous glands: *in vitro* effects of 13-cis retinoic acid and testosterone. J Cell Sci. 1990; 95:125-136.
41. McAteer JA, Douglas WH. Monolayer culture techniques. Methods Enzymol. 1979; 58:132-140.
42. Zouboulis CC, Xia L, Akamatsu H, Seltmann H, Fritsch M, Hornemann S, Rühl R, Chen W, Nau H, Orfanos C. The human sebocyte culture model provides new insights into development and management of seborrhoea and acne. Dermatology. 1998; 196:21-31.
43. Xia L, Zouboulis C, Detmar M, Mayer-da-Silva A, Stadler R, Orfanos CE. Isolation of human sebaceous glands and cultivation of sebaceous gland-derived cells as an *in vitro* model. J Invest Dermatol. 1989; 93:315-321.
44. Toyoda M, Morohashi M. Pathogenesis of acne. Med Electron Microsc. 2001; 34:29-40.
45. Rodriquez-Tudela J, Donnelly J, Arendrup M, Arikan S, Barchiesi F, Bille J, Chryssanthou E, Cuenca-Estrella M, Dannaoui E, Denning D. Subcommittee on Antifungal Susceptibility Testing (AFST) of the ESCMID European Committee for Antimicrobial Susceptibility Testing. EUCAST Technical Note on the method for the determination of broth dilution minimum inhibitory concentrations of antifungal agents for conidiaforming moulds. Clin Microbiol Infect. 2008; 14:982-984.
46. Hamdy A, Kassem H, Awad G, El-Kady S, Benito MT, Doyagüez E, Jimeno M, Lall N, Hussein A. *In-vitro* evaluation of certain Egyptian traditional medicinal plants against *Propionibacterium acnes*. S Afr J Bot. 2017; 109:90-95.
47. Nipanikar S, Chitlange S, Nagore D. Evaluation of anti-inflammatory and antimicrobial activity of AHPL/AYCAP/0413 capsule. Pharmacognosy Res. 2017; 9:273-276.
48. Ye F, Imamura K, Imanishi N, Rhodes L, Uno H. Effects of topical antiandrogen and 5-alpha-reductase inhibitors on sebaceous glands in male fuzzy rats. Skin Pharmacol. 1997; 10:288-297.
49. Rubinchik E, Dugourd D, Algara T, Pasetka C, Friedland HD. Antimicrobial and antifungal activities of a novel cationic antimicrobial peptide, omiganan, in experimental skin colonisation models. Int J Antimicrob Agents. 2009; 34:457-461.
50. Xia L, Zouboulis CC, Ju Q. Culture of human sebocytes *in vitro*. Dermatoendocrinol. 2009; 1:92-95.
51. Thiboutot D, Gilliland K, Cong Z, Jabara S, McAllister JM, Sivarajah A, Clawson G. Human skin is a steroidogenic tissue: Steroidogenic enzymes and cofactors are expressed in epidermis, normal sebocytes, and an immortalized sebocyte cell line (SEB-1). J Invest Dermatol. 2003; 120:905-914.
52. Zouboulis CC, Dessinioti C. Experimental Models of the Sebaceous Gland. In: Pathogenesis and Treatment of Acne and Rosacea (Zouboulis CC, Katsambas AD, Kligman AM, eds.). Springer, Berlin, Heidelberg, 2014; pp. 43-49.
53. Potter JE, Prutkin L, Wheatley VR. Sebaceous gland differentiation. I. Separation, morphology and lipogenesis of isolated cells from the mouse preputial gland tumor. J Invest Dermatol. 1979; 72:120-127.
54. Laurent SJ, Mednieks MI, Rosenfield RL. Growth of sebaceous cells in monolayer culture. In Vitro Cell Dev Biol. 1992; 28A:83-89.
55. Rosenfield RL, Deplewski D, Kentsis A, Ciletti N. Mechanisms of androgen induction of sebocyte differentiation. Dermatology. 1998; 196:43-46.
56. Wheatley VR, Potter JE, Lew G. Sebaceous gland differentiation: II. The isolation, separation and characterization of cells from the mouse preputial gland. J Invest Dermatol. 1979; 73:291-296.
57. Rosenfield RL, Kentsis A, Deplewski D, Ciletti N. Rat preputial sebocyte differentiation involves peroxisome proliferator-activated receptors. J Invest Dermatol. 1999; 112:226-232.
58. Wheatley VR, Brind JL. Sebaceous gland differentiation: III. The uses and limitations of freshly isolated mouse preputial gland cells for the *in vitro* study of hormone and drug action. J Invest Dermatol. 1981; 76:293-296.
59. Glasenhardt K, Erdei L, Bolla B, Tax G, Urbán E, Kemény L, Szabó K. Development of an *in vitro* follicle model to study the interaction of keratinocytes, sebocytes and *Propionibacterium acnes*. J Invest Dermatol. 2016; 136:S223.
60. Schneider MR, Paus R. Sebocytes, multifaceted epithelial cells: Lipid production and holocrine secretion. Int J Biochem Cell Biol. 2010; 42:181-185.
61. Esselin N, Capallere C, Meyrignac C, Plaza C, Coquet C, Busuttil V, Botto J, Domloge N. Generation and quantification of oxidized squalene to develop an acne testing model *in vitro* based on skin tissue engineering. J Invest Dermatol. 2016; 136:S173.
62. Cibula D, Hill M, Vohradnikova O, Kuzel D, Fanta M, Zivny J. The role of androgens in determining acne severity in adult women. Br J Dermatol. 2000; 143:399-404.
63. Griffiths CE, Finkel LJ, Tranfaglia MG, Hamilton TA, Voorhees JJ. An *in vivo* experimental model for effects of topical retinoic acid in human skin. Br J Dermatol. 1993; 129:389-394.
64. De Young LM, Young JM, Ballaron SJ, Spires DA, Puhvel SM. Intradermal injection of *Propionibacterium acnes*: A model of inflammation relevant to acne. J Invest Dermatol. 1984; 83:394-398.
65. Jang YH, Lee KC, Lee S-J, Kim DW, Lee WJ. HR-1 mice: A new inflammatory acne mouse model. Ann Dermatol. 2015; 27:257-264.
66. Rottboell L, de Foenss S, Thomsen K, Christiansen H, Andersen SM, Dam TN, Rosada C, Stenderup K. Exploring valrubicin's effect on *Propionibacterium acnes*-induced skin inflammation *in vitro* and *in vivo*. Dermatol Reports. 2015; 7:6246.
67. Tsai TH, Chuang LT, Lien TJ, Liing YR, Chen WY, Tsai PJ. Rosmarinus officinalis extract suppresses *Propionibacterium acnes*-induced inflammatory responses. J Med Food. 2013; 16:324-333.

68. Bialecka A, Mak M, Biedron R, Bobek M, Kasprowicz A, Marcinkiewicz J. Different pro-inflammatory and immunogenic potentials of *Propionibacterium acnes* and *Staphylococcus epidermidis*: Implications for chronic inflammatory acne. Arch Immunol Ther Exp (Warsz). 2005; 53:79-85.
69. Ryu S, Han HM, Song PI, Armstrong CA, Park Y. Suppression of *Propionibacterium acnes* infection and the associated inflammatory response by the antimicrobial peptide P5 in mice. PLoS One. 2015; 10:e0132619.
70. Lee WR, Kim KH, An HJ, Kim JY, Chang YC, Chung H, Park YY, Lee ML, Park KK. The protective effects of melittin on *Propionibacterium acnes*-induced inflammatory responses *in vitro* and *in vivo*. J Invest Dermatol. 2014; 134:1922-1930.
71. Zhang Z, Mu L, Tang J, Duan Z, Wang F, Wei L, Rong M, Lai R. A small peptide with therapeutic potential for inflammatory acne vulgaris. PLoS One. 2013; 8:e72923.
72. Kahraman E, Güngör S. Polymeric micellar nanocarriers of benzoyl peroxide as potential follicular targeting approach for acne treatment. Colloids Surf B. 2016; 146:692-699.
73. Ravi R, Senthil K, Parthiban S. Formulation and evaluation of the microsponges gel for an anti-acne agent for the treatment of acne. Indian J Pharm Sci Res. 2013; 3:32-38.
74. Vora J, Srivastava A, Modi H. Antibacterial and antioxidant strategies for acne treatment through plant extracts. Inform Med Unlock. 2018; 13:128-132.
75. Wahi AK, Singh A, Singh AK. Determination of minimum inhibitory concentration (MIC) of some novel triazole derivative. Int J Res Pharm Chem. 2011; 1:1108-1114.
76. Budhiraja A, Dhingra G. Development and characterization of a novel antiacne niosomal gel of rosmarinic acid. Drug Deliv. 2015; 22:723-730.
77. Dinant A, Boulos RA. Zolav®: A new antibiotic for the treatment of acne. Drug Des Devel Ther. 2016; 10:1235.
78. Rodríguez-Tudela JL, Barchiesi F, Bille J, Chryssanthou E, Cuenca-Estrella M, Denning D, Donnelly JP, Dupont B, Fegeler W, Moore C, Richardson M, Verweij PE. Method for the determination of minimum inhibitory concentration (MIC) by broth dilution of fermentative yeasts. Clin Microbiol Infect. 2003; 9:1-8.
79. Andrews JM. Determination of minimum inhibitory concentrations. J Antimicrob Chemother. 2001; 48:5-16.

(Received December 10, 2018; Revised December 18, 2018; Accepted December 29, 2018)

Original Article

DOI: 10.5582/ddt.2018.01070

Quantitation of β-carboline and quercetin in alligator weed (*Alternanthera philoxeroides* (Mart.) Griseb.) by LC-MS/MS and evaluation of cardioprotective effects of the methanol extracts

Xinke Zhang[1], Peng Li[2], Shaohua Guo[2], Shuqi Wang[1,*], Dasheng Liu[2,3,*]

[1] *School of Pharmaceutical Science, Shandong University, Ji'nan, Shandong, China;*
[2] *Ecological Society of Shandong, Ji'nan, Shandong, China;*
[3] *Shandong Institute of Environmental Science, Ji'nan, Shandong, China.*

Summary **Plant invasion is one of the major threats to natural ecosystems. The alligator weed grows rapidly within a small span of time and is easily available all over the world. β-Carboline and quercetin are considered as excellent bioactive components of the alligator weed. In our study LC-MS/MS methods were performed for the detection and determination of the bioactive constituents, β-carboline and quercetin in leaves, in multiple reaction monitoring (MRM) mode. The effects of methanol extract on cardiomyocyte apoptosis induced by doxorubicin using H9c2 cells were evaluated by MTT assay and Annexin V-FITC/PI staining assay. A sensitive and selective liquid chromatography tandem mass spectrometry was developed and validated for the determination of β-carboline and quercetin in this plant. According to *in vitro* cell evaluation experiments, methanol extracts significantly prevented cardiomyocyte apoptosis induced by doxorubicin.**

Keywords: *Alternanthera philoxeroides* (Mart.) Griseb., β-caroline, quercetin, MRM, cardiomyocyte apoptosis

1. Introduction

Plant invasion is a worldwide problem and considered to pose as an environmental and economic threat to human beings (*1*). *Alternanthera philoxeroides* (Mart.) Griseb. is an invasive plant, which although originated in South America, can now be found in many parts of the world (*2*). The weed can grow rapidly in a short period of time and generally form a dense tangled mat. Due to its prevalence, it shades the aquatic vegetation from sunlight and reduces water flow. The alligator weed can also cause death of fish and native plants and give favorable habitat for mosquitoes. Though it is a hazardous weed, its abundance all over the world is exceptional (*3*). Thus in this work, we have tried to find some benefits of this invasive plant. Previous chemical investigation on this species revealed a number of compounds (*4-6*). Among those compounds, β-carboline and quercetin are of great interest due to their diverse biological activities (*7,8*). It is reported they have antioxidant, antimicrobial activity as well as cardioprotective effects. In the present study, we will focus on the study of its cardioprotective effects against doxorubicin (DOX).

As it is known, doxorubicin, sold under the trade names adriamycin among others, is a chemotherapy medication used to treat cancer including bladder cancer, breast cancer, Kaposi's sarcoma, lymphoma, and acute lymphocytic leukemia (*9*). It is often used together with other chemotherapy agents. However, their clinical use is markedly hampered by a major risk of cardiotoxicity that may lead to dilated cardiomyopathy and congestive heart failure (*10*). Prevention of this cardiotoxicity remains a critical issue in clinical oncology. Based on that, we wonder maybe we can utilize the compounds of the alligator weed and develop its cardiomyocyte apoptosis prevention induced by doxorubicin.

Firstly we have developed specific methods for the quantitative analysis of the β-carboline and quercetin

**Address correspondence to:*
Dr. Dasheng Liu, Ecological Society of Shandong, Zhijinshi Jie 12, Jinan 250012, Shandong, China.
E-mail: liu_sdiep@126.com

Dr. Shuqi Wang, School of Pharmaceutical Science, Shandong University, 44 West Wenhua Road, Jinan 250012, Shandong, China.
E-mail: wangsq@sdu.edu.cn

in the *A. philoxeroides* using LC-MS/MS. We also investigated the effects of methanol extract (ME) from *A. philoxeroides* on cardiomyocyte apoptosis induced by doxorubicin. The results demonstrated that ME of the alligator weed was able to reduce DOX-induced H9c2 cell apoptosis.

2. Materials and Methods

2.1. *Reagents*

Standards were purchased from Sigma-Aldrich (Sigma-Aldrich, China). The chemicals acetonitrile (ACN, LC-MS grade) was purchased from Sigma-Aldrich. Formic acid additive for LC-MS was from Sigma-Aldrich. All aqueous solutions, including the HPLC mobile phase, were prepared with water purified using a Milli-Q system (Millipore).

2.2. *Preparation of β-carboline and quercetin standards*

Stock solutions of β-carboline and quercetin (1 mg/mL) were prepared in methanol, and working standard solutions were prepared by adequate dilution of stock solutions with methanol. Solutions were stored at 4°C in the dark. The stability of the stock and standard solutions under these conditions were checked and demonstrated for at least 2 weeks.

2.3. *Sample collection and extraction*

Leaves of *A. philoxeroides* were collected in the Jinan, China, on July, August September and October 2012, from eight different individual plants (numbered AP01-AP08). Ten young leaves and ten old leaves were harvested from each plant. The young and old leaves from each plant were freeze-dried, mixed and ground to a fine powder. The eight powdered samples were then stored in a cold room (−20°C) in the dark until analysis.

2.4. *Analysis sample and extract preparation*

A precise amount of 50 mg of each sample was weighed and extracted with 100 mL of methanol by ultrasound for 0.5 h, and macerated in dark overnight. The extracts were filtered and reported to the correct volume used for extraction. 200 g of the whole plant powder was extracted with 1 L methanol for 24 hours at 25°C. After 24 hours, the mixture was filtrated and the filtrate was evaporated to dryness. The weight of the extract was 13.2 g.

2.5. *LC-MS/MS conditions*

Chromatographic analysis was performed using a Shiseido HPLC system (Kyoto, Japan) equipped with pump (3202), auto-injector (5100), and column heater (3004). Chromatographic analysis was achieved with an Agilent Zorbax SB-C18 (150 × 4.6 mm, i.d.) with a particle diameter of 5 μm. Temperature of the column oven was set at T = 25°C during all experiment, and samples were held at a constant temperature of 4°C by the autosampler thermostat. The mobile phase was a mixture of water acidified with 0.1% of formic acid (A) and ACN (B). The elution of analyte was performed using an isocratic method of 90% of B. The flow rate was set at 0.5 mL/min. The injection volume was 2 μL.

An AB SCIEX QTRAP®5500 tandem mass spectrometer (AB, USA) was connected to the LC system though an electrospray ionization (ESI) interface. The ESI source was operated in positive ionization model for β-carboline and negative ionization model for the qucercetin. Quantification was performed using multiple reaction monitoring (MRM) method with the transitions of the precursor ions to the product ions of m/z 169.0 → 115.1 for β-carboline, and m/z 301.0 → 150.9 for quercetin, respectively. The ionization source conditions were see as follows: Entrance Potential (EP) 10 V; curtain gas (CUR) 30 psi; collision gas (CAD): Medium; ion spray voltage (IS): 5500 V for β-carboline and − 4200 V for quercetin; temperature (TEM) 550°C; nebulizer gas (GS1) 55 psi; heater gas (GS2) 55 psi. Compound dependent parameters were shown in Table 1. System control and data analysis were performed by AB Sciex Analyst software (version 1.6.2).

2.6. *Method validation*

Standard solutions of two representative compounds at a constant concentration were injected into the LC-MS/MS system. The procedure was carried out in triplicate for each concentration. The analyte areas obtained were plotted against the corresponding concentrations of the analyte (expressed as ng/mL) and the calibration curves were constructed by means of the least-square method (*11*).

The limits of quantification (LOQ) and limits of detection (LOD) were evaluated at the concentration in which the quantifier transition presented a signal to noise (S/N) ratio of > 10 and > 3 respectively.

Precision assays were carried out on standard solutions and leaf extracts. Standard solutions of the

Table 1. Multiple reaction monitoring (MRM) optimised parameters for the quantitation of β-carboline and quercetin in *A. philoxeroides* leaves

Analytes	Compounds	
	β-Carboline	Quercetin
Precursor ion	169.0	301.0
Product ion	115.1	150.9
Collision energy	35.0	− 24.2
Declustering potential	140	− 120
Entrance potential	10	− 10
Collision cell exit potential	13	13

selected compounds at three different concentrations (low, middle, and high) were analyzed six times within the same day to obtain intra-day precision and six times over six different days to obtain inter-day precision, both expressed as percentage relative standard deviation (RSD%). Similarly, leaf extracts were analyzed six times within the same day to test intra-day precision and six times over six different days to obtain inter-day precision.

Method accuracy was tested by means of percentage recovery assays, adding known amounts of standard solutions of the analytes leaf extracts, which had been already analyzed. The added concentrations corresponded to the lower limit, an middle value and a high value (*12*).

2.7. *Protective effects of methanol extract on doxorubicin-induced apoptosis in H9c2 cells*

Rat cardiac H9c2 cells were cultured in DMEM supplemented with 10% fetal bovine serum, 100 U/mL of penicillin, 100 μg/mL of streptomycin and 5% CO_2 at 37°C. Cells were plated at an appropriate density according to each experimental design. H9c2 cells were incubation with ME (10, 20, 40, 80, 160 mg/mL) for 24 h. After incubation with 10 μM doxorubicin for another 24 h, a modified MTT assay was used to determine cell viability (*13*).

2.8. *Annexin V-FITC/PI staining assay*

Rat cardiac H9c2 cells seeded in 6-well plates (1.5×10^5 per well) were exposed to ME (10, 20, 40, 80, 160 mg/mL) for 24 h. After incubation with 10 μM doxorubicin for another 24 h, cells were harvested and washed with cold PBS. The cell surface phosphatidylserine in apoptotic cells was quantitatively estimated by using Annexin V-FITC/PI apoptosis detection kit according to the manufacturer's instructions (Becton Dickinson, USA). The analysis was performed on a FACScan flow cytometry.

3. Results

3.1. *Preliminary assays*

β-Carboline and quercetin, mass spectra were first acquired in full-scan mode (100-400 m/z) by infusion of reference solutions at 1 μg/mL. We used MRM to quantify the two compounds. The chosen MRM transitions for LC-MS/MS quantitative analysis were: β-carboline (169.0 → 115.1 for qualitative purposes); quercetin (301.0 → 150.9 for qualitative purposes) according to the spectra C and D in Figure 1 . The collision energy used to fragment the β-carboline and quercetin were optimized in the spectra E and F. Base on the data, we selected 35 V for β-carboline and − 24.2 V for quercetin to generate the sufficiently abundant fragmentation ion. The precursor ion and the product ion, together with optimized MS parameters for each compound are given in Table 1.

3.2. *Method validation*

The whole methodology was successfully validated in terms of linearity, precision and accuracy according to International Regulatory Guidelines, thus demonstrating reliability and suitability of this analytical strategy. Good linearity ($r^2 > 0.995$) was obtained over the 0.3-100 ng/mL concentration range for all the analytes. The LOQ and the LOD values were 0.3 ng/mL and 0.1 ng/mL, respectively, for the two compounds. Intra-day and inter-day repeatability were evaluated for each compound. CV% did not exceed a value of 15% for intra-day assay and 20% for inter-day assay. Mean recovery values were always higher than 95%; thus, method accuracy is satisfactory (Table 2).

3.3. *Quantitative results*

The validated method was applied to the analysis of *A. philoxeroides* leaf. Quantitative results are shown in Table 3 and each value is the mean of the results obtained from five analyses. It's shown that β-carboline and quercetin in the extracts from September are richer than those from other months.

3.4. *Cardioprotective effect*

To analyze the protective effects of methanol extract (ME) on doxorubicin-induced cytotoxicity in H9c2 cells, cell proliferation was examined after incubation with methanol extract (10, 20, 40, 80, 160 mg/mL) in the presence of doxorubicin. The result of cell viability was shown on Figure 2. The cell viability of the negative group in the presence of the DOX was 40.75 ± 4.25%, while incubation with different concentrations of ME for 24 h, the cell viability was boosted significantly. With treatment of 10, 20, 40, 80, 160 mg/mL ME, the cell viability was 38.43 ± 11.5%, 66.33 ± 6.03%, 79.00 ± 3.6%, 84.33 ± 5.5%, 83.16 ± 8.12% respectively. The pretreatment had a significant protective effect against doxorubicin-mediated cytotoxicity.

3.5. *Decrease of apoptosis induced by DOX*

Flow cytometry analysis results were shown in Figure 3. It was demonstrated that DOX induced 53.88% H9c2 cell apoptosis, while with the pretreatment of ME at the concentration of 10, 20, 40, 80, 160 mg/mL the cell apoptosis was decreased to 51.18%, 42.5%, 33.18%, 25.2%, 23.46% induced by DOX. It was illustrated that ME could decrease the cell apoptosis induced by DOX. And the protection effect of ME was relevant

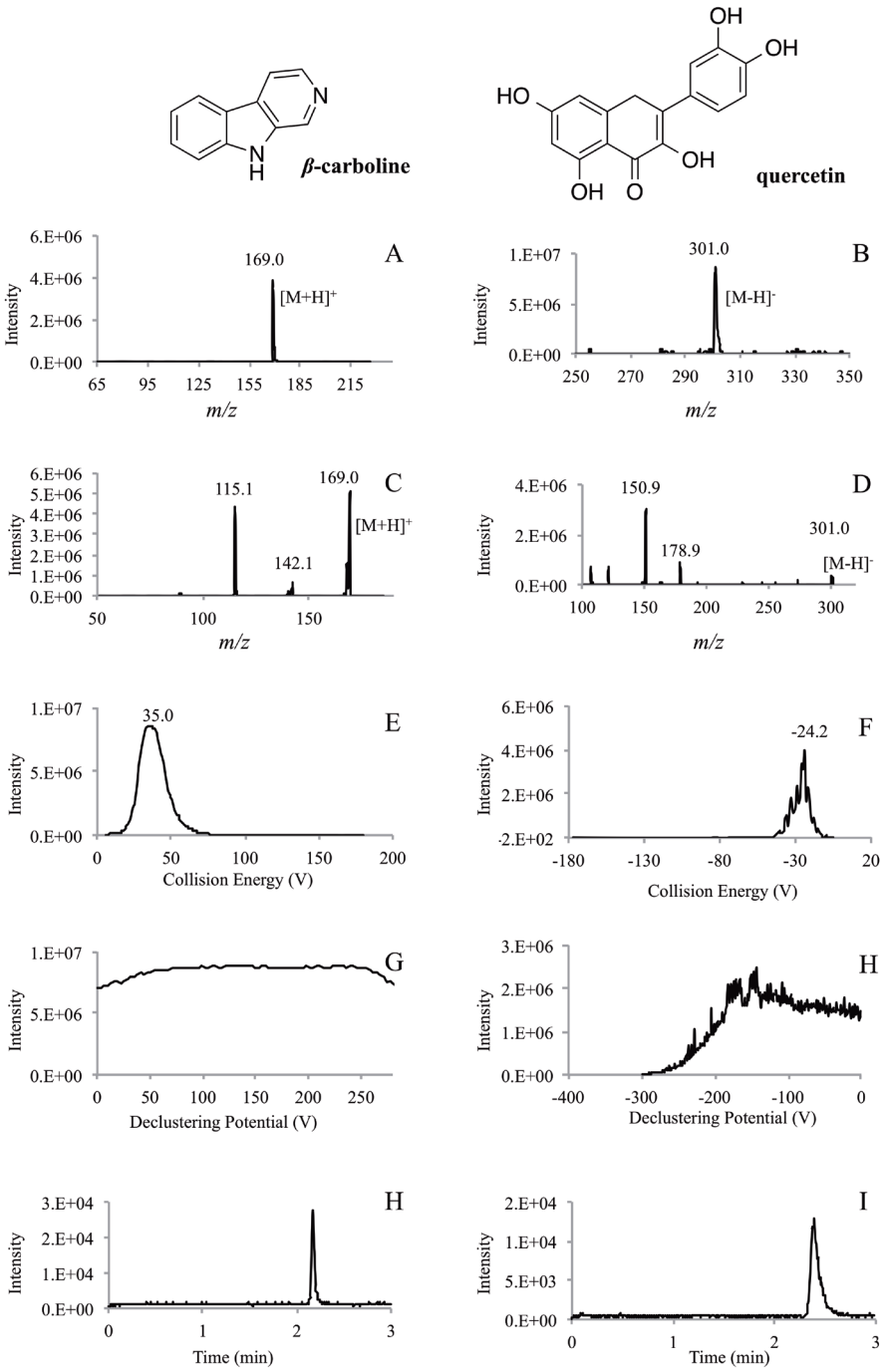

Figure 1. The MS spectra of β-carboline (A) and quercetin (B). MS-MS spectra of β-carboline **(C)** and quercetin **(D)**, obtained at the collision energy of 5 V and − 20V, respectively. According to the spectra, the precursor ions to the product ions of m/z 169.0 → 115.1 for β-carboline, and m/z 301.0 → 150.9 for quercetin were selected for the MRM. E and G were used to modify the value of collision energy and declustering potential for the MRM quantitation of β-carboline, while F and H were for quercetin. Spectra H and I were the MRM ion chromatograms of the β-carboline and quercetin, using the method described in the Material and Methods.

Table 2. Calibration parameters. Linear dynamic range, coefficient of determination (R2), limit of quantification (LOQ), limit of detection (LOD), intra-day, inter-day (CV%), and recovery (%) obtained using solutions of standards and standards addition in *A. philoxeroides* samples

Compounds	Linearity (ng/mL)	Calibration curves	r^2	Inter-day CV (%)	Intra-day CV (%)	Recovery
β-Carboline	0.3 - 100	$Y = 1.01e^5 \bullet X + 5.56e^3$	0.999	8.1%	13.4%	98.2%
Quercetin	0.3 - 100	$Y = 2.34e^5 \bullet X - 2.15e^3$	0.999	6.7%	12.5%	101.5%

to the concentration. When exposed to ME at higher concentration, there was less apoptosis cells.

4. Discussion

It has been reported that alligator weed has numbers of active compounds, such as phytosterol, flavonoid, triterpenes compounds and so on. Based on various constituents, different extractives using different solvents exhibit multiple pharmacological activities such as antinociceptive, antihyperglycemic, antioxidant, anti-microbial activities and a-glucosidase inhibitory effects. Among those compounds, β-carboline and quercetin are of great interest due to their diverse biological activities (*7,8*). For this, we analyzed the important two active components present in the leaf extract (methanolic) of *A. philoxeroides* using LC-MS/MS. Besides, the cardioprotective effect of the leaf extract was also explored by MTT and Annexin V-FITC/PI staining assay. In these two experiments Dox was explored to induced cell apoptosis. Doxorubicin (DOX) is an anti-tumor agent that is widely used in clinical setting for cancer treatment. The application of DOX, however, is limited by its cardiac toxicity which can induce heart failure through an undefined mechanism. So H9c2 cells induced by Dox is commonly used to screen cardioprotective agents. The results demonstrated that ME had obvious protective effects against doxorubicin-mediated cytotoxicity. The mechanism might be that ME could decrease the cell apoptosis induced by DOX, which was illustrated in Annexin V-FITC/PI staining assay. And the protective effects were relevant to the concentration of ME. In our experiments, only β-carboline and quercetin were determined by LC-MS/MS, but other components in ME solution might also have protective effects, which still required validation.

Table 3. Content of β-carboline and quercetin in *A. philoxeroides* leaves (ng/mg dry weight ± SD) (quantified by LC-MS/MS). Values shown are means (± SD) based on triplicate measurements

Samples	Collected Date	β-carboline (μg/g ± SD)	Quercetin (μg/g ± SD)
AP01	Jul 15th	13.3 ± 1.2	52.6 ± 2.7
AP02	Jul 15th	16.7 ± 2.1	45.2 ± 3.4
AP03	Aug 15th	23.2 ± 3.5	47.1 ± 5.4
AP04	Aug 15th	19.6 ± 0.8	49.5 ± 1.6
AP05	Sep 15th	35.1 ± 4.3	62.7 ± 2.5
AP06	Sep 15th	36.5 ± 2.0	70.5 ± 6.3
AP07	Oct 15th	12.7 ± 6.3	22.3 ± 2.7
AP08	Oct 15th	14.3 ± 3.3	25.6 ± 4.3

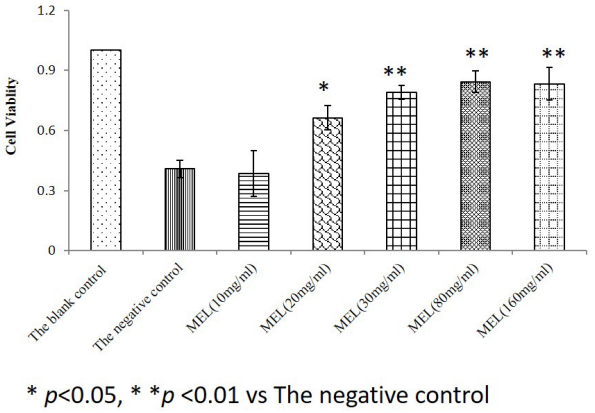

Figure 2. The cell viability results of ME exposed at different concentrations.

Acknowledgements

Financial supported from the Science and Technology Program of Shandong Province (2009GG10008014)

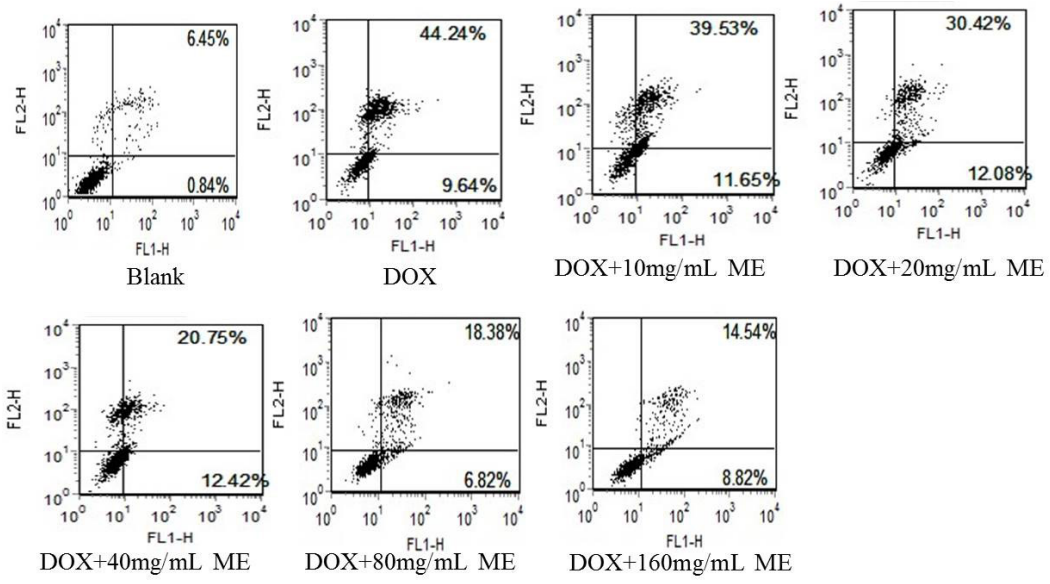

Figure 3. Flow cytometry analysis results illustrating cardioprotective effects of ME on H9c2 cells induced by Dox.

and The key research and development program of Shandong Province(2017GSF218049). We thank Xiao-Fei Wang for assistance with material collection.

References

1. Chen Y, Zhou Y, Yin TF, Liu CX, Luo FL. The invasive wetland plant *Alternanthera philoxeroides* shows a higher tolerance to waterlogging than its native congener *Alternanthera sessilis*. PLoS One. 2013; 11:e81456.
2. Khatun F, Zaman F, Mosaiab T, Mostafa F, Zaman M, Rehana F, Nasrin D, Jamal F, Nahar N, Rahmatullah M. Rahmatullah, M. Evaluation of antinociceptive and antihyperglycemic activities in methanol extracts of whole plants of *Alternanthera philoxeroides* (Mart.) Griseb. (Amaranthaceae) in mice. Pak J Pharm Sci. 2012; 25:583-587.
3. Bhattacherjee A, Ghosh T, Sil R, Datta A. Isolation and characterisation of methanol soluble fraction of *Alternanthera philoxeroides* (Mart.): evaluation of their antioxidant, α-glucosidase inhibitory and antimicrobial activity in *in vitro* systems. Nat Prod Res. 2014; 28:2199-2202.
4. Fang JB, Duan HQ, Zhang YW, Yoshihisa T. Chemical constituents from herb of Alternanthera philoxeroides. Zhongguo Zhong Yao Za Zhi. 2006; 31:1072-1075. (in Chinese)
5. Fang JB, Jia W, Gao WY, Yao Z, Teng J, Zhao AH, Duan HQ. Antitumor constituents from A*lternanthera philoxeroides*. J Asian Nat Prod Res. 2007; 9:511-515.
6. Fang JB, Yao Z, Chen JC, Liu YW, Takaishi Y, Duan HQ. Cytotoxic triterpene saponins from *Altenanthera philoxeroides*. J Asian Nat Prod Res. 2009; 11:261-266.
7. Cao R, Peng W, Wang Z, Xu A. beta-Carboline alkaloids: biochemical and pharmacological functions. Curr Med Chem. 2007; 14:479-500.
8. Chondrogianni N, Kapeta S, Chinou I, Vassilatou K, Papassideri I, Gonos ES. Anti-ageing and rejuvenating effects of quercetin. Exp Gerontol. 2010; 45:763-771.
9. Lipshultz SE, Lipsitz SR, Sallan SE, Dalton VM, Mone SM, Gelber RD, Colan SD. Chronic progressive cardiac dysfunction years after doxorubicin therapy for childhood acute lymphoblastic leukemia. J Clin Oncol. 2005; 23:2629-2636.
10. Bernard Y, Ribeiro N, Thuaud F, Türkeri G, Dirr R, Boulberdaa M, Nebigil CG, Désaubry L. Flavaglines alleviate doxorubicin cardiotoxicity: Implication of Hsp27. PLoS One. 2011; 6:e25302.
11. Mercolini L, Protti M, Saracino MA1, Mandrone M, Antognoni F, Poli F. Analytical profiling of bioactive phenolic compounds in argan (*Argania spinosa*) leaves by combined microextraction by packed sorbent (MEPS) and LC-DAD-MS/MS. Phytochem Anal. 2015; 27:41-49.
12. Della Corte A, Chitarrini G, Di Gangi IM, Masuero D, Soini E, Mattivi F, Vrhovsek U. A rapid LC-MS/MS method for quantitative profiling of fatty acids, sterols, glycerolipids, glycerophospholipids and sphingolipids in grapes. Talanta. 2015; 140:52-61.
13. Han X, Ren D, Fan P, Shen T, Lou H. Protective effects of naringenin-7-O-glucoside on doxorubicin-induced apoptosis in H9C2 cells. Eur J Pharmacol. 2008; 581:47-53.

(Received September 14, 2018; Revised December 22, 2018; Accepted December 29, 2018)

Original Article

DOI: 10.5582/ddt.2018.01082

Microparticles for sustained release of water-soluble drug based on a containment, dry coating technology

Akihiro Matsumoto, Akira Ono, Satoshi Murao, Masahiro Murakami*

Laboratory of Pharmaceutics, Faculty of Pharmacy, Osaka Ohtani University, Tondabayashi, Osaka, Japan.

Summary **Controlled release microparticles in a sub-gram-scale batch were fabricated using a ball mill, dry coating technique, to coat the water-soluble core material. This process also guaranteed the maintenance of the containment's integrity during the dry coating process. Quinine (average diameter, ca. 10 μm) and carnauba wax were used as the core and coating material, respectively. We evaluated the influence of process time, milling speed, and quinine-to-carnauba wax ratio on the particle size of the coated particles and their *in vitro* drug release profiles. Scanning electron microscopic observations suggested that the small wax particles attached to the core (quinine) particles resulted in a smooth film during the dry coating process. The size distribution of the coated particles agreed with the theoretically estimated size distribution. The *in vitro* release test demonstrated that the coated particles released quinine over 2 h in a biphasic mode. These results suggest that dry coating of microparticles less than 50 μm (D_{99}) is feasible on a several-grams-batch scale. This new ball mill-coating technique also enables a guaranteed containment, a prerequisite for the manufacturing of highly bioactive or biohazard substances.**

Keywords: Microsphere, mechanofusion, ball mill coating, small-batch production, controlled release

1. Introduction

A film coating technique is often used in the pharmaceutical industry to: 1) protect active ingredients from moisture, light, or oxygen, 2) improve the product's glossy appearance for marketing, or 3) control the dissolution of drugs from pharmaceutical formulations. The coating methods used in manufacturing medications are generally based on wet coating such as a fluidized bed coating and pan coating, where the coating material solution is sprayed on the surface of the core materials in this coating method.

There is a number of technical limitations in the coating process to be solved as an unmet need in the pharmaceutical field. One such limitation is the applicable size of core materials. With respect to conventional coating machines, over 100 μm of a particle size is generally required for use as a core material. Wurster fluid-bed technique has the advantage of film-coating small particles within the micrometer magnitude. However, even under an appropriate spray liquid flow rate, 20 to 50 μm microaggregates are produced with an associated yield of 60% (*1*). Thus, applying conventional coating methods to microparticles and nanoparticles have proven difficult.

Another limitation of the coating process is the ability to coat in a small scale. In the early stage of drug development, only a milligram order of the active ingredient under investigation is often available. However, most commonly used coating machines require several hundred grams per batch, at the very least. Therefore, formulation studies on controlled release preparations cannot be executed in practice when only a limited amount of the active compound is available. This prompts the need for small-scale manufacturing of highly active pharmaceutical ingredients such as nucleic acids or biomedicines.

Maintaining the integrity of the containment during the coating process is also an unmet need. In the wet coating process, solvents are removed by blow drying,

**Address correspondence to:*
Dr. Masahiro Murakami, Laboratory of Pharmaceutics, Faculty of Pharmacy, Osaka Ohtani University, 3-11-1 Nishikori-kita, Tondabayashi, Osaka 584-0854, Japan.
E-mail: murakm@osaka-ohtani.ac.jp

which may affect the containment's integrity. This inadequate containment may be associated with risks such as leakage of highly bioactive or biohazardous substances, and its exposure to these circumstances.

Mechanofusion is a surface modification method of powder (*2*). Researchers have investigated the mechanofusion method as a dry coating method to propose tentative advancements. These include improving the humidity resistance of magnesium powder (*3*), improving the aerosolization of drug powder through a reduction of the powder's intrinsic cohesion (*4*), improving the flow properties of bulk powder (*5,6*), and controlling the dissolution of a poorly water-soluble drug (*7,8*). According to a study (9), the five types of devices introduced for dry coating include mechanofusion, hybridizer, magnetically assisted impaction coater, rotating fluid bed coater and theta composer. Recently, Nobilta® and Nanocular® (Hosokawa Micron Corporation, Osaka, Japan) have become increasingly popular for dry coating on a small scale. Dry coating on a scale of approximately 10 g is possible using those machines (*4-8*).

Ordered mixing can be used for coating, where the surface of larger particles is loosely coated or covered with smaller particles (*9,10*). Micro- or nanoparticles tend to easily adhere to each other or attach to the surface of larger particles by van der Waals interaction and electrostatic force. This attachment forms aggregates or composite particles. In the field of pharmaceutical manufacturing, high-intensity mixers and grinding machines such as a ball mill, have generally been used for ordered mixing. The aggregates generated during the ordered mixing process can be broken down into primary particles using those machines (*10*). Therefore, the ordered mixing technique may have the advantage of coating microparticles to produce microcapsules below 100 μm, a current technical limitation in the applicable size of core material. However, this technique has not been applied practically, to the coating of materials prepared for controlled release. This lack of application is because of the difficulty in eliminating the gaps present between the attached particles found on the surface of core particles. In addition, exothermic effect is a known undesirable property of the machines. The exothermic heat generated by the collision of particles may affect the stability of the core active material, which may increase related compounds or change the crystalized form of the active material.

Such exothermic property of milling, however, may have the advantage of tight coating. Namely, the exothermic effect should promote the melting of guest particles to form a seamless film on the surface of a host particle (*11*). This indicates that the guest particles consisting of a material with a lower melting point can tightly bind or fuse with each other. This fusion may then be applied to the coating for a controlled drug release particle. In addition, among the high-intensity mixers and grinding machines, only ball milling machines can be operated under a closed condition. Thus, coating with a ball mill, if feasible, may guarantee the integrity of the containment when contained during the coating process.

In the present study, we assessed the feasibility of dry coating microcapsules that are less than 100 μm, used for controlled drug release and created using the ball mill technique. Quinine hydrochloride (m.p., ca. 115ºC) was used as the water-soluble core particle, and was pulverized to microcrystals with an average diameter of approximately 10 μm (the host particle). Carnauba wax (m.p., ca. 85ºC), a common inactive pharmaceutical ingredient, was used as the hydrophobic coating material (the guest particle).

2. Materials and Methods

2.1. *Materials*

Carnauba wax (density, 0.99 g/cm^3) was purchased from Alfa Aesar (Lancashire, UK) while quinine hydrochloride 2-hydrate (quinine) (density, 1.27 g/cm^3) was purchased from Nakarai tesque (Kyoto, Japan). All other chemicals used were of reagent grade.

2.2. *Pulverizing quinine*

Three-hundred milligrams of quinine was pulverized by a planetary mill (pulverisette6, FRITSCH GmbH, Germany) using the ball mill pot (ϕ 40 mm; H 40 mm) with 4 balls (ϕ 10 mm). The ball milling rotated at 250 rpm for 2 h to prepare the pulverized quinine particles.

2.3. *Dry coating by the ball milling method*

The 250-300 mg mixture of pulverized quinine particles (ca. 10 μm) and carnauba wax (ca. 40 μm) was applied to an agate ball mill pot (ϕ 40 mm; H 40 mm) with 4 balls (ϕ 10 mm). The ball mill was then rotated at 22-23ºC using the planetary mill (pulverisette6, FRITSCH GmbH, Germany).

2.4. *Microscopic observations*

The coated samples obtained were observed using a scanning electron microscope (SEM) (JSM-5500LV, JOEL Ltd., Tokyo, Japan). To evaluate aggregation, the coated particles were dispersed in 0.05% Tween 80 aqueous solution, filtrated by 0.22-μm membrane filter and dried on the filter for 2 h at 22-23ºC. The collected particles on the filter were used as samples. Cross sections of the samples were obtained by cutting using a razor. Samples for SEM observation were prepared by depositing gold-palladium at 15 mA for 3 min (Quick Auto Coater JFC-1500, JOEL Ltd.).

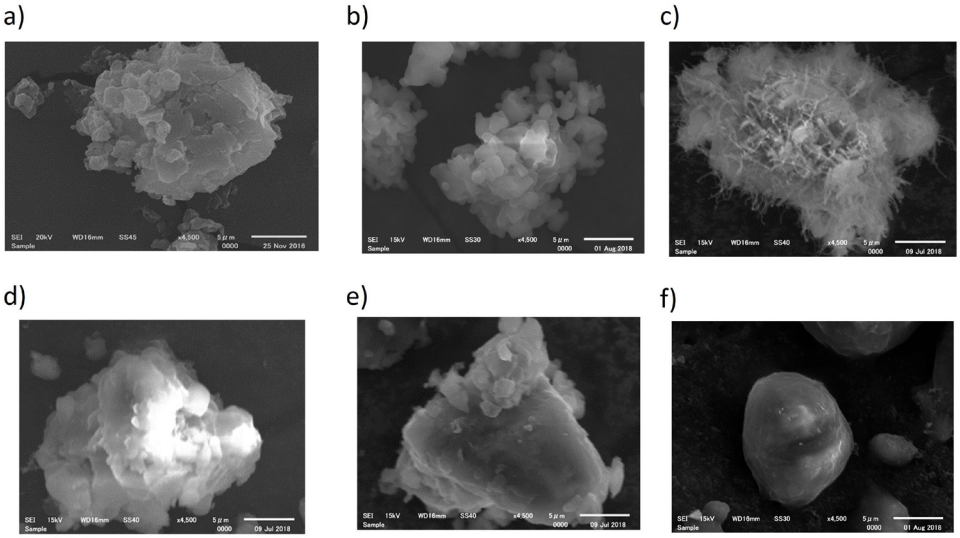

Figure 1. Scanning electron micrographs of the pulverized quinine and the coated particles. a) 2 h-pulverized quinine particles, **b)** 8 h-pulverized quinine particles, and the quinine and carnauba wax (1:1) coated particles prepared at 250 rpm for **c)** 0.5 h, **d)** 3 h, e) 6 h, and **f)** 12 h. Morphology changed during the dry coating process was demonstrated.

2.5. *Differential scanning calorimetry (DSC) analysis*

The particles (2 mg) were analyzed using DSC (DSC-60; Shimadzu Co., Ltd.) under N_2 gas (50 mL/min). The temperature rising speed was 20ºC/min.

2.6. *Determination of particle size*

The size of the pulverized quinine particles and coated particles was determined as a volume-based diameter using a laser diffraction particle size analyzer (SALD-2200, Shimadzu Co. Ltd., Kyoto, Japan). For the dispersion medium, soybean oil-hexane (1:2) and 0.05% Tween 80 aqueous solution were used as the dispersion media for the pulverized quinine and the coated particles, respectively. The size was measured within 1 min after the addition of the dispersion medium. To determine the volume-based diameter of carnauba wax in the coated particles, quinine was washed out of the coated particles through a 3 h incubation in the dispersion medium at 37ºC. The theoretical size of the coated particles was calculated using the following equation that is based on the hypothesis that the quinine particle were coated as the primary particle:

$$\text{Theoretical size } (D_x) = d_x \left[(W_1/\rho_1 + W_2/\rho_2)\right]^{1/3}$$

where D_x and d_x is diameter of coated particles and pulverized quinine microcrystals at the X% of cumulative distribution, respectively. W_1 and W_2 is weight of pulverized quinine and carnauba wax, respectively. ρ_1 and ρ_2 is the density of pulverized quinine and carnauba wax, respectively.

2.7. *In vitro dissolution test*

The dissolution test was performed in triplicate for each batch using the paddle method of the JP dissolution test. Briefly, 0.05% Tween 80 aqueous solution (900 mL), which was degassed at 41ºC for 2 h prior to use, was stirred using a paddle at 50 rpm and 37 ± 0.5ºC, with 20-75 mg (5 mg as quinine hydrochloride 2-hydrate) of particles added to the medium. 1 mL of the medium was periodically collected at predetermined time intervals, followed by the addition of 1 mL of fresh medium during the dissolution test. For the assay of quinine concentration, 100 µL of 0.1 M HCl was added to 400 µL of each collected sample, and the concentration determined by the fluorescent method (Ex., 350 nm; Em., 450 nm) using a hybrid multimode microplate reader (Synergy H4; BioTek Instruments, Winooski, VT, USA).

3. Results

3.1. *Observed morphological changes in the coated particles during dry coating process*

To evaluate the influence of process time, the particles were observed with the SEM at different process times. The typical scanning electron micrographs are shown in Figure 1. For the pulverized quinine crystals, the surface changed from a scale-like shape (2 h, Figure 1a) to aggregates of small particles (8 h, Figure 1b) as the milling process progressed at 250 rpm. For the coated particles, the surface changed from an aggregate with small particles, to one with a smooth surface as the dry coating with quinine and carnauba wax (1:1) at a speed of 250 rpm (Figures 1c, 1d, 1e, 1f) progressed. Interestingly, the coated particles obtained when dry coating was performed once for 30 min with the wax, had a brush surface or a fibrous surface standing upright (Figure 1c). However, the particles became spherical with a rather smooth surface at 12 h (Figure 1f). The

SEM observation of the cross-section of the sample obtained by 12 h of dry coating (Figure 2), revealed that a layer existed around the core section, although the core or quinine crystal was not clear. Through the observation of the well-dispersed particles, the coated particles prepared at 250 rpm in a 1:1 ratio of quinine and carnauba wax were observed as primary particles despite the 6 h or 12 h process time (Figures 3a and 3b). However, the particles prepared at 500 rpm were aggregates of several coated particles (Figure 3c). The particles fabricated in a 1:4 ratio of quinine to carnauba wax at 250 rpm for 6 h, also resulted in aggregates (Figure 3d).

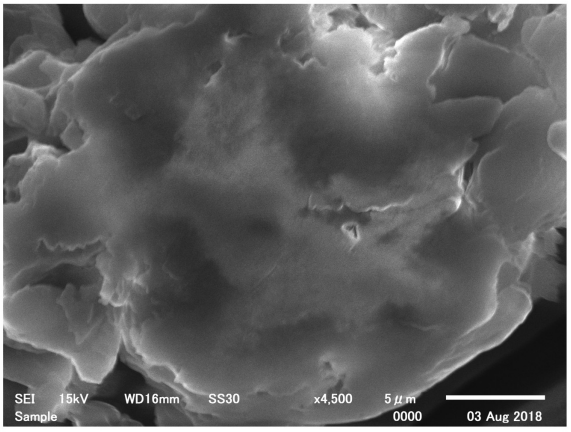

Figure 2. Scanning electron micrograph of the cross section of the coated particles. The coated particle of the quinine and carnauba wax (1:1) were prepared at 250 rpm for 12 h.

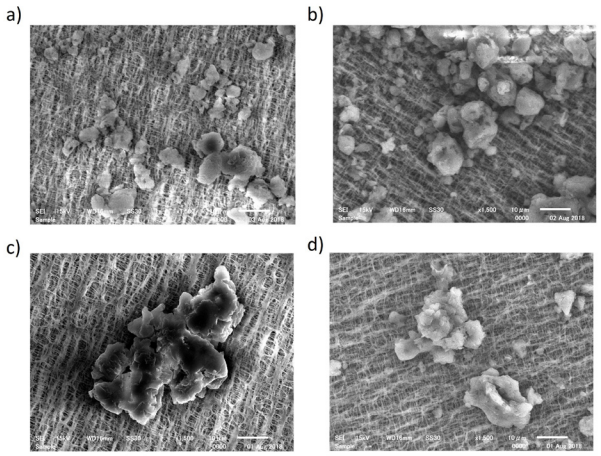

Figure 3. Scanning electron micrographs of the coated particles. The particles prepared by **a)** standard conditions, **b)** process time of 12h, **c)** milling speed of 500rpm, **d)** quinine-to-carnauba wax ratio of 1:4. The conditions of 1:1, 250 rpm, and 6 h for quinine/carnauba wax ratio, milling speed, and process time, respectively, were selected as the standard.

3.2. *Particle size of the coated particles*

The volume-based diameters of the coated particles prepared by the dry coating technique were evaluated using the laser diffraction particle size analyzer. Comparisons between the actual and theoretical diameters were made as shown in Table 1. The average diameter increased as the additive amount of the guest particles increased. For the dry coating process at 250 rpm, the actual average diameters were well in agreement with the theoretical average diameters for the 1:2 and 2:1 ratios of quinine to carnauba wax: this was not observed for the 1:4 ratio. In particular, the coated particles in the 1:1 ratio of quinine to carnauba wax showed that the actual cumulative size distribution was almost identical to the theoretical value (Table 1, Figure 4). With respect to the milling speed in the 1:1 mixture of quinine and carnauba wax, the actual average diameter of the particles prepared at 250 rpm was close to that of the theoretical value when processed for 6 h. Thus, the actual and theoretical average diameters observed were well in agreement after 3 h of processing (data not shown). However, the actual diameter of the coated particles prepared using the 6 h processing time at 100 rpm and 500 rpm was found to be larger than the theoretical values for the identical time. In the later study, the dry coating speed of 250 rpm, process time of 6 h, and the 1:1 ratio of quinine and carnauba wax were selected as the standard conditions.

Quinine as the core material was removed from the coated particles to evaluate the change in size of carnauba wax during the dry coating process. The mean

Table 1. Comparisons between actual and theoretical particle sizes of the coated particles

Quinine/ carbauna wax	Dry-coating condition	Particles size (μm)							
		Mean		D_{25}		D_{50}		D_{75}	
		actual	theoretical	actual	theoretical	actual	theoretical	actual	theoretical
1/1	250 rpm, 6hr	11.8 ± 2.5	12.3	6.7 ± 1.5	7.8	14.6 ± 2.9	15.0	25.0 ± 4.9	23.7
	100 rpm, 6hr	12.3 ± 1.2	12.3	5.0 ± 0.5	7.8	16.9 ± 1.8	15.0	33.0 ± 4.5	23.7
	500 rpm, 6hr	18.4 ± 4.8	12.3	12.8 ± 4.3	7.8	21.3 ± 4.5	15.0	31.6 ± 5.9	23.7
	250 rpm, 12hr	11.6 ± 1.3	12.3	6.9 ± 1.1	7.8	14.5 ± 1.6	15.0	23.8 ± 1.5	23.7
2/1	250 rpm, 6hr	10.9 ± 1.3	11.0	4.6 ± 0.6	7.0	11.0 ± 1.6	13.4	30.3 ± 7.2	21.2
1/2	250 rpm, 6hr	19.4 ± 2.0	14.2	12.1 ± 1.2	9.0	22.9 ± 1.5	17.4	37.8 ± 2.8	27.5
1/4	250 rpm, 6hr	26.1 ± 3.1	17.1	16.5 ± 1.8	10.8	29.4 ± 3.0	20.8	48.9 ± 5.4	33.0
Pulverized quinine		10.1 ± 1.9	-	6.4 ± 1.5	-	12.3 ± 2.8	-	19.5 ± 3.4	-

Data represents mean ± S.D. (n = 3 batchs).

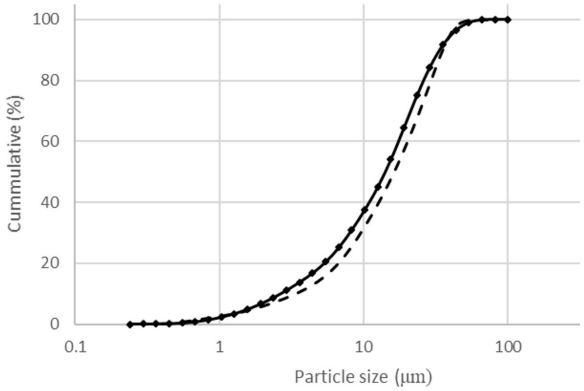

Figure 4. Cumulative particle size distribution of the typical coated particles. The solid and dot lines express the actual size and theoretical size distribution, respectively. The coated particles were prepared by the condition: quinine/carnauba wax ratio 1:1, milling speed 250 rpm, process time 12 h.

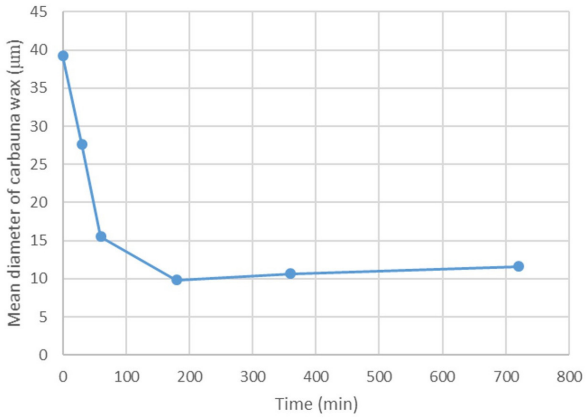

Figure 5. Change in size of carnauba wax particles during the dry coating process. Quinine-to-carnauba wax ratio and milling speed were 1:1 and 250 rpm, respectively.

particle size of the carnauba wax particles decreased while the dry coating process progressed and plateaued at 3 h (Figure 5).

3.3. *DSC analysis of coated particles*

DSC analysis was used to examine the influence of the dry coating process on the thermodynamic properties of carnauba wax and quinine. For the coated particles, the melting point derived from carnauba wax shifted higher while that of quinine experienced a lower shift than that of carnauba wax (Figure 6).

3.4. *In vitro drug release from the coated particles*

The release of quinine from the coated particles is shown in Figure 7. As the process advanced, the initial release at 10 min decreased and the duration of release extended from 10 min to 2 h (Figure 7a). Although up to 95% of the pulverized quinine was dissolved within 5 min, the quinine released from the coated particles obtained by the 12 h processing time, lasted over 2 h.

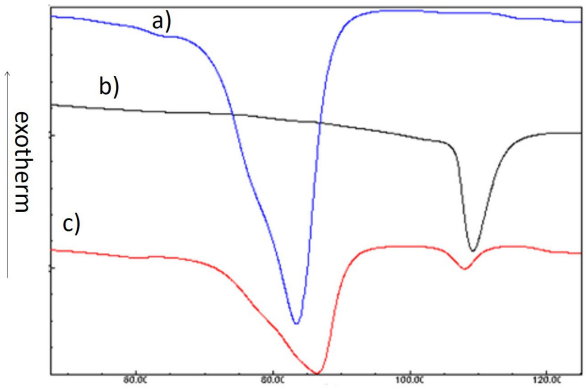

Figure 6. DSC charts. a) carnauba wax, **b)** quinine, **c)** the coated particles perepared by the standard condition: quinine/carnauba wax ratio 1:1, milling speed 250 rpm, process time 6 h.

The analysis conducted by liner fitting indicated that the release of quinine from the coated particles was biphasic (Figure 7b). The particles prepared at 100 and 250 rpm showed similar drug release profiles in the release of approximately 80% of quinine within the initial 30 min. However, the particles prepared at 500 rpm showed a slower drug release, where 80% of quinine was released in 1.5 h (Figure 7c). The influence of the ratio of quinine and carnauba wax on drug release, was evaluated on the coated particles fabricated at the 6 h processing time at 250 rpm. Initial release at 10 min decreased as the amount of carnauba wax increased. However, the initial release plateaued around 50-60% release of the prepared coated particles when the amount of carnauba wax was more than that of quinine (Figure 7d).

4. Discussion

Before we performed the dry coating of quinine by carnauba wax, we selected quinine microcrystals as core particles that were pulverized to a mean diameter of approximate 10 μm, as this size is considered the lower critical limit of pulverization. Dry grinding with a ball mill is a popular technique used in the pharmaceutical industry; however, a lower critical particle size can be achieved through pulverization. In general, it is difficult to reduce particle size below 10 μm by dry milling. This is explained by several theories in terms of the energy for pulverization. For example, according to the theory by Bond (*12*), the energy for pulverizing powder is calculated using the following equation:

$$E = C_B\,(1/\sqrt{x2} - 1/\sqrt{x1})$$

where E is the net specific energy, C_B is a constant, and $x1$ and $x2$ are the feed and pulverized size (D_{80}), respectively. This equation indicates that more energy is required when the particle size gets smaller. Moreover, the lower critical size in pulverizing is explained by

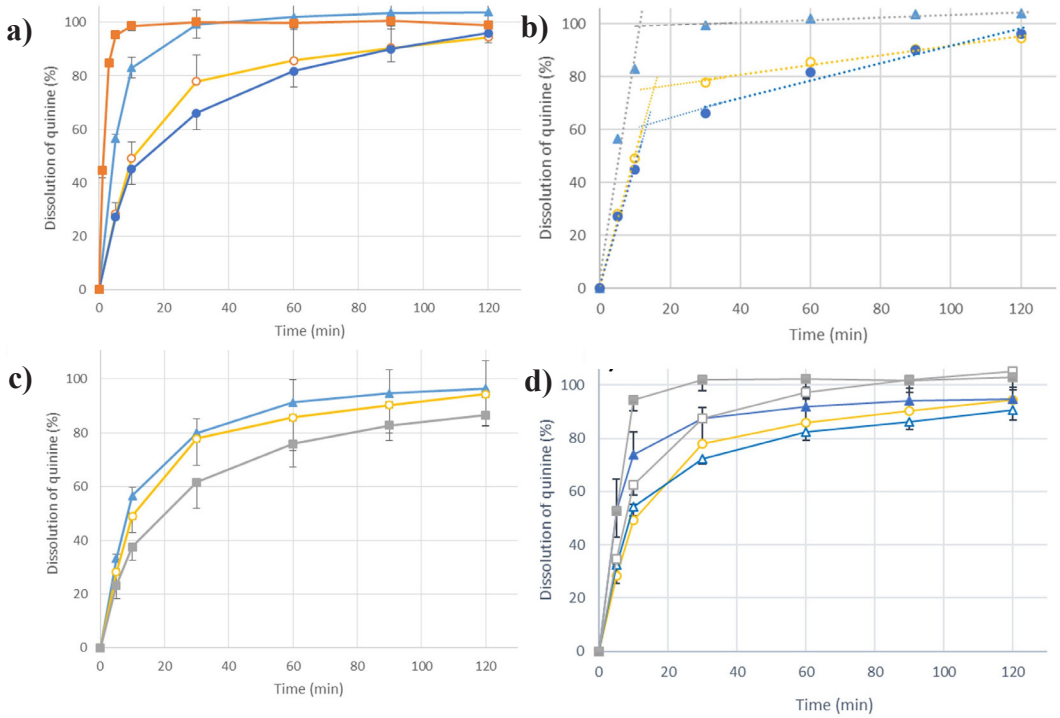

Figure 7. ***In vitro*** **dissolution of quinine from the coated particles.** Effect of the process time on **a)** *in vitro* dissolution profiles and **b)** liner fitting: ■ 0 h (pulverized quinine), ▲ 0.5 h, ○ 6 h, and ● 12 h. **c)** Effect of milling speed on in vitro dissolution profiles: ▲100 rpm, ○ 250 rpm, and ■ 500 rpm. **d)** Effect of quinine-to-carnauba wax ratio on *in vitro* dissolution profiles: ▲4:1, ■ 2:1, ○ 1:1, □ 1:2, and Δ 1:4. The standard conditions were 1:1, 250 rpm, and 6 h for quinine/carnauba wax ratio, milling speed, and process time, respectively. Data represents the means ± S.E. for 3 batches.

the relationship between hardness and size of particles. The hardness of a particle is related to the magnitude of the crack in the particle (*13*), which is considered to be decreased when the particle size is reduced. Thus, more energy is required for pulverization along with a smaller size of particles. Besides the selection of the core particle size, we also chose a moderate milling speed (250 rpm as the standard speed) for the dry coating process so that the reduction in particle size of the core particles would not proceed during the dry coating process. To confirm no reduction of the core particle size, we examined the influence of the pulverization time on the quinine particle size at 250 rpm. When only the quinine particles were pulverized for 8 h, the particles were larger in size than those obtained through 2 h of pulverization (10.1 ± 1.9 µm and 20.8 ± 6.4 µm for the 2 h and 8 h process, respectively; the mean particle size ± S.D. for 3 batches). Considering the SEM image shown in Figure 1b, the increase in the particle size of quinine by the 8 h pulverization may be due to the formation of aggregates. Consequently, the size of cores particle was considered not to reduce during the dry coating process. So, when the dry coating with the pulverized quinine and carnauba wax was performed, it was suggested that the carnauba wax may be dominantly pulverized in the 6 h dry coating process, which had in advance, a 2 h pulverization process.

Under the condition that the size of the core particles (10 µm quinine) would not reduce, we performed the dry coating by 40 µm carnauba wax. The dry coating technology used in the present study is related to mechanofusion, which is mainly used for modifying the surface of particles. For the conventional mechanofusion and dry coating procedures reported, smaller particles were used as guest particles and larger particles as host particles (*3,7,9,14*). In this study, quinine particles used as host particles were smaller than the carnauba wax particles that were used as guest particles to result in the achievement of dry coating. The possible explanation for the conflict is related to the size reduction in carnauba wax during the dry coating process. Since the host quinine particles had a mean particle size similar to the minimum critical particle size obtainable by pulverization, carnauba wax particles may dominantly be milled to become finer particles during the coating process as indicated above. This selected pulverization provides a high surface energy to carnauba wax particles by engendering new surfaces and showing the tendency to attach to other particles. The generated small particles of carnauba wax were gathered with quinine particles and melted to incorporate the quinine particles. This is supported by the electron microscopic observation, where most of the particles changed in morphology from a composite with small particles, to a particle with a smooth surface as the process of dry coating proceeded. The echinoid-shaped particles were produced by the initial 30 min coating, which may have been formed when the

carnauba wax particles were teared off by milling. The production of echinoid-shaped particles may enhance further aggregation of particles by increasing the surface area. Particles forming a composite could not be clearly identified in the microscopic observation (neither carnauba wax nor quinine), although the observation of the cross section suggested this recognition.

To prove the coating of a quinine particle with carnauba wax, we evaluated the particle size distribution and drug release profiles of the coated particles. In the dry coating process, the coated particles decreased in particle size down to the theoretical diameter in the 3 h required to reach a plateau. Similar tendency was observed on the guests obtained when quinine was washed out of the coated particles. Therefore, the observed size reduction is considered to be of carnauba wax. This observation supports that the coating process may proceed with the progress of pulverization of the carnauba wax as mentioned above. Therefore, by the inadequate pulverization of carnauba wax, the actual particle size of all particles including coated particle, quinine and carnauba wax was therefore larger than that of the theoretical size in the early period of the process. This is seen to hold true for other coated particles prepared at a low milling speed. Indeed, the dry coating at 100 rpm produced coated particles with relatively larger sizes, especially in D_{75}. On the other hand, the average diameter of the particles obtained at 500 rpm was found to have a value twice that of the theoretical value. This is not due to inadequate pulverization. This is explained by assuming that the milling at 500 rpm gave rise to excess energy for coating the particles, which may be used to aggregate the coated particles as shown in Figure 3. Thus, it was indicated that 250 rpm is the optimal milling speed to obtain primary coated particles. The volume-based particle sizes, D_{25}, D_{50}, and D_{75}, of the coated particles prepared by 6 or 12 h of dry coating with quinine and carnauba wax (1:1) at 250 rpm, were close to the theoretical values estimated by assuming that the particles were primary particles. In addition, the size distribution of the particles obtained by the 12 h dry coating period coincided with the theoretical size distribution. On the other hand, when the ratio of quinine to carnauba wax was 1:4, the average diameter of the obtained coated particles was larger than the average theoretical diameter. This is probably due to the production of aggregates, judging from the observation of the dispersed particles (Figure 3). This indicates that there are optimum conditions in terms of the host-to-guest ratio and milling speed, to obtain primary particles. For quinine and carnauba wax, the optimum ratio at 250 rpm was found to exist between 2:1 and 1:2.

We then evaluated the influence of process time, coating speed and ratio of host and guest materials on *in vitro* quinine release from the coated particles. With increased processing time, a longer drug release was sustained with a suppressed initial release. The influence of the process time on the drug release can also be explained by the morphological changes of particles shown in Figures 1c-1f. It was indicated that the attachment of only intact, small guest particles (Figure 1c) cannot control drug release as there are gaps between the adhered wax particles; even as close-packed spherical particles provide approximately 0.26% of porosity. The attachment of guest particles on the host particles may be based on the steric repulsive force among the guest particles, besides the attractive force between the host and guest particles. This steric repulsive force prevents close-packing. Changing the shape of the attached particles for controlled drug release is also essential. It was reported that heating melts the adhered particles resulting in the formation of a smooth layer (*15*). For the dry coating process using an electric mortar and a powder surface reforming system, it was reported that a change in shape of the adhering particles is observed as a relaxation process takes place during process progression (*16*). In this study, we observed the changing of the adhered particles (Figure 1c) to the smooth layer (Figures 1d-1f) with process progression. One of the important factors in morphological changes during the process is the melting points of the guest and host particles. Melting points of the guest and host particles used in this study were approximately 85ºC and 115ºC, respectively. Considering that the original quinine particles were not clearly observed in the cross section of the coated particles (Figure 2), carnauba wax and quinine are considered to melt during the dry coating process. The DSC analysis attributed the thermal peaks of the coated particles, to the melting of carnauba wax and quinine. This indicates that quinine exists as a crystallized structure, but may interact with carnauba wax during the dry coating process.

The coated particle obtained at 500 rpm showed a slower release than those obtained at 100 and 250 rpm. Although the dry coating at 500 rpm gave rise to aggregates, the coated particles consisted of quinine and carnauba wax in the ratio, 1:4 at 250 rpm also gave rise to aggregates. These aggregates showed a similar release of quinine particles to those in the 1:1 ratio at 250 rpm, which were suggested to exist as primary particles. The aggregation of the coated particles cannot completely account for the slower release of the coated particles at the 500 rpm. Considering the degree of compaction in a coating layer, the magnitude of the milling speed may affect the coating layer more than the amount of coating material.

It is well-known that drug release through a water-insoluble membrane shows the zero-order pattern. A model proposed by Chien (*17*) has been commonly accepted as a mechanism of drug release by hydrophobic polymer coating particles. Drug molecules underlying the shell of a capsule, left the crystal to penetrate the

polymer wall by a partitioning phenomenon, diffuse through the wall using a driving force that differs in concentration across the wall, dissolve in the solution surrounding the capsule to form saturated and diffusion phases, prior to dispersal in the bulk solution. A modified model proposed by Ito *et al*. (*18*) takes it into consideration the medium penetrating through the coating layer to the core compartment of a capsule, followed by dissolving of the crystallized drug in the core prior to drug release. Drug release from the matrix formulation is proportional to the square of time. In this study, the drug release from the coated particles did not fit a matrix-type kinetic, as it was not proportional to the square of time. This suggests that the particles obtained were not of the matrix type. Although the release did not show zero-order kinetics, biphasic kinetics which involves a zero-order pattern was observed. A decrease in the release in the early phase was observed while the latter phase increased along with the extension period of the dry coating process. This suggests that the coating layer may have two regions of diffusion: a leaky and rigid region, and that a leaky region may be present within the gaps between the guest particles. The leaky region reduces as guest particles bind tighter to each other during the progression of dry coating.

In conclusion, controlled release coating of quinine microcrystals less than 50 μm with carnauba wax was achieved by the ball mill dry coating method. The method selected may avoid the lower size limitation of coating, in the pharmaceutical manufacturing. In addition, the ball milling technique guaranteed that the integrity of the containment is maintained when contained during the dry coating process. Thus, our method may be useful in coating highly bioactive substances that may present a variety of risks when exposed to the environment. Through the use of a dry coating technology with a ball mill, we are proposing that this method may provide a breakthrough solution in the manufacture of controlled release microparticles that undergo contained conditions. Application of nano-order particles should be investigated in a future study.

Acknowledgements

We would like to thank Ms. Kayoko Murakami for her technical assistance and CBC Co., Ltd., for its financial support of this study. We are also grateful to Editage (*www.editage.jp*) for English language editing.

References

1. Ichikawa H, Fukumori Y. Microagglomeration of pulverized pharmaceutical powders using the Wurster process I. Preparation of highly drug-incorporated, subsieve-sized core particles for subsequent microencapsulation by film-coating. Int J Pharm. 1999; 180:195-210.
2. Chen W, Dave R, Pfeffer R, Walton O. Numerical simulation of mechanofusion system. Powder technol. 2004; 146:121-136.
3. Mujumdar A, Wei D, Dave RN, Pfeffer R, Wu C. Improvement of humidity resistance of magnesium powder using dry particle coating. Powder Technol. 2004; 140:86-97.
4. Zhou QT, Qu L, Larson I, Stewart PJ, Morton DAV. Improving aerosolization of drug powders by reducing powder intrinsic cohesion *via* a mechanical dry coating approach. Int J Pharm. 2010; 394:50-59.
5. Zhou QT, Qu L, Gengenbach T, Denman JA, Larson I, Stewart PJ, Morton DAV. Investigation of the extent of surface coating *via* mechnofusion with varying additives levels and the influences on bulk powder flow properties. Int J Pharm. 2011; 413:36-43.
6. Zhou QT, Qu L, Larson I, Stewart PJ, Morton DAV. Effect of mechanical dry particle coating on the improvement of powder flowability for lactose monohydrate: A model cohesive pharmaceutical powder. Powder Technol. 2011; 207:414-421.
7. Hoashi Y, Tozuka Y, Takeuch H. Solventless dry powder coating for sustained drug release using mechanochemical treatment based on the tri-component system of acetaminophen, carnauba wax and glidant. Drug Devel Ind Pharm. 2013; 39:259-265.
8. Tay T, Morton DAV, Gengenbach TR, Stewart PJ. Dissolution of a poorly water-soluble drug dry coated with magnesium and sodium stearate. Eur J Pharm Biopharm. 2012; 80:443-452.
9. Pfeffer R, Dave RN, Wei D, Ramlakhan M. Synthesis of engineered particles with tailored properties using dry particle coating. Powder Tech. 2001; 117:40-67.
10. Hersey JA. Ordered mixing: A new concept in powder mixing practice. Powder Technol. 1975; 11:41-44.
11. Yeung CC, Hersey JA. Ordered powder mixing of coarse and fine particulate systems, Powder Technol. 1979; 22:127-131.
12. Bond FC. The third theory of comminution. Trans. AIME. 1952; 193:484-494.
13. Epstein B. Statistical aspects of fracture problems. J Appl Phys. 1948; 19:140-147.
14. Alonso M, Satoh M, Miyanami K. Mechanism of the combined coating-mechanofusion processing of powders. Powder Technol. 1989; 59:45-52.
15. Pearnchob N, Bodmeier R. Dry powder coating of pellets with micronized Eudragit RS for extended drug release. Pharm Res. 2003; 12:1970-1976.
16. Ishizaka T, Honda H, Kikuchi Y, Ono K, Katano T, Koishi M. Preparation of drug-diluent hybrid powders by dry processing. J Pharm Pharmacol. 1989; 6:361-368.
17. Chien YW. Chapter 4 in Sustained and controlled Release drug delivery systems, 1978 (Robinson JR, ed.). Marcel Dekker, New York, p. 229.
18. Ito R, Golman B, Shinohara K. Controlled release with coating layer of permeable particles. J Control Release. 2003; 92:361-368.

(Received November 26, 2018; Revised December 25, 2018; Accepted December 28, 2018)

Original Article

DOI: 10.5582/ddt.2018.01063

Tissue-dependent induction of antimicrobial peptide genes after body wall injury in house fly (*Musca domestica*) larvae

Minako Andoh, Takayuki Ueno, Kiyoshi Kawasaki*

Faculty of Pharmaceutical Sciences, Doshisha Women's College of Liberal Arts, Kyotanabe, Kyoto, Japan.

Summary **Injury of the insect body wall, which enables environmental microorganisms to invade into insect tissues, induces innate immune responses including the induction of antimicrobial peptides (AMPs) in flies and silkworms. Here, house fly (*Musca domestica*) larvae and pupae were injured using a needle and the effects on the expression of genes encoding AMPs were examined. The expression of AMP genes including *defensin*, *attacin*, *diptericin*, and *sarcotoxin II* dramatically increased in both larvae and pupae after injury of the body wall, indicating that innate immune responses were induced. Furthermore, the injury-dependent expression of AMP genes was examined in larval tissues including fat bodies, hemocytes, salivary glands, and digestive tracts. Injury-dependent AMP gene expression was observed in salivary glands, hemocytes, and fat bodies, but not in digestive tracts. The degree of the transcriptional induction of each gene differed among tissues, suggesting that their expression is governed by complex regulatory machinery and that AMPs have tissue-specific functions. To further examine the properties of the AMPs, we examined the antimicrobial activities of partial synthetic peptides corresponding to portions of the predicted AMP proteins deduced from the AMP genes. A synthetic peptide exhibited antimicrobial activity, indicating that these injury-inducible genes are potential medicinal resources.**

Keywords: Antimicrobial peptide, innate immunity, house fly, larval tissue, insect

1. Introduction

Insects respond to microbial infections *via* the activation of an innate immune system consisting of germline-encoded sensor, signaling, and defense molecules including antimicrobial peptides (AMPs) (*1*). In insects including the flesh fly (*Sarcophaga peregrina*) and silkworm (*Bombyx mori*), innate immune responses including the induction of AMPs have been reported to be induced by injury of the body wall, which enables environmental microorganisms to invade into insect tissues (*2,3*). Additionally, we previously observed that antimicrobial activities were induced in the hemolymph of house fly (*Musca domestica*) larvae after injury (*4*). It has been shown that infectious inflammation signals induced by microbial components derived from microorganisms invaded through the injury sites and non-infectious inflammation signals induced by the physical damage due to the injury induce expression of AMPs in *Drosophila melanogaster* (*5-7*). In insects, the injury-dependent expression of AMPs has been reported to occur in the fat bodies, in which most of the intermediary metabolism takes place, including lipid and carbohydrate metabolism as in the mammalian liver (*8,9*). The recognition of invading microorganisms by sensor molecules induces the synthesis of AMPs, and the AMPs secreted into the hemolymph play an essential role in inhibiting the growth of invading microorganisms (*10*). Furthermore, the excretions or secretions of medicinal maggots of the blowfly (*Lucilia sericata*) contain AMPs in the absence of injury or bacterial invasion (*11*). These observations suggest that some flies express inducible and constitutive AMPs, and the defense system of flies can be established by various AMPs that are expressed constitutively or injury-dependently in a tissue-specific manner.

AMPs contain a region of positively-charged amino acids that specifically bind to negatively-

**Address correspondence to:*
Dr. Kiyoshi Kawasaki, Faculty of Pharmaceutical Sciences, Doshisha Women's College, Kodo, Kyotanabe, Kyoto 610-0395, Japan.
E-mail: kkawasak@dwc.doshisha.ac.jp

charged microbial surface molecules such as bacterial lipopolysaccharide (*12-14*). This interaction disrupts the microbial membrane and leads to cell lysis and/or cell death (*15-17*). In addition to the general characteristics of AMPs, insect AMPs possess certain structural features, and they are classified into four families based on their structures. These four families are cysteine-rich peptides (such as defensin and drosomycin), glycine-rich peptides/proteins (such as attacin, sarcotoxin II, and diptericin), α-helical peptides (such as cecropin and sarcotoxin I) and proline-rich peptides (such as drosocin) (*18,19*).

AMPs are a novel class of antibiotics because of their broad-spectrum antimicrobial activities and their low tendency to induce resistance in microbes (*20*). Chemically synthesized AMPs have been developed based on the amino acid sequences of insect AMPs. For example, the synthetic peptide KLKLLLLLKLK-NH_2, which was developed from the *S. peregrina* AMP sapecin B, exhibits broad-spectrum antimicrobial activities (*21*). Furthermore, the same synthetic peptide synthesized using D-amino acids displayed a higher antimicrobial activity than its L-form counterpart (*22,23*). The potential utility of AMPs as an adjuvant has been examined because of their activity to induce immune responses in mammals (*24-26*). These observations demonstrate the importance of natural AMPs as medicinal resources.

The house fly (*M. domestica*) genome encodes a larger number of AMPs than any other dipteran genome (*27*). Thus, we expected that the AMPs encoded by the *M. domestica* genome are potential medicinal resources. In this study, we examined the properties of AMP genes in *M. domestica*. Particularly, we focused on the larval tissue-dependent induction of AMP genes.

2. Materials and Methods

2.1. *Reagents*

Dimethyl sulfoxide and bovine serum albumin (fraction V) were purchased from Sigma-Aldrich (St. Louis, MO, USA). AMPs were commercially synthesized by Toray Research Center (Tokyo, Japan). The C-terminal of each synthetic peptide was modified by amidation. All peptides were initially solubilized in dimethyl sulfoxide and then used for the analysis.

2.2. *Injury of fly larvae and pupae, and collection of tissues from injured larvae*

Non-sterile third-instar larvae of *M. domestica* provided by E's, Inc. (Tokyo, Japan) were injured by inserting the tip of a stainless steel hypodermic needle (Dentronics, Tokyo, Japan) into the abdominal cavity. The injured larvae were incubated in contact with insect saline solution (130 mM NaCl, 5 mM KCl, and 1 mM $CaCl_2$) in plastic containers at 30°C for the indicated times. As an experimental control, intact larvae were also incubated in the same manner as described above.

To analyze gene expression in the whole body, injured larvae were directly stored in a tube at −80°C. For the analysis of gene expression in tissues, the fat bodies, salivary glands, and digestive tracts were dissected from larval bodies using fine tweezers and a surgical knife under a binocular microscope following anesthesia on ice. In this study, we defined the digestive tract as the alimentary canal from mouth to anus with the caecum of ventriculus and Malpighian tubule. The dissection was performed based on a previously published anatomical drawing of *M. domestica* larvae (*28*). To collect hemocytes, hemolymph was collected in a tube on ice by cutting off the anterior tip of the larvae using fine scissors. Hemocytes were then collected by the centrifugation of hemolymph at 4°C for 10 min at 2,000 × g. The collected tissues were stored at −80°C until use.

To collect pupae, third-instar larvae were incubated with gauze in plastic containers containing insect saline solution at 30°C until pupation. At 20-24 h after pupation, the pupae were injured using a stainless steel hypodermic needle and incubated for a further 20-24 h at 30°C in plastic containers. As an experimental control, intact pupae were also incubated in the same manner. After incubation, the pupae were stored at –80°C.

2.3. *RNA extraction and synthesis of first-strand cDNA*

Total RNA was extracted from larval whole bodies, fat bodies, hemocytes, digestive tracts, salivary glands, and pupal whole bodies using a MagExtractor™ nucleic acid purification kit (TOYOBO, Osaka, Japan) according to the manufacturer's protocol. Total RNA was then treated with DNase I (TaKaRa Bio, Kusatsu, Japan) as previously described (*29*) and was reverse-transcribed using a PrimeScript™ RT reagent kit (TaKaRa Bio) with oligo(dT) primers and random hexamer primers according to the manufacturer's protocol.

2.4. *Real-time polymerase chain reaction (PCR)*

Real-time PCR was performed with a LuminoCt™ SYBR® Green qPCR ready mix (Sigma-Aldrich) using an Eco™ real-time PCR system (Illumina, San Diego, CA, USA) according to the manufacturer's protocol. Primers were synthesized by FASMAC (Atsugi, Japan) or Nippon Gene (Tokyo, Japan). The primer sequences are listed in Table S1 (*http://www.ddtjournal.com/action/getSupplementalData.php?ID=36*). The optimized thermal cycler settings for the PCR reactions were as follows: initial denaturation at 95°C for 20 s, followed by 45 amplification cycles of denaturation (95°C for 5 s) and annealing/extension. The annealing/extension conditions used are indicated in Table S1. The amount

of transcript was normalized to that of *glyceraldehyde-3-phosphate dehydrogenase (gapdh) or ribosomal protein 18 (rps18)* (*30*).

2.5. *Droplet digital PCR (ddPCR)*

The ddPCR procedure was performed using a QX100™ droplet digital PCR system (Bio-Rad Laboratories, Hercules, CA, USA). The reaction mixture (20 µL) containing 1 × ddPCR supermix for probes (Bio-Rad Laboratories), 900 nM primers, 250 nM hydrolysis probe, and sample cDNA was loaded into a DG8 cartridge (Bio-Rad Laboratories) together with 70 µL of droplet generator oil (Bio-Rad Laboratories). Then, a cartridge was loaded into the QX100™ droplet generator (Bio-Rad Laboratories) to generate PCR droplets. The droplets were then transferred to a 96-well PCR plate (Eppendorf, Hamburg, Germany). PCR thermal cycling was performed using a C1000 Touch™ thermal cycler (Bio-Rad Laboratories) as follows: initial incubation at 95°C for 10 min, 40 cycles of 94°C for 30 s and 60°C for 60 s, followed by a final incubation at 98°C for 10 min and holding at 12°C. After reaction, the droplets from each well of the plate were read using a QX100™ droplet reader (Bio-Rad Laboratories). The quantification data were analyzed with the QuantaSoft™ analysis software (Bio-Rad Laboratories). PCR primers and a hydrolysis probe, whose sequences are listed in Table S2 (*http://www.ddtjournal.com/action/getSupplementalData.php?ID=36*), were designed and synthesized by TaKaRa Bio. The hydrolysis probe was labeled with carboxyfluorescein at the 5′ end and Black Hole Quencher® 1 at the 3′ end.

2.6. *Primer design for real-time PCR and ddPCR*

Primers for the amplification of transcripts by real-time PCR or ddPCR were designed based on the house fly genome sequence in the National Center for Biotechnology Information (NCBI) database. The sequences *LOC101887540*, *LOC101887872*, and *LOC101887709* were designated as *M. domestica defensin* genes. Six cysteine residues that are characteristic of the mature defensin peptide were conserved in the amino acid sequences of the proteins encoded by these genes, and a common potential cleavage signal (Lys-Arg) was found in each sequence (*31-33*) (Figure S1) (*http://www.ddtjournal.com/action/getSupplementalData.php?ID=36*). Primers for *defensin* were designed to amplify these genes (Table S1), since their nucleotide sequences were highly similar. Another three genes, namely *LOC101888225*, *LOC105261620*, and *LOC105261775*, were designated as *defensin-like 1*, *defensin-like 2*, and *defensin-like 3*, respectively. The conserved cleavage signal (Lys-Arg) was not found in their amino acid sequences, but the characteristic six cysteine residues were conserved in the genes (Figure S1). Primers were designed to simultaneously amplify both *defensin-like 1* and *defensin-like 2* (Table S1) because of their similar sequences. A further four genes, namely *LOC101893190*, *LOC101893350*, *LOC101893688*, and *LOC101893852* were designated as *M. domestica sarcotoxin II*. A short proline-rich domain and two glycine-rich domains that are characteristic of *sarcotoxin II* were found in their amino acid sequences (Figure S2) (*http://www.ddtjournal.com/action/getSupplementalData.php?ID=36*) (*34-36*). Primers for *sarcotoxin II* were designed to amplify these four genes because of their close similarity. The two genes *LOC101901352* and *LOC101889632* were designated as *M. domestica sarcotoxin I-B*. A hydrophilic domain that was rich in charged residues and a hydrophobic domain that was rich in nonpolar amino acid residues, both of which are present in *S. peregrina sarcotoxin I-B*, were found in *M. domestica sarcotoxin I-B* (Figure S3) (*http://www.ddtjournal.com/action/getSupplementalData.php?ID=36*) (*37*). Primers for *sarcotoxin I-B* were designed to amplify these two genes. The genes *LOC101889508* and *LOC101887777* were designated as *M. domestica attacin and attacin-like*, respectively (*27,38*). A signal peptide and two glycine-rich domains were found in the amino acid sequence of *LOC101889508* as well as that of *Drosophila melanogaster attacin*, while no signal peptide was found in the sequence of *LOC101887777* (*35*) (Figure S4) (*http://www.ddtjournal.com/action/getSupplementalData.php?ID=36*). The genes *LOC101897067* and *LOC101896897* were designated as *diptericin* according to their annotations in the NCBI database, and primers for *diptericin* were designed to amplify these two genes (Table S1). The genes *LOC101900398*, *LOC101895233*, *LOC101892543*, and *LOC101896200* were designated as *M. domestica salivary gland-expressed bHLH* (*sage*), *cytochrome P450 4aa1* (*cyp4aa1*), *larval serum protein 2* (*lsp2*), and *eater*, respectively, because of their 43%, 69%, 59%, and 44% identities with the genes of the same names in *D. melanogaster*, respectively. The lengths of the PCR amplicons were confirmed to correspond to the predicted lengths by agarose gel electrophoresis to ensure the specificity of the designed primers.

2.7. *Culture of bacteria*

Escherichia coli W3110 (NBRC12713) cells were grown at 37°C with aeration in Luria-Bertani (LB) medium (Nacalai Tesque, Kyoto, Japan). All experiments were conducted using bacterial cells in the logarithmic phase of growth.

2.8. *Determination of minimum inhibitory concentrations (MICs) of AMPs*

Bacterial suspensions in LB medium were adjusted to

an optical density at 600 nm = 0.016. Two-fold dilution series of peptide solutions were prepared in 10 mM phosphate buffer (pH 6) containing 130 mM sodium chloride, 0.2% bovine serum albumin, and 2% dimethyl sulfoxide. Each peptide solution (100 µL) was mixed with 100 µL of bacteria suspension. Bacterial cultures were incubated overnight at 37°C. The MIC was defined as the lowest concentration of antibiotic at which there was no visible growth of the organism (*39*).

2.9. *Determination of colony-forming units (CFUs)*

Bacterial suspensions were diluted appropriately with growth medium, and 500 µL of the suspension was mixed with 500 µL of peptide solution prepared as described above. The peptide/bacteria suspensions were incubated at 37°C for 1 h, then the suspensions were diluted and spread onto LB agar plates. After cultivation of the plates, the number of CFUs in each peptide/bacteria suspension was calculated based on the average of triplicate plates.

2.10. *Statistical analysis*

Statistical analysis were performed using one way ANOVA and Scheffe's test or Welch's *t*-test using Statcel3 (OMS publishing, Tokyo, Japan), and $p < 0.05$ was considered significant.

3. Results

3.1. *Needle injury induces the expression of AMP genes in both larvae and pupae*

In this study, we first examined whether the expression of *defensin*, *attacin*, *diptericin*, and *sarcotoxin II* would be induced by needle injury of the body wall in *M. domestica* larvae. Our analysis of gene expression by real-time PCR using transcripts from larval whole bodies revealed that the expression levels of the AMP genes in injured larvae were 24-300 times higher than those in intact larvae (Figure 1A). These observations indicated that needle injury induced the expression of AMP genes in *M. domestica* larvae. Furthermore, we examined whether needle injury would also induce the expression of AMP genes in pupae. As shown in Figure 1B, the expression levels of the AMP genes in injured pupae were 6-2,600 times higher than those in intact pupae. These observations indicate that the injury-dependent induction of AMP genes, which is a representative event of the innate immune response in some insects, occurred in pupae and larvae of the house fly (*M. domestica*).

3.2. *Expression of AMP genes in larval tissues upon injury*

We examined the expression of AMP genes in larval fat

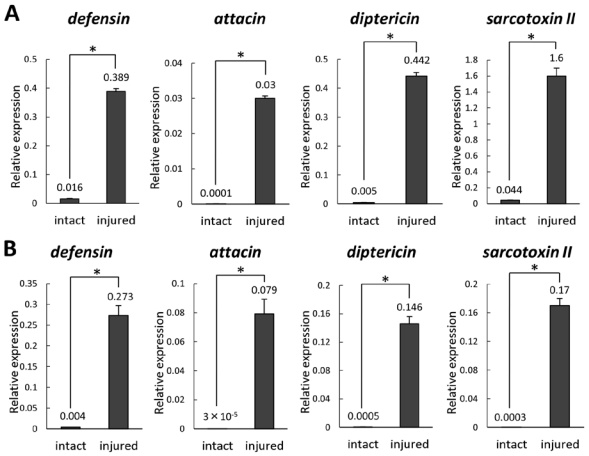

Figure 1. Needle injury induces the expression of antimicrobial peptide genes in *Musca domestica* larvae and pupae. The expression levels of *defensin*, *attacin*, *diptericin*, and *sarcotoxin II* in injured and intact *M. domestica* larvae **(A)** and pupae **(B)** were examined by real-time polymerase chain reaction (PCR). Larvae and pupae were used for mRNA extraction at 20-24 h after injury, and 10 larvae or 20 pupae were used as one batch. The expression level of each gene is given as a ratio to that of the internal control gene *gapdh*. The bars represent the mean relative expression level of triplicate assay of a batch and the error bars represent the standard deviation. An average values are shown above the bars. Data were analyzed by the Welch's *t*-test. *p < 0.05. The results shown were representative of two independent experiments.

bodies to examine whether the fat body in *M. domestica* larvae is a tissue in which innate immune responses are induced by needle injury of the body wall. The expression levels of AMP genes in the fat bodies of injured larvae were much higher than those in the fat bodies of intact larvae at 6, and 24 h after injury (Figure 2), and the expression levels peaked at 6 h after injury (Figure 2). These observations indicate that the injury-dependent expression of AMP genes was transient in fat bodies, peaking at approximately 6 h after injury and remaining significantly elevated at 24 h after injury.

To further explore the injury-dependent expression of AMP genes in larval tissues, we examined their expression in the salivary glands, digestive tracts, and hemocytes in addition to fat bodies. In these experiments, we examined various structural types of AMPs, including cysteine-rich peptides (*defensin*, *defensin-like 1*/*defensin-like 2*, and *defensin-like 3*), glycine-rich peptides (*attacin*, *attacin-like*, *sarcotoxin II*, and *diptericin*), and an α-helical peptide (*sarcotoxin I-B*). The structural features of the AMPs are shown in Figures S1-S5 (*http://www.ddtjournal.com/action/getSupplementalData.php?ID=36*). Additionally, *LOC101888779*, which was previously classified as a *diptericin* gene based on its sequence (*27*), was analyzed, although *LOC101888779* was annotated as an uncharacterized protein in the NCBI database.

Before we analyzed the expression of AMP genes in the larval tissues, we examined whether the tissues were appropriately collected using the following tissue-specific marker genes: a salivary gland marker gene,

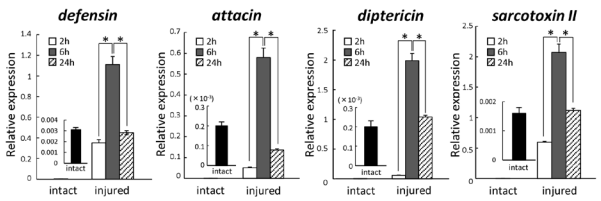

Figure 2. Transient expression of antimicrobial peptide genes in fat bodies after injury. The expression levels of *defensin*, *attacin*, *diptericin*, and *sarcotoxin II* in fat bodies were examined by real-time PCR. Fat bodies were prepared from larvae at 2, 6, and 24 h after injury or from intact larvae. Fat bodies were collected from 40 larvae as one batch at each time point. The expression level of each gene is given as a ratio to that of *gapdh*. Values represent the mean relative expression level of triplicate assay of a batch and the error bars represent the standard deviation. Data were analyzed by the one way ANOVA and Scheffe's test. *p < 0.05. Insets are enlarged views of parts of the panels. The results shown were representative of two independent experiments.

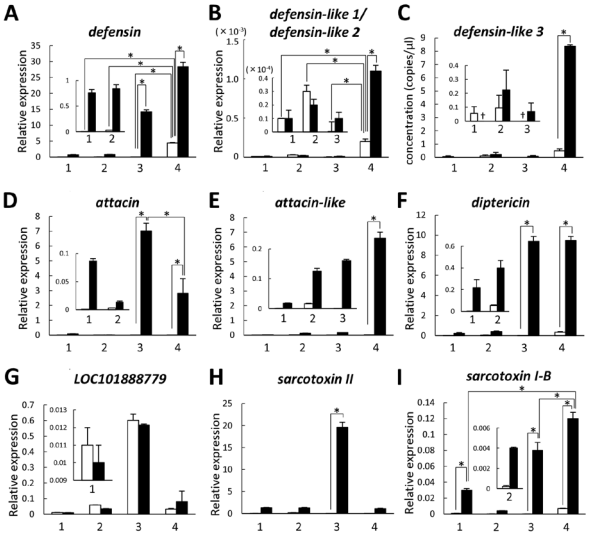

Figure 3. Expression of antimicrobial peptide genes in larval tissues after injury. The expression levels of *defensin* **(A)**, *defensin-like 1/defensin-like 2* **(B)**, *defensin-like 3* **(C)**, *attacin* **(D)**, *attacin-like* **(E)**, *diptericin* **(F)**, *LOC101888779* **(G)**, *sarcotoxin-II* **(H)**, and *sarcotoxin I-B* **(I)** in the salivary gland (1), digestive tract (2), fat body (3), and hemocyte (4) were measured by real-time PCR **(A, B, D-I)** or droplet digital PCR **(C)**. Tissue samples were prepared from larvae at 20-24 h after injury or from intact larvae. Salivary glands, digestive tracts, and fat bodies were collected from 5-15 larvae as one batch. Hemocytes were collected from approximately 100-400 larvae as one batch. For real-time PCR analysis, the expression level of each gene is given as a ratio to that of *rps18*. For droplet digital PCR analysis, gene expression data are represented as the copy number per μL of first-strand cDNA solution. In both analyses, values represent the means of triplicate assay of a batch from intact larvae (white bars) or injured larvae (black bars) and the error bars represent the standard deviations. Dagger (†) indicates that the expression was not detected. Insets in panels A, B, C, D, E, F, G, and I are enlarged views of parts of the panels. Data were analyzed by the one way ANOVA and Scheffe's test. *$p < 0.05$. The results from another batch were shown in Figure S7.

sage; a digestive tract (hindgut) marker gene, *cyp4aa1*; a fat body marker gene, *lsp2*; and a hemocyte marker gene, *eater*. It is well established that these four genes are expressed in a tissue-specific manner in *D. melanogaster* larvae (*40-43*). These genes also showed tissue-specific expression in *M. domestica* larvae, indicating the validity of the tissue collection (Figure S6) (*http://www.ddtjournal.com/action/getSupplementalData.php?ID=36*).

The expression of *defensin* was increased in fat bodies and hemocytes after injury (Figure 3A). Interestingly, significant *defensin* expression was also observed in hemocytes from intact larvae at a higher level than that in salivary glands, digestive tracts and fat bodies from intact larvae. The expression of *defensin-like 1* and *2* was also observed in hemocytes from intact larvae to some extent, and their expression was apparently increased after injury (Figure 3B). By contrast, the expression of *defensin-like 1* and *2* did not increase after injury in other tissues including fat bodies (Figure 3B). The injury-dependent induction of *defensin-like 3* expression was also apparent in hemocytes (Figure 3C). These results indicated that defensin and defensin-related peptides were induced after injury, but their induction levels or patterns differed among tissues. Furthermore, some defensin peptides were constitutively expressed in hemocytes. These observations imply that defensin and defensin-related peptides might have some tissue-specific functions in *M. domestica* larvae.

The expression of *attacin* increased in hemocytes and fat bodies after injury, whereas that of *attacin-like* increased in hemocytes but not in fat bodies (Figures 3D and E). These observations suggest that attacin-related peptides also have tissue-specific functions in *M. domestica* larvae.

The expression of *diptericin* was strongly induced in fat bodies and hemocytes (Figure 3F). By contrast, the expression of *LOC101888779* was observed in all tissues examined in intact larvae to some extent and its injury-dependent induction was not apparent (Figure 3G). These observations indicate that *diptericin* is injury-inducible but *LOC101888779* is not. The amino acid sequences of diptericins in *Phormia terraenovae* and *D. melanogaster* possess a short proline-rich domain and a long glycine-rich domain, both of which are characteristic features of diptericin (*34*). The *diptericin* encoded by *LOC101897067* and *LOC101896897* in *M. domestica* possesses both these domains, indicating that it is a typical diptericin (Figure S5). However, no sequence similar to the proline-rich domain or the glycine-rich domain was found in the deduced amino acid sequence of *LOC101888779* (Figure S5). Combined with the fact that the expression of *LOC101888779* was not injury-inducible, *LOC101888779* might not belong to the diptericin family or function as an AMP.

The expression of *sarcotoxin II* increased strongly in fat bodies after injury (Figure 3H). The expression of *sarcotoxin I-B* increased in salivary glands, fat bodies and hemocytes after injury (Figure 3I).

The reproducibility of the results described above was confirmed (Figure S7) (*http://www.ddtjournal.com/*

Table 1. MICs of synthetic peptide fragments derived from defensin-related genes in *M. domestica* against *E. coli*

Gene designation	Sequence	MIC (μg/mL)
sapecin B	RSLCLLHCRLK	150
defensin	HSACAAHCLLRGNR	> 300
defensin-like 1	KDSVCAAHCLLIGKS	> 300
defensin-like 2	HSVCAAHCLLLGKS	> 300
defensin-like 3	KVSCQAHCLLLKKR	300

The experiments were performed two times independently and obtained same results.

action/getSupplementalData.php?ID=36). In Figure S7, injury-dependent inductions of *defensin*, *attacin*, *sarcotoxin II*, and *sarcotoxin I-B* were observed in salivary glands. Since the reproducibility of significant inductions of *defensin*, *attacin*, and *sarcotoxin II* were not confirmed in salivary glands (Figure 3), precise analysis is required for the AMP genes inductions in the salivary glands. These results, taken together, indicated that AMP genes were induced in the fat body, hemocyte, and/or salivary gland in response to injury. However, the induction pattern differed among tissues. These findings suggest that AMPs have tissue-specific functions and that their expression is governed by complex regulatory machinery.

3.3. *A peptide fragment from a defensin-related peptide shows antimicrobial activity*

The peptide fragment RSLCLLHCRLK-NH_2 from sapecin B, an AMP belonging to the defensin family in the flesh fly (*S. peregrina*), exhibits an antimicrobial activity against *Staphylococcus aureus*, *E. coli*, and *Candida albicans* (*21*). Since *M. domestica* defensin and defensin-related peptides possess a region that is similar to the peptide RSLCLLHCRLK-NH_2, we examined the antimicrobial activities of four peptide fragments corresponding to that region of four predicted *M. domestica* AMPs against *E. coli* (Table 1).

The MICs of these peptide fragments against *E. coli* were determined (Table 1). The peptide fragment derived from *defensin-like 3*, namely KVSCQAHCLLLKKR-NH_2, showed a significant antimicrobial activity (Table 1). However, other peptide fragments derived from *defensin*, *defensin-like 1*, and *defensin-like 2* did not show any antimicrobial activity (Table 1). Furthermore, a CFU assay revealed that KVSCQAHCLLLKKR-NH_2 exhibited its antimicrobial activity (Figure 4). These results indicated that the peptide region from *defensin-like 3* possessed an antimicrobial activity. These observations indicate the potential of the injury-inducible AMPs of *M. domestica* as medicinal resources.

4. Discussion

In this paper, we have demonstrated that the expression of genes encoding AMPs in the house fly (*M. domestica*)

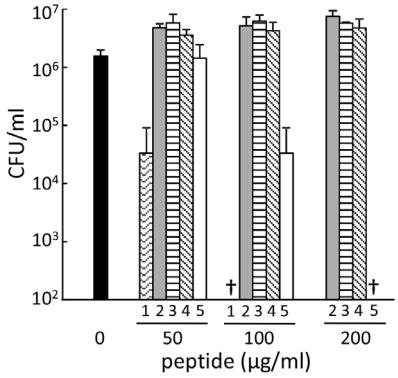

Figure 4. Antimicrobial activities of synthetic fragment peptides derived from defensin-related genes in *M. domestica*. The antimicrobial activities of synthetic fragment peptides from *M. domestica* antimicrobial peptides against *E. coli* were examined by determining the number of colony-forming units in the assay mixture containing synthetic fragment peptides derived from *sapecin B* (1), *defensin* (2), *defensin-like 1* (3), *defensin-like 2* (4), or *defensin-like 3* (5). The sequences of the peptide fragments are indicated in Table 1. Values represent the mean of triplicate samples and the error bars represent the standard deviation. Dagger (†) indicates that no bacteria were detected.

was induced by needle injury. The needle injury can induce infectious inflammation signal by microbial components derived from environmental microorganisms invaded through the wound, and it can also induce non-infectious inflammation signals by physical damage. The inductions of AMP genes were observed in both larvae and pupae. Our analysis of larval tissues revealed that the induction of AMP genes occurred in hemocytes, fat bodies, and salivary glands, but not in digestive tracts. The degree of induction for each gene differed among tissues, suggesting that complex regulatory machinery governs their expression.

Previously, Tang *et al*. showed that the expression of AMP genes in *M. domestica* larvae was induced by the injection of bacteria (*44*). Our observation that the expression of AMP genes was induced by injury is consistent with their result. The injury-dependent expression of AMP genes was revealed to also occur in pupae. Furthermore, our analysis of larval tissues revealed that the induction of the genes was regulated in a complex manner. For example, *attacin* was induced in both fat bodies and hemocytes by injury, but *attacin-like* was induced only in hemocytes. At present, the molecular machinery and physiological functions of the localized induction of AMPs remains unknown, but this phenomenon implies that the AMPs have tissue-specific functions. Additionally, our results revealed that some defensin-related peptides were constitutively expressed in hemocytes and their expression increased further after injury. In addition to their acute induction in response to injury, the constitutive expression of AMPs in hemocytes might have some functions in intact larvae.

It is noteworthy that almost all the studied AMP genes, except *sarcotoxin II*, were induced in hemocytes after injury and that some AMP genes were not induced

in the fat body, which was previously characterized as the dominant organ of injury-dependent AMPs synthesis (*8*). Our findings suggest that hemocytes are the most sensitive tissue to the induction of innate immune responses after injury.

The *M. domestica* genome encodes a larger number of AMPs than any other Dipteran genome (*27*). Our results demonstrate that the *M. domestica* AMP genes show tissue-specific and injury-inducible expression, and their complex induction machinery might imply that they have tissue-specific functions against infection. The merit of multiple expressions of AMPs in larval tissues is the combinatorial activity of AMP against invaded microorganisms. The larvae of *L. sericata*, which are known as medicinal maggots, expressed attacins, cecropins, diptericins, and sarcotoxins in addition to lucifencin, and the AMPs showed additive as well as synergetic activity (*11,45*). Also, insect AMP complexes, in contrast to individual AMP, has been shown to be well protected from resistance development in bacteria (*46*). Examinations of AMP combinations in natural products, including insect hemolymph and insect tissues, are valuable for development of combinatorial products of AMP, because the AMP combinations in natural products may be suitable for the merits described above.

In this study, we showed that a synthetic peptide fragment from the injury-inducible AMP gene exhibit antimicrobial activity. This observation implies that injury-inducible AMP genes in house fly were potential resource for some applications including medicine. AMP, such as polymyxin B and colistin, is clinically used as an antimicrobial agent (*47*). Interestingly, some AMPs showed biological activities, such as immunomodulation, angiogenesis, and wound healing, against mammalian cells and tissues (*48-50*). The usefulness of injury-inducible AMP genes in house fly is limited now, and the further study of the AMP is necessary for the formation of grounds of the practical use.

Acknowledgements

This work was supported in part by the Adaptable and Seamless Technology transfer Program through Target-driven R&D (A-STEP) from the Japan Science and Technology Agency (JST). The authors declare no conflict of interest associated with this work.

References

1. Hoffmann JA. The immune response of Drosophila. Nature. 2003; 426:33-38.
2. Okada M, Natori S. Purification and characterization of an antibacterial protein from haemolymph of *Sarcophaga peregrina* (flesh-fly) larvae. Biochem J. 1983; 211:727-734.
3. Brey PT, Lee WJ, Yamakawa M, Koizumi Y, Perrot S, Francois M, Ashida M. Role of the integument in insect immunity: epicuticular abrasion and induction of cecropin synthesis in cuticular epithelial cells. Proc Natl Acad Sci U S A. 1993; 90:6275-6279.
4. Kawasaki K, Andoh M. Properties of induced antimicrobial activity in *Musca domestica* larvae. Drug Discov Ther. 2017; 11:156-160.
5. Gottar M, Gobert V, Michel T, Belvin M, Duyk G, Hoffmann JA, Ferrandon D, Royet J. The *Drosophila* immune response against Gram-negative bacteria is mediated by a peptidoglycan recognition protein. Nature. 2002; 416:640-644.
6. Kleino A, Silverman N. The Drosophila IMD pathway in the activation of the humoral immune response. Dev Comp Immunol. 2014; 42:25-35.
7. Kenmoku H, Hori A, Kuraishi T, Kurata S. A novel mode of induction of the humoral innate immune response in *Drosophila* larvae. Dis Model Mech. 2017; 10:271-281.
8. Hoffmann JA, Hetru C, Reichhart JM. The humoral antibacterial response of *Drosophila*. FEBS Lett. 1993; 325:63-66.
9. Arrese EL, Soulages JL. Insect fat body: energy, metabolism, and regulation. Annu Rev Entomol. 2010; 55:207-225.
10. Lemaitre B, Nicolas E, Michaut L, Reichhart JM, Hoffmann JA. The dorsoventral regulatory gene cassette spatzle/Toll/cactus controls the potent antifungal response in *Drosophila* adults. Cell. 1996; 86:973-983.
11. Cerovsky V, Zdarek J, Fucik V, Monincova L, Voburka Z, Bem R. Lucifensin, the long-sought antimicrobial factor of medicinal maggots of the blowfly *Lucilia sericata*. Cell Mol Life Sci. 2010; 67:455-466.
12. Vaara M, Viljanen P. Binding of polymyxin B nonapeptide to gram-negative bacteria. Antimicrob Agents Chemother. 1985; 27:548-554.
13. Gunn JS, Lim KB, Krueger J, Kim K, Guo L, Hackett M, Miller SI. PmrA-PmrB-regulated genes necessary for 4-aminoarabinose lipid A modification and polymyxin resistance. Mol Microbiol. 1998; 27:1171-1182.
14. Kawasaki K, China K, Nishijima M. Release of the lipopolysaccharide deacylase PagL from latency compensates for a lack of lipopolysaccharide aminoarabinose modification-dependent resistance to the antimicrobial peptide polymyxin B in *Salmonella enterica*. J Bacteriol. 2007; 189:4911-4919.
15. Shai Y. Mechanism of the binding, insertion and destabilization of phospholipid bilayer membranes by alpha-helical antimicrobial and cell non-selective membrane-lytic peptides. Biochim Biophys Acta. 1999; 1462:55-70.
16. Matsuzaki K. Why and how are peptide-lipid interactions utilized for self-defense? Magainins and tachyplesins as archetypes. Biochim Biophys Acta. 1999; 1462:1-10.
17. Huang HW. Molecular mechanism of antimicrobial peptides: the origin of cooperativity. Biochim Biophys Acta. 2006; 1758:1292-1302.
18. Yi HY, Chowdhury M, Huang YD, Yu XQ. Insect antimicrobial peptides and their applications. Appl Microbiol Biotechnol. 2014; 98:5807-5822.
19. Iwai H, Nakajima Y, Natori S, Arata Y, Shimada I. Solution conformation of an antibacterial peptide, sarcotoxin IA, as determined by 1H-NMR. Eur J Biochem. 1993; 217:639-644.
20. Zasloff M. Antimicrobial peptides of multicellular organisms. Nature. 2002; 415:389-395.
21. Yamada K, Natori S. Characterization of the antimicrobial peptide derived from sapecin B, an antibacterial protein of

Sarcophaga peregrina (flesh fly). Biochem J. 1994; 298 (Pt 3):623-628.
22. Alvarez-Bravo J, Kurata S, Natori S. Novel synthetic antimicrobial peptides effective against methicillin-resistant *Staphylococcus aureus*. Biochem J. 1994; 302 (Pt 2):535-538.
23. Manabe T, Kawasaki K. D-form KLKLLLLLKLK-NH_2 peptide exerts higher antimicrobial properties than its L-form counterpart *via* an association with bacterial cell wall components. Sci Rep. 2017; 7:43384.
24. Okuyama-Nishida Y, Akiyama N, Sugimori G, Nomura K, Ogawa K, Homma KJ, Sekimizu K, Tsujimoto M, Natori S. Prevention of death in bacterium-infected mice by a synthetic antimicrobial peptide, L5, through activation of host immunity. Antimicrob Agents Chemother. 2009; 53:2510-2516.
25. Fritz JH, Brunner S, Birnstiel ML, Buschle M, Gabain A, Mattner F, Zauner W. The artificial antimicrobial peptide KLKLLLLLKLK induces predominantly a TH2-type immune response to co-injected antigens. Vaccine. 2004; 22:3274-3284.
26. Schellack C, Prinz K, Egyed A, Fritz JH, Wittmann B, Ginzler M, Swatosch G, Zauner W, Kast C, Akira S, von Gabain A, Buschle M, Lingnau K. IC31, a novel adjuvant signaling *via* TLR9, induces potent cellular and humoral immune responses. Vaccine. 2006; 24:5461-5472.
27. Sackton TB, Lazzaro BP, Clark AG. Rapid expansion of immune-related gene families in the house fly, *Musca domestica*. Mol Biol Evol. 2017; 34:857-872.
28. Hewitt CG. Memoirs: The structure, development, and bionomics of the house-fly, *Musca domestica*, Linn. Q J Microsc Sci. 1908; s2-52:495-545.
29. Ueno T, Kawasaki K, Kubo T. Preparation of single-cohort colonies and hormone treatment of worker honeybees to analyze physiology associated with role and/or endocrine system. J Vis Exp. 2016; 115. doi: 10.3791/54240.
30. Zhong M, Wang X, Wen J, Cai J, Wu C, Aly SM. Selection of reference genes for quantitative gene expression studies in the house fly (*Musca domestica* L.) using reverse transcription quantitative real-time PCR. Acta Biochim Biophys Sin (Shanghai). 2013; 45:1069-1073.
31. Douglass J, Civelli O, Herbert E. Polyprotein gene expression: generation of diversity of neuroendocrine peptides. Annu Rev Biochem. 1984; 53:665-715.
32. Matsuyama K, Natori S. Purification of three antibacterial proteins from the culture medium of NIH-Sape-4, an embryonic cell line of *Sarcophaga peregrina*. J Biol Chem. 1988; 263:17112-17116.
33. Dimarcq JL, Hoffmann D, Meister M, Bulet P, Lanot R, Reichhart JM, Hoffmann JA. Characterization and transcriptional profiles of a *Drosophila* gene encoding an insect defensin. A study in insect immunity. Eur J Biochem. 1994; 221:201-209.
34. Wicker C, Reichhart JM, Hoffmann D, Hultmark D, Samakovlis C, Hoffmann JA. Insect immunity. Characterization of a *Drosophila* cDNA encoding a novel member of the diptericin family of immune peptides. J Biol Chem. 1990; 265:22493-22498.
35. Hedengren M, Borge K, Hultmark D. Expression and evolution of the Drosophila attacin/diptericin gene family. Biochem Biophys Res Commun. 2000; 279:574-581.
36. Kimbrell DA. Insect antibacterial proteins: not just for insects and against bacteria. Bioessays. 1991; 13:657-663.
37. Okada M, Natori S. Primary structure of sarcotoxin I, an antibacterial protein induced in the hemolymph of *Sarcophaga peregrina* (flesh fly) larvae. J Biol Chem. 1985; 260:7174-7177.
38. Hojland DH, Jensen KM, Kristensen M. Adaptation of *Musca domestica* L. field population to laboratory breeding causes transcriptional alterations. PLoS One. 2014; 9:e85965.
39. Andrews JM. Determination of minimum inhibitory concentrations. J Antimicrob Chemother. 2001; 48 (Suppl 1):5-16.
40. Chung H, Sztal T, Pasricha S, Sridhar M, Batterham P, Daborn PJ. Characterization of *Drosophila melanogaster* cytochrome P450 genes. Proc Natl Acad Sci U S A. 2009; 106:5731-5736.
41. Deutsch J, Laval M, Lepesant JA, Maschat F, Pourrain F, Rat L. Larval fat body-specific gene expression in *D. melanogaster*. Dev Genet. 1989; 10:220-231.
42. Evans CJ, Liu T, Banerjee U. *Drosophila* hematopoiesis: Markers and methods for molecular genetic analysis. Methods. 2014; 68:242-251.
43. Li TR, White KP. Tissue-specific gene expression and ecdysone-regulated genomic networks in *Drosophila*. Dev Cell. 2003; 5:59-72.
44. Tang T, Li X, Yang X, Yu X, Wang J, Liu F, Huang D. Transcriptional response of *Musca domestica* larvae to bacterial infection. PLoS One. 2014; 9:e104867.
45. Poppel AK, Vogel H, Wiesner J, Vilcinskas A. Antimicrobial peptides expressed in medicinal maggots of the blow fly *Lucilia sericata* show combinatorial activity against bacteria. Antimicrob Agents Chemother. 2015; 59:2508-2514.
46. Chernysh S, Gordya N, Suborova T. Insect antimicrobial peptide complexes prevent resistance development in bacteria. PLoS One. 2015; 10:e0130788.
47. Nation RL, Li J, Cars O, Couet W, Dudley MN, Kaye KS, Mouton JW, Paterson DL, Tam VH, Theuretzbacher U, Tsuji BT, Turnidge JD. Framework for optimisation of the clinical use of colistin and polymyxin B: the Prato polymyxin consensus. Lancet Infect Dis. 2015; 15:225-234.
48. Vandamme D, Landuyt B, Luyten W, Schoofs L. A comprehensive summary of LL-37, the factotum human cathelicidin peptide. Cell Immunol. 2012; 280:22-35.
49. Nakagami H, Nishikawa T, Tamura N, Maeda A, Hibino H, Mochizuki M, Shimosato T, Moriya T, Morishita R, Tamai K, Tomono K, Kaneda Y. Modification of a novel angiogenic peptide, AG30, for the development of novel therapeutic agents. J Cell Mol Med. 2012; 16:1629-1639.
50. Tomioka H, Nakagami H, Tenma A, Saito Y, Kaga T, Kanamori T, Tamura N, Tomono K, Kaneda Y, Morishita R. Novel anti-microbial peptide SR-0379 accelerates wound healing *via* the PI3 kinase/Akt/mTOR pathway. PLoS One. 2014; 9:e92597.

(Received October 5, 2018; Revised December 6, 2018; Accepted December 21, 2018)

Original Article

DOI: 10.5582/ddt.2018.01068

Invasive fungal infections in critically ill patients: A prospective study from a tertiary care hospital in India

Chitikela Sindhura Durga[1], Nitin Gupta[1], Manish Soneja[1,*], Manasvini Bhatt[1], Immaculata Xess[2], Pankaj Jorwal[1], Gagandeep Singh[2], Animesh Ray[1], Neeraj Nischal[1], Piyush Ranjan[1], Ashutosh Biswas[1], Naveet Wig[1]

[1] *Department of Medicine, All India Institute of Medical Sciences, New Delhi, India;*
[2] *Department of Microbiology, All India Institute of Medical Sciences, New Delhi, India.*

Summary **Invasive fungal infections (IFI) are commonly seen in immunosuppressed individuals but their epidemiology in critically ill patients has not been well described. The aim of this study was to determine the frequency, risk factors and outcome of invasive fungal infections in a medical intensive care unit. A prospective observational study was carried out between August 2016 and March 2018 in the medical intensive care unit. Patients above the age of 14 years with endotracheal intubation and/or central venous catheter for at-least three days and sepsis (not responding to 48 hours of intravenous antibiotic therapy) were included in the study. Suitable samples were collected and were subjected to fungal diagnostics. Invasive fungal disease was defined according to standard guidelines. Of the 100 recruited patients, a total of 11 patients had invasive aspergillosis, three patients had invasive candidiasis and one patient had both invasive aspergillosis and mucormycosis. IFI was more commonly seen in patients with auto-immune diseases (p = 0.002, odds ratio-10.13 (95% CI: 2.3-44)). A mortality of 73% was observed in patients with IFI. In conclusion, IFI, especially aspergillosis is grossly under-reported in critical settings. Early suspicion, thorough investigation and timely diagnosis may alleviate patients of significant mortality and morbidity.**

Keywords: *Aspergillus*, *Candida*, mucormycosis, intensive care unit

1. Introduction

The course of hospital stay in critically ill patient is often complicated by hospital acquired infections. While bacterial infections are known to be very common in critical care settings, the incidence of invasive fungal infections (IFI) is also on the rise. Invasive candidiasis has been found to be the commonest IFI in such settings (*1-3*). Majority of these cases are ascribed to the rampant use of broad spectrum antibiotics and disruption of normal skin and mucosal barriers with multiple devices (*4-6*). Invasive aspergillosis is the second most common IFI. Although, it is predominantly reported in hematopoietic stem cell transplant recipients (*7*) and solid organ transplant recipients (*8*), invasive aspergillosis is increasingly being reported in intensive care units (ICU). ICU patients are at high risk for colonization with *Aspergillus* because of defective mucosal clearance and mechanical ventilation. Hospital environment and construction works have been implicated as the source of spores (*9,10*). Other fungal infections like those caused by *Mucorales* and *Scedosporium* are relatively rare in the medical ICUs and seen mostly in patients with background immunosuppression (*11,12*). While there is enough literature regarding the incidence and outcome of fungal infections in immunosuppressed populations (transplant recipients/malignancy/human immunodeficiency infection virus), the literature on the epidemiology of fungal infections in critically ill patients is scarce. The primary objective of the study was to therefore, determine the frequency, risk factors and outcome of invasive fungal infections in a medical intensive care unit.

**Address correspondence to:*
Dr. Manish Soneja, Department of Medicine, Teaching block, 3rd floor, All India Institute of Medical Sciences, New Delhi-110029, India.
E-mail: manishsoneja@gmail.com

2. Methods

A prospective observational study was carried out in accordance with the ethical standards laid down in the 1964 Declaration of Helsinki and its later amendments after taking approval from the Institute's ethical committee. The study was carried out in the medical intensive care unit at a tertiary care hospital in New Delhi, India between August 2016 and March 2018. All patients above the age of 14 years with endotracheal intubation and /or central venous catheter for 3 or more days and sepsis (not responding to 48 hours of intravenous antibiotic therapy) were included in the study after taking informed consent. Those patients already diagnosed with an IFI before enrolment, those who were neutropenic at the time of enrolment, those who were already diagnosed with human immunodeficiency virus infection or malignancy, transplant recipients and those who had received antifungals in the two weeks prior to enrolment were excluded from the study.

The recruited patients were evaluated for risk factors implicated in the development of IFI. Suitable samples for diagnostic purposes like bronchio-alveolar lavage (BAL)/mini-BAL, blood, sputum, urine, cerebrospinal fluid (CSF), ascitic fluid and pleural fluid were collected and subjected to potassium hydroxide (KOH) mount, gram stain, India ink preparation and fungal cultures (BACTEC, Becton Dickinson, USA). Each culture set was examined daily for first week & twice weekly thereafter for next three weeks. Cultures were deemed negative if there was no growth after four weeks of incubation. Positive cultures were identified and speciated based on the culture morphology and microscopic features. Antifungal susceptibility was done for yeast isolates using micro-broth dilution method as per Clinical and Laboratory Standards Institute (CLSI) guidelines. Additionally, those with features suggestive of invasive aspergillosis were subjected to serum and BAL galactomannan (Platelia *Aspergillus* enzyme immunoassay, Bio-Rad Laboratories, Munich, Germany) tests as per manufacturer instructions. A complete urine analysis, chest X-ray and bacterial cultures were done for all the patients. A computed tomography (CT) of the chest was also done, wherever indicated.

IFI was defined and categorized into proven, probable and possible based on the revised European Organization for the Research and Treatment of Cancer/ Mycoses Study Group (EORTC/MSG) guidelines (*13*). In cases of suspected invasive pulmonary aspergillosis, where the patients could not be classified according to EORTC/MSG guidelines, algorithm given by Blot *et al*. was used to further classify them into putative aspergillosis and colonization (*14*). Putative aspergillosis was also included in the IFI category.

Statistical analyses were performed using the Stata version 12.1. Categorical variables were expressed as percentage and continuous variables were expressed as mean ± standard deviation. Patients with IFI and without IFI were compared using appropriate statistical tests. Odds ratios (ORs) with 95% confidence interval (CI) were calculated. A *p*-value of less than 0.05 was considered significant.

3. Results

A total of 100 patients who satisfied the inclusion and exclusion criteria were recruited in the study. Of these, 53 patients were male and 47 were female. Most patients were between the age range of 60 and 79 years (41%). The mean age for the study population was 48.9 ± 19.8 years. Pneumonia (39%), acute febrile illness (14%), urinary tract infection (13%), meningoencephalitis (6%) and gastroenteritis (5%) were the most common primary diagnosis in these patients. Diabetes (29%), chronic kidney disease (18%), chronic lung disease (15%), auto-immune disease (9%) and chronic liver disease (6%) were the most common co-morbidities in the recruited patients.

A total of 15 patients were diagnosed with IFI amounting to a frequency of 15% (95% CI 7.88-22.12). Of the 15 patients with IFI, 11 patients had invasive aspergillosis, three had invasive candidiasis and one patient had both invasive aspergillosis and mucormycosis. A total of 123 blood cultures were sent, of which three cultures grew *Candida* spp. (*Candida albicans*, *Candida krusei* and *Candida tropicalis*). *Candida krusei* was resistant to fluconazole. Candida albicans and Candida tropicalis were sensitive to all the tested drugs (amphotericin B, voriconazole, fluconazole, caspofungin and micafungin). Out of the 178 mini-BAL cultures sent, 23 samples tested positive for molds. A total of 12 patients (Probable-6, Putative-6) satisfied the criteria for invasive fungal infection. Of these twelve patients, ten patients were culture positive: *A. fumigatus* (n = 5), *A. flavus* (n = 1), *A. terreus* (n = 1), *A. fumigatus* + *A. flavus* (n = 1), *A. fumigatus* + *A. terreus* (n = 1), *A. flavus* + *Lichtheimia corymbifera* (n = 1). Two patients satisfied the criteria for IFI but were culture negative. Of the 140 urine cultures sent, 18 cultures were positive for *Candida* spp. In absence of suggestive clinical findings and concurrent positive blood cultures, these were regarded as colonization. Mean time taken for culture positivity from the day of admission for blood, mini-BAL and urine was 15.6, 8 and 8 days respectively.

There was no statistically significant association between occurrence of IFI and baseline sequential organ failure assessment (SOFA) score, acute physiology and chronic health evaluation (APACHE) II score, duration of mechanical ventilation, duration of central venous catheterization, duration of ICU stays and duration of antibiotics (Table 1). Risk factors other than presence of auto-immune conditions (p = 0.002, odds ratio-10.13

Table 1. Comparison of risk factor between patients with/without Invasive fungal infections (IFI)

Variable	In patients without IFI (Median, IQR), *N* = 85	In patients with IFI (Median, IQR), *N* = 15	*P* value
SOFA score	11 (9 – 13)	10 (5 – 14)	0.55
APACHE II score	22 (17 – 27)	25 (13 – 28)	0.97
Mechanical ventilation (days)	11 (7 – 22)	10 (8 – 18)	0.88
Central venous catheterization (days)	11 (8 – 20)	13 (10 – 22)	0.37
Length of stay in Intensive care unit (days)	12 (7 – 20)	13 (8 – 19)	0.57
Duration of broad spectrum antibiotics (days)	19 (11 – 31)	20 (11 – 25)	0.97

Table 2. Occurrence of Invasive fungal infections (IFI) with respect to various risk factors

Variable	Risk factor absent (%)	Risk factor present (%)	*P* value
Chronic kidney disease	15.85%	11.11%	1.00
Chronic lung Disease	12.94%	26.67%	0.23
Chronic liver disease	13.83%	33.33%	0.22
Autoimmune conditions	10.99%	55.56%	0.003
Diabetes mellitus	15.49%	13.79%	1.00
Hemodialysis	16.92%	11.43%	0.57

(95% CI: 2.3-44)) did not affect the rate of IFI (Table 2). Out of 15 patients with IFI, 11 patients (73.3%) expired whereas 55 (64.7%) expired out of the 85 patients without IFI.

4. Discussion

Invasive fungal infections in non-immunosuppressed critically ill patients is a less explored area with most studies concentrating on invasive candidiasis (candidemia and deep seated tissue infections) alone. Incidence of candidemia in literature ranges from 6.51 to 54 per 1,000 patients in various studies, most of which are from European countries (*16-18*). The mean interval from ICU admission to the occurrence of candidemia in our patients was 15.67 days. Although, studies from Europe report similar findings, this duration was reported as 8 days from an Indian study (*18-20*).

According to a systematic review, 80% of IFI in critically ill patient are due to *Candida* spp. while only 0.3-19% of these infections are caused by invasive aspergillosis (*21*). Two studies in Italy reported an incidence of invasive aspergillosis of 2.3 per 1,000 admissions and 6.8 per 1,000 admissions respectively (*16,17*). Meersseman *et al*. conducted a multi-center retrospective study in Belgium and reported a frequency of invasive aspergillosis in critically ill patients without malignancy to be 6.9% (*22*). The frequency of aspergillosis in most studies may be grossly under-reported because of the uncertainty in diagnostic criteria. In our study, out of 15 cases of IFI, only three were caused by *Candida* spp. and the rest by *Aspergillus* spp. This differential distribution might have been due to *i*) Use of expanded criteria for diagnosis of invasive aspergillosis- EORTC/MSG criteria has long been used for diagnosis of invasive aspergillosis but it is often difficult to classify invasive aspergillosis in non-neutropenic critically ill patient with these criteria alone. To resolve this issue, we used the Blot's criteria in those patients where classification could not be done based on EORTC/MSG criteria (Probable-6, Putative-6, colonization-9), *ii*) lack of traditional risk factors for invasive candidiasis in medical ICUs like total parenteral nutrition and gastro-intestinal surgery, *iii*) Presence of risk factors for aspergillosis like chronic lung diseases, chronic liver disease and auto-immune disorders, *iv*) ubiquitous presence of *Aspergillus* spores coupled with constructional activities in hospital (*9*).

The mean duration of ICU stay before positivity of mini-BAL culture (calculated from the day of admission in ICU) in patients with invasive aspergillosis in our study population was eight days. Various other studies have reported this duration to be in the range of 4 to 15.6 days (*17,23,24*). Most common species isolated from the mini-BAL of patients with invasive aspergillosis was *Aspergillus fumigatus* (70%) followed by *Aspergillus flavus* (30%) and *Aspergillus terreus* (20%). Most studies from Europe revealed *Aspergillus fumigatus* (82-92%) as the commonest fungus causing invasive Aspergillosis (*17,24*).

Statistically significant relationship was established between autoimmune diseases and occurrence of IFI. Out of the nine patients admitted with auto-immune diseases, five patients developed invasive aspergillosis ((p = 0.003) with an odds ratio of 10.125 (p = 0.002)). Patients with chronic lung disease (p = 0.23) and chronic liver disease (0.22) also had increased frequency of IFI but this finding was not statistically significant. Meersseman et al. found the use of corticosteroids for more than 3 weeks and chronic liver disease as an important risk factor for invasive aspergillosis in critically ill patients (*22*). Garnacho-Montero et al. also concluded that COPD and use of corticosteroids was associated with positive culture for

Aspergillus from lower respiratory samples (*25*).

A crude mortality rate of 30-81% and an attributable mortality of 5-71% has been reported for invasive candidiasis in various studies whereas a mortality rate of up to 80% has been reported for invasive aspergillosis (*2,3,21-23,25*). Owing to the fact that ours is an apex care center receiving referral from most parts of India, the study population had a higher mean age, high frequency of co-morbidities and high base-line APACHE-2/SOFA scores. This was probably the reason for high mortality across both the groups.

The incidence of IFI, particularly invasive aspergillosis, is grossly under-reported in critical care settings. Early suspicion and thorough investigation, especially in presence of established risk factors such as use of immunosuppressive agents and chronic lung diseases, should be carried out. These infections are associated with high mortality. Institutional measures like infection control and anti-microbial stewardship are the need of the hour.

Limitations

Beta-d glucan test could not be done in these patients which has a higher sensitivity than blood culture for making a diagnosis of invasive candidiasis. This may have led to under-reporting of invasive candidiasis cases.

Declarations

Ethics approval was taken from the institute's ethics committee and informed consent to participate in the study was taken from all patients/ surrogates. Competing interests: The authors declare that they have no competing interests. Funding: The authors have no funding source to declare. Acknowledgements: The authors thank the medical and nursing staff of the medical intensive care unit.

References

1. Bassetti M, Taramasso L, Nicco E, Molinari MP, Mussap M, Viscoli C. Epidemiology, species distribution, antifungal susceptibility and outcome of nosocomial Candidemia in a tertiary care hospital in Italy. PLoS One. 2011; 6:e24198.
2. Horn DL, Neofytos D, Anaissie EJ, Fishman JA, Steinbach WJ, Olyaei AJ, Marr KA, Pfaller MA, Chang CH, Webster KM. Epidemiology and outcomes of candidemia in 2019 patients: Data from the prospective antifungal therapy alliance registry. Clin Infect Dis. 2009; 48:1695-1703.
3. Zaoutis TE, Argon J, Chu J, Berlin JA, Walsh TJ, Feudtner C. The epidemiology and attributable outcomes of candidemia in adults and children hospitalized in the United States: A propensity analysis. Clin Infect Dis. 2005; 41:1232-1239.
4. Méan M, Marchetti O, Calandra T. Bench-to-bedside review: *Candida* infections in the intensive care unit. Crit Care. 2008; 12:204.
5. Marchetti O, Bille J, Fluckiger U, Eggimann P, Ruef C, Garbino J, Calandra T, Glauser MP, Täuber MG, Pittet D; Fungal Infection Network of Switzerland. Epidemiology of candidemia in Swiss tertiary care hospitals: Secular trends, 1991-2000. Clin Infect Dis. 2004; 38:311-320.
6. Richards MJ, Edwards JR, Culver DH, Gaynes RP. Nosocomial infections in combined medical-surgical intensive care units in the United States. Infect Control Hosp Epidemiol. 2000; 21:510-515.
7. Kontoyiannis DP, Marr KA, Park BJ, *et al.* Prospective surveillance for invasive fungal infections in hematopoietic stem cell transplant recipients, 2001-2006: Overview of the Transplant-Associated Infection Surveillance Network (TRANSNET) Database. Clin Infect Dis. 2010; 50:1091-1100.
8. Pappas PG, Alexander BD, Andes DR, *et al*. Invasive fungal infections among organ transplant recipients: Results of the Transplant-Associated Infection Surveillance Network (TRANSNET). Clin Infect Dis. 2010; 50:1101-1111.
9. Haiduven D. Nosocomial aspergillosis and building construction. Med Mycol. 2009; 47 (Suppl 1):S210-216.
10. Vonberg RP, Gastmeier P. Nosocomial aspergillosis in outbreak settings. J Hosp Infect. 2006; 63:246-254.
11. Bitar D, Lortholary O, Le Strat Y, Nicolau J, Coignard B, Tattevin P, Che D, Dromer F. Population-based analysis of invasive fungal infections, France, 2001-2010. Emerg Infect Dis. 2014; 20:1149-1155.
12. Perlroth J, Choi B, Spellberg B. Nosocomial fungal infections: Epidemiology, diagnosis, and treatment. Med Mycol. 2007; 45:321-346.
13. De Pauw B, Walsh TJ, Donnelly JP, et al. Revised definitions of invasive fungal disease from the European Organization for Research and Treatment of Cancer/ Invasive Fungal Infections Cooperative Group and the National Institute of Allergy and Infectious Diseases Mycoses Study Group (EORTC/MSG) Consensus Group. Clin Infect Dis. 2008; 46:1813-1821.
14. Blot SI, Taccone FS, Van den Abeele AM, Bulpa P, Meersseman W, Brusselaers N, Dimopoulos G, Paiva JA, Misset B, Rello J, Vandewoude K, Vogelaers D; AspICU Study Investigators. A clinical algorithm to diagnose invasive pulmonary aspergillosis in critically ill patients. Am J Respir Crit Care Med. 2012; 186:56-64.
15. Reference method for broth dilution antifungal susceptibility testing of yeasts, approved standard. CLSI document M27-A3. 2008.
16. Montagna MT, Caggiano G, Lovero G, De Giglio O, Coretti C, Cuna T, Iatta R, Giglio M, Dalfino L, Bruno F, Puntillo F. Epidemiology of invasive fungal infections in the intensive care unit: Results of a multicenter Italian survey (AURORA Project). Infection. 2013; 41:645-653.
17. Tortorano AM, Dho G, Prigitano A, *et al*. Invasive fungal infections in the intensive care unit: A multicentre, prospective, observational study in Italy (2006-2008). Mycoses. 2012; 55:73-79.
18. Chakrabarti A, Sood P, Rudramurthy SM, *et al*. Incidence, characteristics and outcome of ICU-acquired candidemia in India. Intensive Care Med. 2015; 41:285-295.
19. Yapar N, Akan M, Avkan-Oguz V, Ergon CM, Hancer M, Doluca M. Risk factors, incidence and outcome of candidemia in a Turkish intensive care unit: A five-year retrospective cohort study. Anaesth Pain Intensive Care.

2014; 18:265-271.
20. Laupland KB, Gregson DB, Church DL, Ross T, Elsayed S. Invasive *Candida* species infections: A 5 year population-based assessment. J Antimicrob Chemother. 2005; 56:532-537.
21. Bassetti M, Garnacho-Montero J, Calandra T, Kullberg B, Dimopoulos G, Azoulay E, Chakrabarti A, Kett D, Leon C, Ostrosky-Zeichner L, Sanguinetti M, Timsit JF, Richardson MD, Shorr A, Cornely OA. Intensive care medicine research agenda on invasive fungal infection in critically ill patients. Intensive Care Med. 2017; 43:1225-1238.
22. Meersseman W, Vandecasteele SJ, Wilmer A, Verbeken E, Peetermans WE, Van Wijngaerden E. Invasive aspergillosis in critically ill patients without malignancy. Am J Respir Crit Care Med. 2004; 170:621-625.
23. Vandewoude K, Blot S, Benoit D, Depuydt P, Vogelaers D, Colardyn F. Invasive aspergillosis in critically ill patients: Analysis of risk factors for acquisition and mortality. Acta Clin Belg. 2004; 59:251-257.
24. Taccone FS, Van den Abeele AM, Bulpa P, Misset B, Meersseman W, Cardoso T, Paiva JA, Blasco-Navalpotro M, De Laere E, Dimopoulos G, Rello J, Vogelaers D, Blot SI; AspICU Study Investigators. Epidemiology of invasive aspergillosis in critically ill patients: Clinical presentation, underlying conditions, and outcomes. Crit Care. 2015; 19:7.
25. Garnacho-Montero J, Amaya-Villar R, Ortiz-Leyba C, León C, Alvarez-Lerma F, Nolla-Salas J, Iruretagoyena JR, Barcenilla F. Isolation of *Aspergillus* spp. from the respiratory tract in critically ill patients: Risk factors, clinical presentation and outcome. Crit Care. 2005; 9:R191-199.

(Received November 20, 2018; Revised December 12, 2018; Accepted December 28, 2018)

Original Article

DOI: 10.5582/ddt.2018.01080

The outcome of combined treatment with ombitasvir-paritaprevir-ritonavir, sofosbuvir with or without ribavirin as salvage therapy for Egyptian HCV experienced patients: A single center study

Waleed Abdelfattah Ismail, Fady Maher Wadea*

Internal Medicine Department, Gastroenterology and Hepatology Unit, Faculty of Medicine, Zagazig University, Zagazig, Egypt.

Summary **We aimed to investigate the efficacy and safety of combination of sofosbuvir with ombitasvir, paritaprevir, and ritonavir ± ribavirin as a retreatment option for experienced Egyptian patients who failed previous sofosbuvir, daclatasvir ± ribavirin therapy. A total of 75 treatment-experienced patients were allocated for the completion of their treatment period according to criteria formed by the national committee for control of viral hepatitis. The enrolled patients were followed up throughout treatment, at the end of treatment and 3 months after the end of the treatment by clinical evaluation and laboratory investigations. 27 patients were treated with sofosbuvir with ombitasvir, paritaprevir, and ritonavir plus ribavirin for 12 weeks while 48 patients were treated with sofosbuvir with ombitasvir, paritaprevir, and ritonavir without ribavirin for 24 weeks. The per-protocol sustained virological response at week 12 (SVR12) rate was 100% in both groups while the intention-to-treat SVR12 was 93.4% in all patients, 97.9% in the 24 weeks group and 85.2% in the 12 weeks group. The regimen was well tolerated and the most common adverse effects observed across treatment and during follow-up period included fatigue (38.6%) and headache (29.3%), withdrawal due to adverse effects occurred in 6.6%. We can conclude that retreatment with sofosbuvir with ombitasvir, paritaprevir, and ritonavir ± ribavirin is well tolerated and achieved high SVR12 rates in chronic HCV Egyptian patients with previous sofosbuvir plus daclatasvir treatment failure. Ribavirin free regimen for 24 weeks exerted significant lesser adverse effects.**

Keywords: Hepatitis C, salvage therapy, Egypt

1. Introduction

HCV is near to be epidemic in Egypt. Seroprevalence has been reported in about 8 million individuals (10% of Egyptians). Estimated 7-10% of Egyptian populations are chronically infected (*1-3*). Genotype 4 (GT4) infection accounts for 13-20% of HCV infections worldwide; in Egypt, it is present in about 93% of chronic HCV patients (*4*).

With the emergence of many HCV direct-acting antiviral therapy options, the Egyptian National Committee for Control of Viral Hepatitis (NCCVH) began to recruit HCV patients for treatment in September 2014 (*5*). According to the AASLD guidelines, the recommendations for treatment were sofosbuvir/daclatasvir (SOF/DCV) for 24 weeks without ribavirin (RBV) or 12 weeks with weight-based ribavirin (*6*). This regimen was associated with high rates of sustained virological response among "difficult to cure" patients (*7*).

In November 2015, generic SOF/DCV (± RBV) became the main treatment option for chronic HCV in the national program in Egypt. This therapy was evaluated later on in an Egyptian study included 18378 patients, SVR12 was achieved in 95.4% in SOF/DCV group and in 94.7% in SOF/DCV/RBV group. Relapse and nonresponder rates were 3.7% and 3.3% in both groups respectively (*8*).

SOF is a potent pan-genotypic NS5B polymerase inhibitor with a high barrier to resistance (*9*). Ombitasvir

**Address correspondence to:*
Dr. Fady Maher Wadea, Internal Medicine Department, Gastroenterology and Hepatology Unit, Faculty of Medicine, Zagazig University, Zagazig, Egypt.
E-mail: fadymaher41@yahoo.com

is an NS5A protein inhibitor and paritaprevir is an NS3/4A protease inhibitor are co-dosed with ritonavir (r) to increase drug exposures (*10*). These drugs are given in combination to increase their efficacy and prevent HCV resistance-associated substitutions (*11*). The most favorable plan for retreatment of HCV experienced patients with previous direct-acting antivirals (DAAs) failure is sofosbuvir plus other class drugs not previously used and ribavirin unless it is contraindicated to consider triple or quadruple DAAs treatment (*12*).

Minimal data and clinical trials for retreatment in Egyptian patients with HCV GT4 who failed prior DAAs treatments are present as most of the studies focused on the treatment of patients with genotype 1 infection which has the highest worldwide prevalence (*13*), therefore, this study was conducted for evaluation of the efficacy and safety of the combination of quadruple DAAs; SOF/ombitasvir/paritaprevir/ritonavir/±RBV as salvage therapy for retreatment of experienced Egyptian patients who failed previous treatment with SOF/DCV therapy.

2. Patients and Methods

2.1. *Patients*

This study included a total of 75 experienced patients with chronic hepatitis C and all stages of liver fibrosis (F0-F4) indicated for treatment according to inclusion and exclusion criteria who failed to achieve SVR12 following previous treatment with sofosbuvir and daclatasvir regimens.

All patients were recruited from Faqous general hospital specialized center affiliated to the NCCVH in Egypt, Sharkia governorate, Egypt in the period from Jan 2017 to April 2018. The study was conducted in accordance with the ethical standards of the responsible committee on human experiment (institutional and national) and with the Declaration of Helsinki. An informed consent was written by all patients before starting treatment to allow the use of their clinical data and for publication.

Inclusion criteria for treatment according to the supreme council and the national committee for control of viral hepatitis (NCCVH), December 2016: males and females ≥ 18 years; detectable HCV viremia by PCR; HbA1C < 9 % for diabetic patients; alpha-fetoprotein (AFP) < 100 ng/mL (Triphasic CT was ordered for exclusion of HCC if AFP > 100 ng/mL); female patients practicing contraception; wife of a male patient practicing contraception; patients older than 65 years old should undergo cardiac evaluation by ECG, echocardiography and cardiac consultation before treatment; noncirrhotic and compensated cirrhosis (Child's class A) who failed previous treatment with sofosbuvir and daclatasvir (easy to treat group) or sofosbuvir, daclatasvir and ribavirin (difficult to treat group).

Exclusion criteria for treatment according to the supreme council and the national committee for control of viral hepatitis (NCCVH), December 2016: patients with Child's class B and C; patients with hepatocellular carcinoma except after 6 months of successful radical curative intervention aiming at a cure with no activity as detected with dynamic imaging as CT or MRI; apregnant female or inability to implement effective contraception; inadequate control of diabetes (HA1C % > 9); extrahepatic malignancy excepts after 2 years of a disease-free interval; patients with hypersensitivity to drugs.

2.2. *Methods*

All subjects underwent thorough history taking (including a history of hepatic encephalopathy, ascites, previous HCV treatment, adherence to previous treatment, previous endoscopies or upper GIT bleeding, diabetes, hypertension, smoking, and contraceptive pills usage or other drug histories) and through physical examination.

2.3. *Routine Biochemical measurements*

Serum total and direct bilirubin, albumin, serum alanine transaminase (ALT) level, aspartate transaminase (AST), urea, creatinine, CBC, prothrombin time (PT), prothrombin concentration, partial thromboplastin time (PTT), International Normalizing Ratio (INR), fasting, postprandial blood sugar, HA1c, AFP, HBs antigen, pregnancy test, and PCR for HCV-RNA (the lower limit of detection of HCV-RNA was 12 IU/ML).

2.4. *Radiological investigations*

Pelvi-abdominal ultrasonography for examination of the liver, portal vein diameter, spleen, detection of hilar varices, focal lesions and ascites.

2.5. *Staging of liver fibrosis*

Was assessed by Metavir Score (if available), FIB-4 or Transient elastography scoring (Fibro scan if available) at any time prior to enrolment. Cirrhosis was diagnosed when patients show cirrhosis in their liver biopsy, liver stiffness by Fibroscan of 12.5 kPa or more or Fib-4 > 2.5.

2.6. *Treatment protocols*

Generic SOF was supplied to the Ministry of Health centers by many manufacturing Egyptian facilities as AUG Pharma, Marcyrl, and Pharco while generic ribavirin was supplied by Amriya pharmaceutical, Egypharma, Mash Pharmaceuticals, Pharco, and T3A pharmaceuticals. Ombitasvir, paritaprevir, ritonavir was supplied as Qurevo® by Abbvie pharmaceuticals.

SOF/OBV/PTV/r + RBV group (ribavirin eligible

subjects): received treatment for 12 weeks: Sofosbuvir 400 mg once daily; ombitasvir 25 mg + paritaprevir 150 mg and ritonavir100mg (two capsules) PO q Day with the meal; Ribavirin (RBV) was supplied in 200 mg capsule, recommended dose: 1,200 mg daily if weight > 75 kg or 1,000 mg daily if weight ≤ 75kg divided daily dose BID with food.

SOF/OBV/PTV/r group (ribavirin ineligible subjects): received treatment for 24weeks: Sofosbuvir 400mg once daily; ombitasvir25mg + paritaprevir 150 mg and ritonavir100mg (two capsules) PO q Day with the meal.

RBV ineligible/intolerance was defined as: Neutrophils < 750 cells/mm^3, results within the past protocol therapy; Haemoglobin < 10g/dL, results within the past protocol therapy; Platelets < 50,000 cells/mm^3, results within the past protocol therapy; Autoimmune hepatitis or other autoimmune condition is known to be exacerbated by ribavirin; Known hypersensitivity to ribavirin within the past protocol therapy.

Monitoring of treatment and adverse effects was done by: Quantitative PCR 12 weeks after the end of the treatment protocol to confirm viral eradication and detect SVR12; ALT, AST every month; Bilirubin (total and direct) and CBC every 2 weeks in patients subjected to 12 weeks therapy and every month in patients subjected to 24 weeks therapy. Ribavirin dose was reassessed according to hemoglobin level and ministry of health (MOH) protocol. Discontinuation of treatment was planned on the experience of severe adverse effects as severe anemia, jaundice or new liver decompensation.

2.7. *Endpoints*

The primary endpoint represents a sustained virological response (HCV RNA < 12 IU/mL), observed 12 weeks after the end of the treatment (SVR12).

2.8. *Statistical analysis*

The obtained data were analyzed statistically using SPSS program version 20 (SPSS, Chicago, IL). Data were expressed as means ± standard deviation in quantitative variables; and numbers and percentages for qualitative variables. T-Test for variables with normal distribution, Mann-Whitney *U* test for variables with abnormal distribution, Chi-Square tests (χ^2) were used when appropriate. The results were considered statistically significant if the *p* value was < 0.05.

3. Results

3.1. *Basic characteristics and demographic data of studied patients*

Ribavirin eligible treatment-experienced patients (*27*) were treated with SOF with OBV/PTV/r plus RBV for 12 weeks while ribavirin ineligible treatment-experienced patients (*48*) were treated with SOF with OBV/PTV/r for 24 weeks.

The two groups of treatment were matched regarding age, sex, comorbid factors as diabetes, hypertension, and smoking. A significant difference between the two groups was found as regards total bilirubin, INR, and FIB4 score, as well as the number of cirrhotic patients, being higher in SOF with OBV/PTV/r group that were ribavirin intolerant. Also, albumin, WBC's count, hemoglobin concentration, and platelets count were significantly lower. However, no significant difference as regards other variables were found ($p > 0.05$) (Table 1).

3.2. *SVR rates*

Per-protocol SVR rates were 100% with no treatment failure in both investigated groups while the intention-to-treat results were 93.4% in all patients, 97.9% in SOF with OBV/PTV/r group and 85.2% in SOF with OBV/PTV/r + RBV group (Figure 1 and 2).

3.3. *Adverse effects and discontinuations*

The regimen was generally well tolerated and the most common adverse effects observed across treatment and during the follow-up period included fatigue (38.6%), headache (29.3%), and hyperbilirubinemia (21.3%) (Table 2). These adverse effects were slightly significantly more notable in the ribavirin group ($p < 0.05$).

Current study data revealed there were no deaths, but discontinuations of therapy recorded due to adverse effects as severe jaundice and pruritis occurred in five patients (6.6%) that was slightly more significant in SOF with OBV/PTV/r + RBV group ($p < 0.05$) (Figure 2, Table 2).

4. Discussion

Treatment of HCV with the new era of DAAs offered a renewed hope to Egyptian patients. According to NCCVH treatment protocol (December 2016), the first option was combining 400 mg sofosbuvir and 60 mg daclatasvir in two separate tablets that was introduced in November 2015 and it was the most prevalent treatment option used due to the availability of low price local generics. The second option was treatment with the fixed-dose combination of ombitasvir, paritaprevir and ritonavir in two tablets given daily with food and weight-based ribavirin and was approved for use in Egypt in October 2015, however, this option was restricted to patients with renal failure.

Retreatment of HCV with DAA of the same class plus an addition of DAA with another mechanism of action and/or new DAA can achieve high SVR in patients that had previous treatment failure with DAAs treatments (*14*) for this reason combination therapy of

Table1. Basic characteristics and demographic data of studied patients

Items	SOF/OBV/PTV/r, (*n* = 48, 24 Weeks)	SOF/OBV/PTV/r + RBV, (*n* = 27, 12 Weeks)	*p*-value
Age (y) (M ± SD)	52.6 ± 9.02	48.2 ± 10.6	0.66
Male	35 (72.9%)	18 (66.6%)	0.56
Female	13 (27.1%)	9 (33.4%)	
Diabetes	6 (12.5%)	3 (11%)	0.85
Hypertension	5 (10.4%)	4 (14.8%)	0.57
Smoking	9 (18.7%)	5(18.5%)	0.98
Laboratory data (M ± SD)			
Total bilirubin (mg/dL)	1.2 ± 0.31	0.81 ± 0.21	< 0.001*
ALT (ULN:40U/L)	63.3 ± 53.8	62.1 ± 31.4	0.91
AST (ULN:40U/L)	58.5 ± 30.8	56.4 ± 23.3	0.75
Albumin (g/dL)	3.6 ± 0.45	3.8 ± 0.17	0.03*
INR	1.4 ± 0.4	0.9 ± 0.5	< 0.001*
WBC ($\times 10^3/mm^3$)	5.3 ± 1.5	6.3 ± 1.2	0.004*
Haemoglobin (g/dL)	11 ± 0.86	12 ± 1.15	< 0.001*
Platelets ($\times 10^3/mm^3$)	120.6 ± 22.6	142.8 ± 22.06	< 0.001*
HCV PCR (IU/mL)	690234.36 ± 1803147.07	515033.27 ± 1337072.7	0.66
Type of patient			
Non cirrhotic	10 (20.8%)	12 (44.4%)	0.03*
Cirrhotic	38 (79.2%)	15 (55.6%)	
Previous treatment			
[a]SOF/DCV	3 (6.25%)	0 (0%)	0.64
[b]SOF/DCV/RBV	45 (93.75%)	27 (100%)	
FIB4	3.21 ± 0.9	2.42 ± 1	0.001*

*Significant value, [a]sofosbuvir/daclatasvir, [b]sofosbuvir/daclatasvir/ribavirin, ALT: alanine transaminase; AST: aspartate transaminase; INR: international normalized ratio; WBC: white blood cell count.

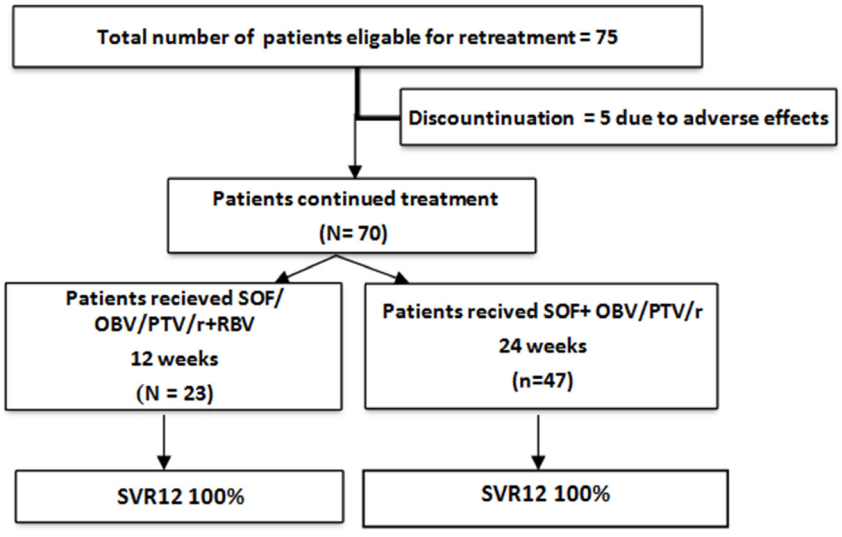

Figure 1. Per protocol SVR12 among patients completed the study.

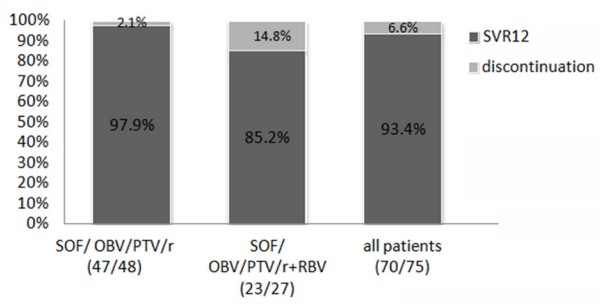

Figure 2. Intention to treat SVR12 and discontinuation percentages among treatment groups.

ombitasvir, paritaprevir, and ritonavir plus sofosbuvir was used and was the only treatment option available in Egypt for experienced patients who failed previous treatment with SOF/DCV therapy.

Optimizing treatment outcomes in patients with cirrhosis includes either the addition of RBV or prolonging treatment duration (*15,16*) for this reason, 48 patients in our study who were ribavirin ineligible were subjected to prolonged treatment period for 24 weeks.

Current study results showed that the per-protocol SVR12 rate was (100%; 70/70) in both studied groups

Table 2. Adverse effects among treatment groups

Items	SOF/OBV/P/r		SOF/OBV/PTV/r+ RBV		Total		*p*-value
	No	%	No	%	No	%	
Hyperbilirubinemia	6	12.5	10	37	16	21.3	0.01*
Diarrhea	5	10.4	7	25.9	12	16	0.78
Headache	10	20.8	12	44.4	22	29.3	0.03*
Itching/Rash/pruritus	5	10.4	8	29.6%	13	17.3	0.03*
Loss of appetite	8	16.6	6	22	14	18.6	0.55
Nausea	3	6.25	4	14.8	7	9.3	0.22
Insomnia	5	10.4	4	14.8	9	12	0.57
Fatigue	14	29.1	15	55.5	29	38.6	0.02*
Anaemia	1	2	5	18.5	6	8	0.01*

*Significant value.

without treatment failure while the intention-to-treat were (93.4%; 70/75) in all patients, (97.9%; 47/48) in SOF with OBV/PTV/r group, and (85.2%; 23/27) in SOF with OBV/PTV/r plus RBV group, near results obtained by Abdel-Moneim *et al*. (17) who evaluated retreatment efficacy of SOF/OBV/PTV/r + RBV for 12 weeks in HCV genotype 4 experienced patients who failed treatment with DAAs-based regimens and found overall per-protocol SVR12 rate (97%; 109/113), SVR12 was achieved by (98%; 81/83) of non-cirrhotic patients and (93%; 28/30) of cirrhotic patients. The SVR12 results differences between the current study and Abdel-Moneim *et al*. may be due to more limited number of cases in the current study. However, in the current study similar SVR12 for both cirrhotic and noncirrhotic patients who completed treatment protocol duration was found.

Sanai *et al*. (*18*) assessed the efficacy of co-formulated ombitasvir/paritaprevir/ritonavir in the treatment of HCV GT4 ± RBV with chronic kidney disease stage 4-5. This study included treatment-naïve and peginterferon/RBV-experienced GT4-infected patients (n = 32) treated for 12-24 weeks, 19.4% were treated without RBV; Overall, 97.1% patients achieved SVR12, including 100% of those with a post-treatment follow-up (modified ITT analysis) with no virological failures. The virological response was equal in both treatment naive and experienced, cirrhotic and noncirrhotic and those who received or not received ribavirin.

Despite the recommendation for the addition of RBV in the product label and in guidelines, 48 patients who were ribavirin ineligible were treated without RBV for 24 weeks. All patients who received a RBV-free regimen achieved SVR12, however, they recommended that the role of RBV must be further explored in larger clinical trials. Our study shows that RBV-free cohort (24 weeks) achieved high SVR12 with less significant side effects than RBV-containing one (12 weeks).

According to current results, neither baseline demographic features as age and sex nor comorbid factors as DM, hypertension, and smoking affected SVR12. In addition, the virological response was unaffected by the degree of viremia, previous treatment protocols nor fibrosis degree assessed by FIB4 results, a similar conclusion was reached by other studies who confirmed that age, body mass index, HCV-RNA levels, GT4 subtype, and IL-28B genotype, may not impact significantly on the virological response (*17,18*).

The regimen was generally well tolerated and the most common adverse effects observed across treatment and after follow-up were fatigue and headache. Our findings were in agreement with the studies of Abdel-Moneim *et al*. (*17*) and Sanai *et al*. (*18*).

Hyperbilirubinemia is the most observed laboratory abnormality and was responsible for discontinuations of therapy in five patients due to severe jaundice and pruritis, this may be explained by ribavirin-induced hemolysis and known inhibition of the organic anion transporting polypeptide 1B1 bilirubin transporter by protease inhibitors (*19*).

In conclusion, the combination of sofosbuvir with ombitasvir, paritaprevir, ritonavir ± RBV is well tolerated and achieved high SVR12 rates in chronic HCV GT4 Egyptian patients with previous SOF/DCV treatment failure. Ribavirin free regimen for 24 weeks had high SVR12 as 12 weeks ribavirin regimen with lesser adverse effects and offered a hope for treatment of patients who are ribavirin intolerant.

References

1. Waked I, Doss W, El-Sayed MH, Estes C, Razavi H, Shiha G, Yosry A, Esmat G. The current and future disease burden of chronic hepatitis C virus infection in Egypt. Arab J Gastroenterol. 2014; 15:45-52.
2. Bruggmann P, Berg T, Ovrehus AL, *et al*. Historical epidemiology of hepatitis C virus (HCV) in selected countries. J Viral Hepat. 2014; 21:5-33.
3. Sievert W, Altraif I, Razavi HA, *et al*. A systematic review of hepatitis C virus epidemiology in Asia, Australia, and Egypt. Liver Int. 2011; 31:61-80.
4. Gower E, Estes C, Blach S, Razavi-Shearer K, Razavi H. Global epidemiology and genotype distribution of the hepatitis C virus infection. J Hepatol. 2014; 61:45-57.
5. El Sayed M. Access to innovation: Hepatitis C and the Egyptian national experience. *https://www.wto.org/english/tratop_e/trips_e/trilat_symp15_e/Manal_*

trilatsymp_e.pdf. (Accessed January 14, 2016).
6. AASLD/IDSA HCV Guidance Panel. Hepatitis C guidance: AASLD-IDSA recommendations for testing, managing, and treating adults infected with hepatitis C virus. J Hepatol. 2015; 62:932-954.
7. Estrabaud E, Vidaud M, Marcellin P, Asselah T. Genomics and HCV infection: Progression of fibrosis and treatment response. J Hepatol. 2012; 57:1110-1125.
8. Omar H, El Akel W, Elbaz T, *et al*. Generic daclatasvir plus sofosbuvir, with or without ribavirin, in treatment of chronic hepatitis C: Real-world results from 18 378 patients in Egypt. Aliment Pharmacol Ther. 2018; 47:421-431.
9. Lawitz E, Mangia A, Wyles D, *et al*. Sofosbuvir for previously untreated chronic hepatitis C infection. N Engl J Med. 2013; 368:1878-1887.
10. DeGoey DA, Randolph JT, Liu D, *et al*. Discovery of ABT267, a pan-genotypic inhibitor of HCV NS5A. J Med Chem. 2014; 57:2047-2057.
11. Pawlotsky JM. Hepatitis C. Virus resistance to direct-acting antiviral drugs in interferon-free regimens. Gastroenterol. 2016; 151:70-86.
12. Buti M, Esteban R. Management of direct antiviral agent failures. Clin Mol Hepatol. 2016; 22:432-438.
13. Asselah T, Boyer N, Saadoun D, Martinot-Peignoux M, Marcellin P. Direct-acting antivirals for the treatment of hepatitis C virus infection: Optimizing current IFN-free treatment and future perspectives. Liver Int. 2016; 36:47-57.
14. Tamori A, Enomoto M, Kawada N. Recent advances in antiviral therapy for chronic hepatitis C. Mediators Infamm. 2016; 2016:6841628.
15. Nelson DR, Cooper JN, Lalezari JP, *et al*. All-oral 12-week treatment with daclatasvir plus sofosbuvir in patients with hepatitis C virus genotype 3 infection: ALLY-3 phase III study. J Hepatol. 2015; 61:1127-1135.
16. Majumdar A, Kitson MT, Roberts SK. Systematic review: Current concepts and challenges for the direct-acting antiviral era in hepatitis C cirrhosis. Aliment Pharmacol Ther. 2016; 43:1276-1292.
17. Abdel-Moneim A, Aboud A, Abdel-Gabbar M, Zanaty M, Ramadan M. Retreatment efficacy of Sofosbuvir/Ombitasvir/Paritaprevir/Ritonavir+Ribavirin for hepatitis C virus genotype 4 patients. Dig Dis Sci. 2018; 63:1341-1347.
18. Sanai FM, Alghamdi AS, Afghani AA Alswat K, AlZanbagi A, Alghamdi MN, AlMousa A, Aseeri M, Assiri AM, Babatin MA. High efficacy of ombitasvir/paritaprevir/ritonavir plus dasabuvir in hepatitis C genotypes 4 and 1-infected patients with severe chronic kidney disease. Liver Int. 2018; 38:1395-1401.
19. Manns MP, Bourliere M, Benhamou Y, *et al*. Potency, safety, and pharmacokinetics of the NS3/4A protease inhibitor BI201335 in patients with chronic HCV genotype-1 infection. J Hepatol. 2011; 54:1114-1122.

(Received December 12, 2018; Revised December 21, 2018; Accepted December 29, 2018)

Case Report

DOI: 10.5582/ddt.2018.01064

Two cases of Osteoarticular Mucor menace: A diagnostic and management conundrum

Manasvini Bhatt[1], Manish Soneja[1,*], Farhan Fazal[1], Surabhi Vyas[2], Prabhat Kumar[1], Pankaj Jorwal[1], Upendra Raj[1], Janya Sachdev[3], Gagandeep Singh[3], Immaculata Xess[3], Shah Alam[4], Ashutosh Biswas[1]

[1] *Department of Medicine, All India Institute of Medical Sciences, New Delhi, India;*
[2] *Department of Radiodiagnosis, All India Institute of Medical Sciences, New Delhi, India;*
[3] *Department of Microbiology, All India Institute of Medical Sciences, New Delhi; India;*
[4] *Department of Orthopedics, All India Institute of Medical Sciences, New Delhi, Inida.*

Summary **Mucormycosis is an uncommon aggressive fungal infection usually seen in immunocompromised hosts or patients with burns and trauma. The common presentations include rhino-orbital-cerebral and pulmonary involvement. Osteoarticular involvement is a rare presentation of this disease. We present two cases of osteoarticular mucormycosis of pelvis and long bones of the lower limb, one in a patient with burn injury and other one in a patient with chronic granulomatous disease, hitherto a rarely reported association. Delayed diagnosis in a setting where tuberculosis is a common cause of chronic osteomyelitis, challenges in medical and surgical management of these patients are discussed in this report.**

Keywords: Mucormycosis, bone mucormycosis, chronic granulomatous disease

1. Introduction

Mucormycosis is an infection caused by ubiquitous fungi of the order Mucorales and the genera most commonly reported to cause disease includes *Rhizopus*, *Mucor* and *Rhizomucor.* The disease is mostly seen in patients with diabetes mellitus, hematological malignancies, hematopoietic cell and solid organ transplantation, trauma, burns and those on glucocorticoid therapy. This angioinvasive fungal disease can present with varied clinical manifestations, including rhino-orbital-cerebral, pulmonary, cutaneous, gastrointestinal, disseminated and miscellaneous forms (*1-3*).

Osteoarticular mucormycosis (excluding extension following rhinosinusitis) is a rare manifestation of this disease. In a systematic review, 34 reported cases were identified between 1978 and 2014 (*4*). We reported a case of long bone mucormycosis and *Mycobacterium abscessus* infection recently (*5*). Mucormycosis can involve bones and joints with the site depending on the mechanism of infection; long bones may be affected after trauma or surgery, or a wide variety of bones may be involved after hematogenous dissemination. Diagnosis is challenging particularly in a setting with rampant tuberculosis. The destructive nature of Mucorales, in addition to the predisposing risk factors presents a formidable challenge in management of these patients. We highlight the above issues in two patients diagnosed with this rare form of the disease.

**Address correspondence to:*
Dr. Manish Soneja, Department of Medicine, All India Institute of Medical Sciences, New Delhi, India.
E-mail: manishsoneja@gmail.com

2. Case Report

2.1. *Case 1*

A 22-year-old male with no prior comorbidities, apparently well 3 months back, presented with complain of intermittent low-grade fever (documented 100-101° F), associated with continuous dull aching low back pain and weakness of bilateral lower limbs. The weakness was insidious onset, started in left lower limb and gradually progressed to right lower limb over a period of 15 days with bowel and bladder incontinence. He was evaluated at a local hospital, where a magnetic resonance imaging (MRI) of lumbosacral spine with bilateral hip joints was done and category 1 anti-tubercular therapy was initiated with a provisional diagnosis of tubercular sacroiliitis. A month after onset

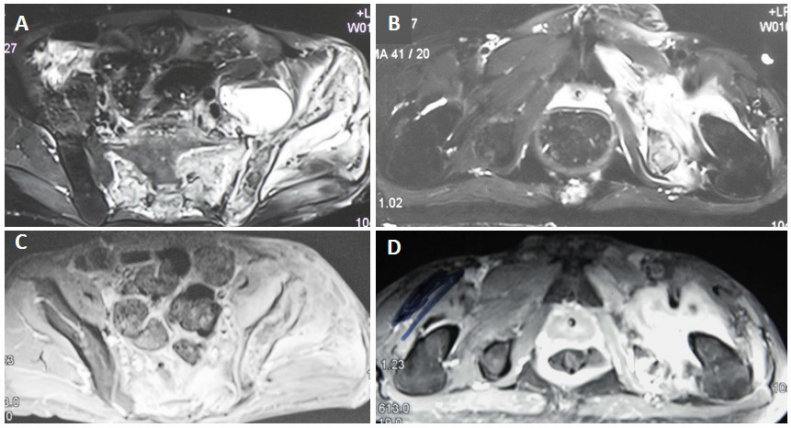

Figure 1. MRI images. Axial fat suppressed T2 images at the level of sacroiliac joints **(A)** and ischial tuberosity **(B)** at the time of admission showing left ilio-psoas collection and bony involvement of the sacrum and left hemipelvis (more on left side and left SI joint). Corresponding images post first debridement **(C,D)** showing mild reduction in the left side collection; however, the sacral involvement appears more extensive.

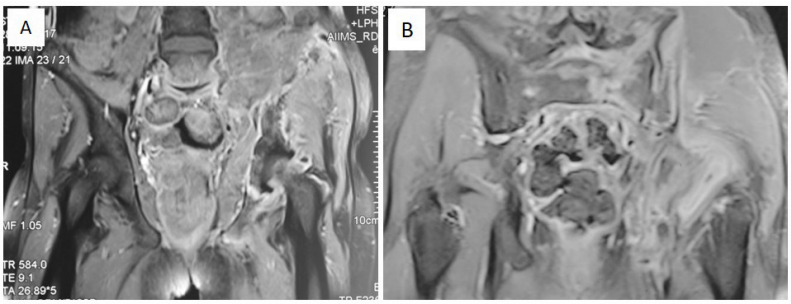

Figure 2. MRI images. Coronal post contrast images at admission **(A)** and follow-up **(B)** showing increased bony involvement and left sided collection.

of fever, he noticed a swelling over the left hip which progressively increased in size and ruptured with black-colored discharge from the wound 10 days later. The area was surgically debrided and histopathological examination was suggestive of aseptate broad hyphae compatible with mucormycosis. He was referred to our institute for further management.

Local examination revealed two ulcers in left gluteal region and left sacral region of size 2 × 3 cm and 3 × 1 cm respectively, with a clean base and granulation tissue. On neurological examination, power grade was 2/5 with deep tendon reflexes absent in left lower limb and mute plantar; power grade was 4/5 in right lower limb. Rest of the general and systemic examination was unremarkable, and vitals were stable. He denied any history of trauma or intramuscular injections.

MRI films were reviewed which revealed left sacroiliitis, left hip arthritis and left psoas collection (Figures 1A, 1B, and 2A). Differentials of a fungal infection (mucormycosis of left pelvic bone), multidrug resistant tuberculosis, non-tubercular mycobacterial infection and chronic bacterial osteomyelitis were considered. Ultrasonography (USG) guided aspiration of gluteal abscess was done, wherein gram stain/culture, fungal stain/culture and GeneXpert were negative. Hematological investigations revealed normocytic normochromic anemia and raised inflammatory markers (Table 1). Liposomal amphotericin B (L-AmB) was initiated at a dose of 10 mg/kg.

MRI was repeated after three weeks of treatment, which did not reveal any improvement, hence caspofungin was added as a rescue therapy. He was evaluated for primary and secondary immunodeficiency which revealed low B and T-cell counts, low neutrophil oxidase activity, feature consistent with chronic granulomatous disease (CGD). A 2-deoxy-2-(^{18}F)fluoro-D-glucose positron emission tomography/computed tomography (^{18}F-FDG PET/CT) scan was performed to determine the disease extent which revealed left paraaortic, prevertebral, common iliac, internal iliac, left external iliac and left inguinal lymph nodes with hepatosplenomegaly. No uptake in liver and spleen was seen.

Meanwhile, he developed drug reaction and leucopenia, secondary to amphotericin, hence it was withheld and later re-started at a lower dose (5 mg/kg). Surgical debridement of pelvis was done, which reconfirmed the diagnosis of mucormycosis (Figure 3). A repeat MRI was done after 4 weeks of surgery revealed worsening in the form of increased left gluteal and iliopsoas collection (Figures 1 C, 1D, and 2B). The collections were drained under USG guidance and

Table 1. Hematological and biochemical profile of the 2 patients

Date	Patient 1/At admission	Patient 1/At discharge	Patient 2/At admission	Patient 2/At discharge
Hb (gm/dL)	8.1	10.3	9.7	8.2
Platelet count (/mm^3)	574 × 10^6	270 × 10^6	2.57 × 10^6	112 × 10^6
TLC (/mm^3)	8,500	5,600	9,000	5,400
Urea (mg/dL)	25	31	25	71
Creatinine (mg/dL)	0.2	1.2	0.4	2.4
Na (mEq/L)	139	134	135	135
K (mEq/L)	3.5	4.4	4.3	3.5
Bilirubin (mg/dL)	0.5	0.4	0.2	0.3
Total protein (g/dL)	6.2	6.4	7.4	6
Albumin (g/dL)	2.7	3.0	3.4	3.8
Globulin (g/dL)	3.5	3.4	4	2.2
SGOT (IU/L)	20	19	17	7
SGPT (IU/L)	19	11	10	6
ALP (IU/L)	322	239	225	236
ESR (mm/hr)	66	52	75	32
CRP (mg/L)	66	20.6	28	16

Hb: Hemoglobin, TLC: Total leukocyte count, Na: Sodium, K: Potassium, SGOT: Aspartate transaminase, SGPT: Alanine transaminase, ALP: Alkaline phosphatase, ESR: Erythrocyte sedimentation rate, CRP: C-reactive protein.

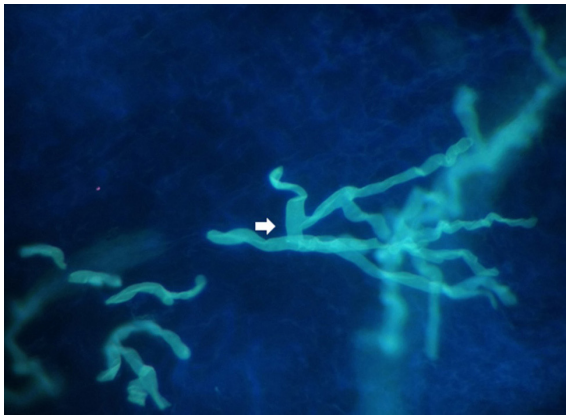

Figure 3. Microscopy findings. Broad aseptate hyphae are observed with right angle branching (arrow) and ribbon like folding under 40x in Calcofluor white-KOH mount indicating mucormycosis.

broad-spectrum antibiotics were initiated to cover for superadded bacterial infection. Due to repeated drug-related toxicities, L-AmB was withheld (total dose 35 grams) and oral posaconazole was initiated. He showed clinical improvement and started ambulating with support. A repeat MRI performed 3 months after surgery revealed partial response.

2.2. *Case 2*

A 40-year-old male, with no prior comorbidities, presented with chronic discharging sinus on the anterior aspect of right leg for 5 months. The sinus developed following debridement performed for burn injury over the leg. He also complained of severe intensity pain in the leg and recurrent episodes of fever (documented 100-101° F) with chills. He was evaluated at a local healthcare facility and diagnosed to have chronic osteomyelitis and referred to our institute. On evaluation, patient was conscious and oriented and vitals were stable. Local examination revealed 10 × 6 cm ulcer present over anterior aspect of lower third of tibia with black eschar with pale granulation tissue with active discharge from the wound. Rest of the general physical and systemic examination was unremarkable. He had anemia and raised inflammatory markers (Table 1).

In view of active discharging sinus, broad-spectrum antibiotics were initiated. A bone biopsy from tibia done outside, was reviewed which showed dead bone trabeculae along with right angle branching broad septate hyphae consistent with mucormycosis. Patient was started on L-AmB at a dose of 5 mg/kg which had to be stopped after second dose in view of deranged renal parameters. Orthopedic opinion was taken and debridement with wash with sinus tract excision with sequestrectomy and saucerization of right tibia was performed. Patient had an uneventful intraoperative and post-operative period and was discharged on oral posaconazole (200 mg QID), due to recurrent acute kidney injury on introduction of L-AmB. A repeat MRI performed 4 weeks after surgery revealed spread of bony lesions to left femur (Figures 4A-4D). The patient was re-admitted, and an above knee amputation was performed after thorough discussion and informed consent. The intraoperative and postoperative events were uneventful. At 2 months follow-up, he was asymptomatic and repeat MRI revealed mild T2/STIR hyperintensity in thigh muscles suggestive of residual disease.

3. Discussion

Osteoarticular mucormycosis is an uncommon manifestation of mucormycosis. In a systematic review of database from 1978 to 2014, only 34 cases were reported (*4*). The review excluded cases of bone

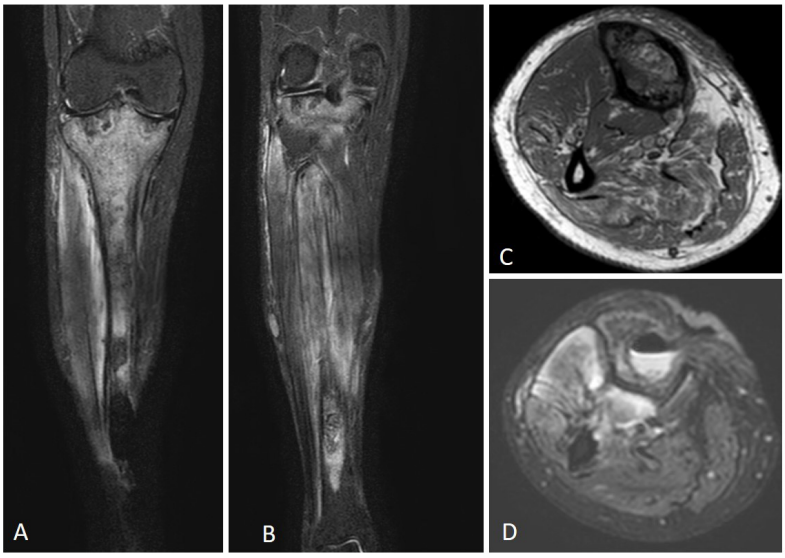

Figure 4. MRI images. (A and B) Fat suppressed T2 coronal images showing extensive marrow signal alteration involving the tibia. **(C)** Axial T1 weighted image showing cortical irregularity and erosions of the tibia. The fibula (*) shows normal marrow and cortical signal. **(D)** Axial fat suppressed T2 weighted image shows an air fluid level within the tibial marrow cavity with sinus tract extending to the skin surface (*). Note also the extensive edema involving the surrounding muscles (arrow).

extension following rhinosinusitis, which is a common site of presentation for mucormycosis. Both our patient had proven mucormycosis as aseptate hyphae was demonstrated in histopathology sections.

Osteoarticular mucormycosis has been reported most frequently after surgical procedures (41%) and trauma (21%); diabetes mellitus (18%) and corticosteroid use (21%) being other significant predisposing factors (*4*). Our second patient had a prior burn injury and underwent surgical procedure; however, the first patient did not have any of the above predisposing conditions. Further, he did not have other source for hematogenous spread of infection, as there was no FDG uptake at any other site on 18F FDG PET-CT scan. His primary immunodeficiency work up revealed low total B and T-cell counts, with low neutrophil oxidase activity (dihydrorhodamine (DHR) assay) suggestive of CGD. Patients with CGD are uniquely susceptible to invasive aspergillosis, but invasive mucormycosis is rare and occurs mostly if patient is receiving corticosteroids (*6*). In a series of 278 patients with CGD, only 5 patients had invasive mucormycosis and all of them were on corticosteroids (*6*). However, neither of our patients received corticosteroids.

The most common presenting features are local symptoms including swelling, tenderness, pain and restriction of movements, while fever is reported in around one-fourth of the patients (*4*). The local features were present in both our patients; fever was present in the first patient since disease onset, while superadded infection was the probable cause of fever in second patient. The reported median diagnostic delay from onset of symptoms is 60 days (*4*). The treatment in our patients was initiated 3 and 5 months respectively, after initial symptoms. Diagnosis of this rare manifestation is challenging in a setting with high burden of tuberculosis, like ours. Biopsy is the mainstay of diagnosis as imaging features are non-specific (*4*).

The cornerstone of management is combined surgical and medical approach. L-AmB is the mainstay of medical therapy and posaconazole is used as maintenance therapy, while debridement (38%) is the most common surgical procedure followed by bone grafting (21%), amputation (15%) and full excision (15%) depending on the site of involvement (*4*). Our first patient had extensive local infiltrative disease, making radical excision a difficult choice and hence, local debridement was opted for. The second patient at presentation had a localized disease and hence, initially a conservative approach with debridement was adopted. However, the rapid spread of disease led to the decision of amputation to preserve the unaffected part of the limb.

The recommended first line of medical therapy for mucormycosis is liposomal or lipid-complex amphotericin B at a minimum dose of 5 mg/kg/day, while posaconazole is recommended as salvage therapy (*7*). The efficacy of L-AmB in mucormycosis is variable across studies depending upon site and extent of involvement, timing of initiation and underlying predisposing conditions. Distinctive immunopathogenesis features contribute to poor response in mucormycosis compared to other invasive fungal infections (*8*). In systematic review of osteoarticular variant of disease, the mortality rate reported was 24% (*4*). Delay in diagnosis may be one of the factors contributing to high failure rates. Management of our patients was further complicated by adverse effects of the drug particularly in the second patient. The drug related nephrotoxicity varies depending on the patient profile, drug dosage

and duration of therapy. In a recent retrospective analysis of 103 treatment courses of L-AMB, 19.4% of patients were classified at risk, 13.6% met an injury classification, and 5.8% were categorized as developing renal failure according to the RIFLE category for renal injury (*9*). Long term L-AmB therapy is associated with more adverse effects (*10*). We discontinued L-AmB in both patients and shifted them to oral posaconazole (800 mg/d). It has been used both in combination with L-AmB and as second line therapy with reported complete and partial response rates of approximately 65% and 7% respectively (*11*). The currently available evidence supports the use of posaconazole as a reserve drug for de-escalation, refractory cases, or patients intolerant to L-AmB (*1,7,12*). The benefit of combination of L-Amb with echinocandin has been reported previously; however, there is insufficient evidence of its efficacy (*13,14*). We used caspofungin in combination with L-AmB as a rescue therapy in the first patient. The two patients have partial response to therapy with clinical resolution of symptoms and improved, albeit persisting radiological findings and are currently on posaconazole. The duration of treatment is not defined and in osteoarticular mucormycosis median time of LAmB use is 45 (5-573) days (*4*).

Osteoarticular mucormycosis is a rare disease and associated with significant morbidity and mortality. Increased awareness will prompt the clinician to suspect this condition in an appropriate setting and attempt early diagnosis by requesting for biopsy with histopathology, staining and culture for fungal etiology. Combined surgical and medical management is the cornerstone for therapy. The duration of antifungals is not defined and it is prudent to continue therapy till there is both clinical and radiological resolution of the disease.

References

1. Riley TT, Muzny CA, Swiatlo E, Legendre DP. Breaking the mold: A review of mucormycosis and current pharmacological treatment options. Ann Pharmacother. 2016; 50:747-757.
2. Tansir G, Rastogi N, Ramteke P, Kumar P, Soneja M, Biswas A, Kumar S, Jorwal P, Baitha U. Disseminated mucormycosis: A sinister cause of neutropenic fever syndrome. Intractable Rare Dis Res. 2017; 6:310-313.
3. Sriranga R, Pawar S, Khot W, Nischal N, Soneja M, Venkatesh HA, Nair RR, Kanna R, Sharma MC, Sharma SK. Isolated renal mucormycosis. J Assoc Physicians India. 2017; 65:77-81.
4. Taj-Aldeen SJ, Gamaletsou MN, Rammaert B, Sipsas NV, Zeller V, Roilides E, Kontoyiannis DP, Henry M, Petraitis V, Moriyama B, Denning DW, Lortholary O, Walsh TJ; International Osteoarticular Mycoses Consortium. Bone and joint infections caused by mucormycetes: A challenging osteoarticular mycosis of the twenty-first century. Med Mycol. 2017; 55:691-704.
5. Gupta N, Banerjee S, Timitrov, Sharma R, Roy SG, Shende TM, Ansari MT, Singh G, Nischal N, Wig N, Soneja M. Osteomyelitis due to multiple rare infections in a patient with idiopathic CD4 lymphocytopenia. Intractable Rare Dis Res. 2017; 6:206-210.
6. Vinh DC, Freeman AF, Shea YR, Malech HL, Abinun M, Weinberg GA, Holland SM. Mucormycosis in chronic granulomatous disease: Association with iatrogenic immunosuppression. J Allergy Clin Immunol. 2009; 123:1411-1413.
7. Cornely OA, Arikan-Akdagli S, Dannaoui E, *et al*. ESCMID and ECMM joint clinical guidelines for the diagnosis and management of mucormycosis 2013. Clin Microbiol Infect. 2014; 20 (Suppl 3):5-26.
8. Katragkou A, Walsh TJ, Roilides E. Why is mucormycosis more difficult to cure than more common mycoses? Clin Microbiol Infect. 2014; 20 (Suppl 6):74-81.
9. Stanzani M, Vianelli N, Cavo M, Maritati A, Morotti M, Lewis RE. Retrospective cohort analysis of liposomal amphotericin B nephrotoxicity in patients with hematological malignancies. Antimicrob Agents Chemother. 2017; 61 pii:e02651-16.
10. Loo AS, Muhsin SA, Walsh TJ. Toxicokinetic and mechanistic basis for the safety and tolerability of liposomal amphotericin B. Expert Opin Drug Saf. 2013; 12:881-895.
11. Vehreschild JJ, Birtel A, Vehreschild MJ, Liss B, Farowski F, Kochanek M, Sieniawski M, Steinbach A, Wahlers K, Fätkenheuer G, Cornely OA. Mucormycosis treated with posaconazole: Review of 96 case reports. Crit Rev Microbiol. 2013; 39:310-324.
12. Pagano L, Cornely OA, Busca A, *et al*. Combined antifungal approach for the treatment of invasive mucormycosis in patients with hematologic diseases: A report from the SEIFEM and FUNGISCOPE registries. Haematologica. 2013; 98:e127-130.
13. Reed C, Bryant R, Ibrahim AS, Edwards J Jr, Filler SG, Goldberg R, Spellberg B. Combination polyene-caspofungin treatment of rhino-orbital-cerebral mucormycosis. Clin Infect Dis. 2008; 47:364-371.
14. Walsh TJ, Kontoyiannis DP. Editorial commentary: What is the role of combination therapy in management of zygomycosis. Clin Infect Dis. 2008; 47:372-374.

(Received October 18, 2018; Revised December 18, 2018; Accepted December 27, 2018)

Case Report

DOI: 10.5582/ddt.2018.01069

Apremilast induced chronic diarrhea and malnutrition

Bipadabhanjan Mallick*, Dibya L. Praharaj, Preetam Nath, Sarat C. Panigrahi

Department of Gastroenterology and Hepatology, Kalinga Institute of Medical Science, Bhubaneswar, India.

Summary **Apremilast is used as a systemic therapy for the treatment of psoriasis and psoriatic arthritis. This drug is considered relatively safe with a very low incidence of serious side effects. Common side effects are diarrhea, nausea, headache, nasopharyngitis, upper respiratory tract infections which are mild to moderate in severity. Diarrhea tends to occur within 2 weeks of starting treatment and resolve spontaneously within 4 weeks without dose adjustment or discontinuation of therapy. Chronic diarrhea and malnutrition due to apremilast have not been reported yet. We report a case of apremilast induced chronic diarrhea leading to malnutrition, necessitating discontinuation of therapy.**

Keywords: Apremilast, chronic diarrhea, malnutrition

1. Introduction

Apremilast is an oral phosphodiesterase 4 (PDE-4) inhibitor and it is used as a systemic therapy for psoriasis and psoriatic arthritis (*1*). This drug is relatively safe at approved dose of 30 mg twice daily, causes a few self resolving mild to moderate side effects which generally do not require discontinuation of therapy (*2*). Common side effects are diarrhea, nausea, headache, nasopharyngitis, upper respiratory tract infections and the reported incidence of diarrhea is close to 10 per 100 person-years (*3*). Diarrhea due to apremilast is secretory in nature which resolves spontaneously and do not require medical intervention, dose adjustment or discontinuation (*3*). We report a case of apremilast induced chronic diarrhea leading to malnutrition.

2. Case Report

A 56-year-old man with psoriasis and psoriatic arthritis of 10 years duration now presented with chronic diarrhea, nausea and weight loss of 10 kg for the past 6 months. He had hemoglobin level was 9.2 g/dL; total leukocyte count was 15,000 × 10^3/dL; and platelet count was 3.25 × 10^3/dL. He had hypoproteinemia and hypoalbuminemia with protein and albumin level of 4.6 g/dL and 1.9 g/dL respectively. The results of other liver function test and kidney function test were normal, and her total bilirubin level was 0.4 mg/dL; aspartate transaminase level was 31 IU/L; alanine transaminase level was 21 IU/L; alkaline phosphatase level was 123 IU/L; urea level was 10 mg/dL and creatinine level was 0.7 mg/dL. To determine the cause of diarrhea, we performed the routine stool examination and culture, which were non-contributory. Further, the result of serological examination for celiac disease (IgA anti-tissue transglutaminase antibody) was negative and thyroid function test were normal. His upper gastrointestinal endoscopy, colonoscopy and computed tomography (CT) enterography was normal. Histopathological examination of duodenal mucosa and right sided colonic mucosa were also normal. Human immunodeficiency virus serology was negative. On drug review he had been treated with steroid, cyclosporine and methotrexate of variable duration. The patient had been prescribed only apremilast 30 mg twice daily for psoriasis for the past 6 months without other immunomodulators. After discontinuation of apremilast his diarrhea subsided and at 2 month follow-up he has gained significant weight with serum albumin level of 3.4 g/dL and for psoriasis he has been started on steroid.

3. Discussion

Apremilast causes phosphodiesterase 4 (PDE-4) inhibition and it interrupts the inflammatory cascade

**Address correspondence to:*
Dr. Bipadabhanjan Mallick, Department of Gastroenterology and Hepatology, Kalinga Institute of Medical Science, Bhubaneswar, India.
E-mail: drbipadabhanjan@gmail.com

by blocking the degradation of cyclic adenosine monophosphate (cAMP) leading to increase in intracellular levels of cAMP which downgrade the production of several pro-inflammatory cytokines, like tumour necrosis factor (TNF)-α and interleukin (IL)-17 and IL-23 (*4*). This oral medication is well tolerated with minimal risk of serious side effects. Commonly reported side effects are diarrhea, nausea, headache, nasopharyngitis, upper respiratory tract infection which are generally self resolving and do not require dose adjustment or discontinuation of therapy (*3*).

Diarrhea due to apremilast is secretory in nature as it causes increases in intracellular cAMP levels within small intestinal crypt cells which activate chloride channels (*5*). Activated chloride channels promote fluid secretion into the gut lumen leading to development of diarrhea. Diarrhea usually resolves within 4 weeks and it might be due to effect of compensatory up-regulation of other phosphodiesterases in the small intestinal crypt cells (*6*). Recommended management of apremilast induced diarrhea is to begin with non-pharmacologic interventions such as ensuring adequate hydration, having small frequent meals and limiting consumption of other potential triggers for diarrhea (*3*). Patients not responding to non-pharmacologic interventions can be treated with over the counter medications like fibre supplement, bismuth subsalicylate or loperamide (*3*).

Most of the trials have reported that apremilast induced diarrhea were mild to moderate in severity, develop within 2 weeks of starting treatment and resolve spontaneously within 4 weeks (*2,6*). This drug has been approved 4 years ago and chronic diarrhea leading malnutrition due to apremilast has not been reported yet. With increased use of apremilast, incidence of chronic diarrhea and malnutrition like our case is expected to be reported more frequently.

References

1. Poole RM, Ballantyne AD. Apremilast: first global approval. Drugs. 2014; 74:825-837.
2. Cutolo M, Myerson GE, Fleischmann RM, Liote F, Diaz-Gonzalez F, Van den Bosch F, Marzo-Ortega H, Feist E, Shah K, Hu C, Stevens RM, Poder A. A phase III, randomized, controlled trial of apremilast in patients with psoriatic arthritis: Results of the PALACE 2 trial. J Rheumatol. 2016; 43:1724-1734.
3. Langley A, Beecker J. Management of common side effects of apremilast. J Cutan Med Surg. 2018; 22:415-421.
4. Schafer P. Apremilast mechanism of action and application to psoriasis and psoriatic arthritis. Biochem Pharmacol. 2012; 83:1583-1590.
5. Lambert JA, Raju SV, Tang LP, McNicholas CM, Li Y, Courville CA, Farris RF, Coricor GE, Smoot LH, Mazur MM, Dransfield MT, Bolger GB, Rowe SM. Cystic fibrosis transmembrane conductance regulator activation by roflumilast contributes to therapeutic benefit in chronic bronchitis. Am J Respir Cell Mol Biol. 2014; 50:549-558.
6. Crowley J, Thaci D, Joly P, Peris K, Papp KA, Goncalves J, Day RM, Chen R, Shah K, Ferrandiz C, Cather JC. Long-term safety and tolerability of apremilast in patients with psoriasis: Pooled safety analysis for ≥ 156 weeks from 2 phase 3, randomized, controlled trials (ESTEEM 1 and 2). J Am Acad Dermatol. 2017; 77:310-317 e311.

(Received November 21, 2018; Revised December 12, 2018; Accepted December 29, 2018)

Commentary

DOI: 10.5582/ddt.2018.01047

Inquiry into some gap among oseltamivir use and severe abnormal behavior in Japanese children and adolescents with influenza

Yasushi Ohkusa[1,*], Tamie Sugawara[1], Kiyosu Taniguchi[2], Chiaki Miyazaki[3], Mariko Y. Momoi[4], Nobuhiko Okabe[5]

[1] *Infectious Disease Surveillance Center, National Institute of Infectious Diseases, Tokyo, Japan;*
[2] *National Hospital Organization Mie National Hospital, Tsu, Mie, Japan;*
[3] *Fukuoka Welfare Center for the Disabled, Fukuoka, Fukuoka, Japan;*
[4] *Ryoumou Seishi Ryogoen for Severely Disabled, Kiryu, Gunma, Japan;*
[5] *Kawasaki City Institute for Public Health, Kawasaki, Kanagawa, Japan.*

Summary **The Fukushima research has examined data form a cohort study of 10,000 Japanese children under 18 years old with influenza during three months to demonstrate that the relative risk of A-type abnormal behavior of patients with oseltamivir was 30 times greater than without oseltamivir. By contrast, our research group found that patients who had been administered no neuraminidase inhibitors (NI) or those administered peramivir had higher risk of abnormal behavior than those administered oseltamivir, zanamivir, or laninamivir. A plausible explanation for this gap is that the two studies specifically examined different criteria to report abnormal behavior. In actually, some A-type abnormal behavior might not be life-threatening. Our definition of severe abnormal behavior is better matched to public health concerns and comparison among incidents according to the administered drug is more appropriate as an analytical procedure.**

Keywords: Influenza, abnormal behavior, oseltamivir, neuraminidase inhibitors

Since two influenza-infected Japanese junior high school students jumped from a great height and died in February 2007, abnormal behavior in influenza patients, especially teenagers, has been the subject of international public health concern. On March 22, 2007, the Ministry of Health, Labour (MHLW) issued emergent safety information to prohibit the administration of oseltamivir to 10-19 years-old influenza patients (*1*). Given those circumstances, epidemiological research efforts of two types were activated.

One research effort was a cohort study of 10,000 patients under 18 years old during three months in 2007 (*2*). This was unparalleled huge and amazing survey. Moreover, this research group continued the analyses for ten years. "Oseltamivir use and severe abnormal behavior in Japanese children and adolescents with influenza: Is a self-controlled case series study applicable?" (Hereinafter, the Fukushima research) was the latest result reported by this group (*3*). We are strongly impressed by their inquisitive approach that is focused on finding truth. The research found that the relative risk of A-type abnormal behavior, the most severe abnormal behavior in the data, of patients with oseltamivir was 30 times greater than without oseltamivir, although they did not emphasize that point in their conclusion because they were unable to isolate the effect of oseltamivir use from the effect of high fever.

Our research group started studying abnormal behavior of influenza patients in 2007. That study is continuing today under a granted by MHLW and Agency for Medical Research and Development in Japan (*4-6*). This group did not set up a cohort because abnormal behavior leading to death is apparently very rare. Instead of the cohort, it asked all physicians to report abnormal behavior of influenza patients with details of abnormal behavior and administered drugs

**Address correspondence to:*
Dr. Yasushi Ohkusa, Infectious Disease Surveillance Center, National Institute of Infectious Diseases, 1-23-1 Toyama, Shinjuku-ku, Tokyo 162-8640, Japan.
E-mail: ohkusa@nih.go.jp

such as several neuraminidase inhibitors (NI) or acetaminophen. In other words, it set a nationwide cohort to capture very rare events. Results of that study demonstrated that patients who have taken all types of NI showed severe abnormal behavior. Moreover, patients without the antivirals showed severe abnormal behavior. Therefore, it was concluded that influenza itself causes the severe abnormal behavior, even if drugs of some kinds might exacerbate it. The study also found that the rate of incidences of abnormal behavior were not different among types of NI such as oseltamvir, zanamivir and laninamivir, with the exception of peramivir. Therefore, zanamivir and laninamivir carry almost equivalent risk to that of oseltamivir. The incidence with peramivir or no antivirals administered were significantly higher than those associated with oseltamivir, zanamivir or laninamivir. However, the numbers of the un-administered patients or those taking peramivir were smaller than for the other NI. This evidence also reinforces the view that influenza itself causes the severe abnormal behavior. Hereinafter, we designate this effort as our research.

How should we interpret these different results related to the putative association between oseltamivir and abnormal behavior? The key point for understanding might be the frequency and definition of abnormal behavior.

The survey used for the Fukushima study found 28 cases of A-type abnormal behavior. The incidence was therefore 0.28% (28/10,000). By contrast, our research found 106 severe cases and 120 moderate cases in the same period.

Unfortunately, the precise number of influenza patients nationwide was not available in 2007. In fact, it is not notifiable disease in Japan, but it is monitored by sentinel in the National Official Sentinel Surveillance of Infectious Diseases (NOSSID) based on Japanese Infectious Disease Control Law. In an almost equivalent period (1st to 13th epidemiological week) NOSSID reported 896,136 influenza patients. NOSSID received the number of influenza patients from 5,000 sentinels, which accounts for almost one-tenth of all hospital and clinics. Therefore we can estimate the total number of influenza patients nationwide during the same period as 8.96 million. Nevertheless, NOSSID does not publish the age distribution of influenza patients for that period. Recently, almost all medical claims have become available for research since 2010. We designate such a huge database as the National Database of Medical Claims (NDBEMC). Our research group applied to MHLW to use it as the denominator of the incidence rate of abnormal behavior. That use was approved. Actually, NDBEMC shows the average proportion of patients younger than 20 years old in the 2010/2011-2013/2014 seasons as 52.5%. Consequently, the number of influenza patients younger than 20 years old was estimated as 4.71 million (8.96 million × 52.5%) during that period. The incidence of severe abnormal behavior in our research group was estimated as 0.0023% (106/4.71 million).

Conversely, our research group requested all physicians at the influenza sentinel to report moderate abnormal behavior cases. Influenza patients younger than 20 years old were 0.471 million (0.896 million × 52.5%) if we presume that the age distributions nationwide and of the sentinel are the same. Therefore, the incidence rate of moderate abnormal behavior in our research group was 0.025% (120/0.471million).

In other words, the incidence of A-type abnormal behavior in the Fukushima research was 100 times higher than severe abnormal behavior and ten times higher than moderate abnormal behavior, as judged by the our research group. The reason is that the two research efforts specifically examined different definitions or criteria to report abnormal behavior.

For instance, in the Fukushima research, A-type abnormal behavior was defined as "Abnormal behavior potentially leading to an accident or harm to another person." By contrast, our research group considered severe abnormal behavior as active motion behavior that can be life-threatening given no intervention, including behaviors such as sudden running away, jumping from a high place, or rampaging involving self-injury. Moreover, it defined the moderate abnormal behavior as unusual behavior that might not be life-threatening.

Therefore, some behaviors considered as A-type abnormal in the Fukushima study might not meet the definition of life-threatening severe abnormal behavior in our study, but might be included as a moderate abnormal behavior. These differences of case definition might affect the study outcome.

However, the severe abnormal behavior examined in our research also might result from underreporting. We cannot evaluate the degree of underreporting, but reports of only a few fatality cases with abnormal behavior of influenza patients have been published by mass media since 2007. Moreover, we have sent request letters from government to almost all hospital and clinics, more than 60 thousands, every year. Therefore, we consider that the bias of underreporting might not be so serious for severe abnormal behavior.

Both studies emphasize different aspects of abnormal behavior. If we were to construct a cohort study like the Fukushima research to examine life-threatening behavior specifically, we need 0.1 million cohort for 2.8 cases with life-threatening abnormal behavior based on our research group's result. Comparison of incidence according to the administered drug seems to be more appropriate as an analytical procedure. Moreover, we consider that our definition of severe abnormal behavior better matches for public health concerns.

Be that as it may, the final conclusion in Fukushima research "we could not deny the possibility that

abnormal behavior was induced by influenza itself" is fully acceptable from the view point of our research group. Our discussion presented in this paper might be useful for new anti-influenza virus drug including endonuclease inhibitor, baroxabil malboxyl.

Acknowledgment

This research was financially supported by the Japan Agency for Medical Research and Development in 2018, 18mk0101059h0003.

References

1. Chugai Pharmaceutical Co., Ltd. The Dear Healthcare Professional Letters of Emergent Safety Communications (Yellow Letter) about abnormal behavior after administrated Tamiflu. *http://www.pmda.go.jp/files/000147877.pdf* (in Japanese). (accessed 24 November, 2017)
2. Fujita T, Fujii Y, Watanabe Y, Osaka H, Wada T, Mori M, Yokota S. A pharmacoepidemiologic study on the relationship between neuropsychiatric symptoms and therapeutic drugs after influenza infection, Jpn J Pharmacoepidemiol. 2010; 15:73-92. (in Japanese)
3. Fukushima W, Ozasa K, Okumura A, Mori M, Hosoya M, Nakano T, Tanabe T, Yamaguchi N, Suzuki H, Mori M, Hatayama H, Ochiai H, Kondo K, Ito K, Ohfuji S. Oseltamivir use and severe abnormal behavior in Japanese children and adolescents with influenza: Is a self-controlled case series study applicable? Vaccine. 2017; 35:4817-4824.
4. Nakamura Y, Sugawara T, Ohkusa Y, Miyazaki C, Momoi M Y, Okabe N. Abnormal behavior during influenza in Japan during the last seven seasons: 2006-2007 to 2012-2013. J Infect Chemother. 2014; 20:789-793.
5. Nakamura Y, Sugawara T, Ohkusa Y, Miyazaki C, Momoi M Y, Okabe N. Life-threatening abnormal behavior incidence in 10-19 year old patients administered neuraminidase inhibitors. PLoS One. 2015; 10:e0129712.
6. Nakamura Y, Sugawara T, Ohkusa Y, Miyazaki C, Momoi MY, Okabe N. Severe abnormal behavior incidence after administration of neuraminidase inhibitors using the national database of medical claims. J Infect Chemother. 2018; 24:177-181.

(Received September 3, 2018; Revised December 23, 2018; Accepted December 27, 2018)

DD&T
Drug Discoveries & Therapeutics

Guide for Authors

1. Scope of Articles

Drug Discoveries & Therapeutics welcomes contributions in all fields of pharmaceutical and therapeutic research such as medicinal chemistry, pharmacology, pharmaceutical analysis, pharmaceutics, pharmaceutical administration, and experimental and clinical studies of effects, mechanisms, or uses of various treatments. Studies in drug-related fields such as biology, biochemistry, physiology, microbiology, and immunology are also within the scope of this journal.

2. Submission Types

Original Articles should be well-documented, novel, and significant to the field as a whole. An Original Article should be arranged into the following sections: Title page, Abstract, Introduction, Materials and Methods, Results, Discussion, Acknowledgments, and References. Original articles should not exceed 5,000 words in length (excluding references) and should be limited to a maximum of 50 references. Articles may contain a maximum of 10 figures and/or tables.

Brief Reports definitively documenting either experimental results or informative clinical observations will be considered for publication in this category. Brief Reports are not intended for publication of incomplete or preliminary findings. Brief Reports should not exceed 3,000 words in length (excluding references) and should be limited to a maximum of 4 figures and/or tables and 30 references. A Brief Report contains the same sections as an Original Article, but the Results and Discussion sections should be combined.

Reviews should present a full and up-to-date account of recent developments within an area of research. Normally, reviews should not exceed 8,000 words in length (excluding references) and should be limited to a maximum of 100 references. Mini reviews are also accepted.

Policy Forum articles discuss research and policy issues in areas related to life science such as public health, the medical care system, and social science and may address governmental issues at district, national, and international levels of discourse. Policy Forum articles should not exceed 2,000 words in length (excluding references).

Case Reports should be detailed reports of the symptoms, signs, diagnosis, treatment, and follow-up of an individual patient. Case reports may contain a demographic profile of the patient but usually describe an unusual or novel occurrence. Unreported or unusual side effects or adverse interactions involving medications will also be considered. Case Reports should not exceed 3,000 words in length (excluding references).

News articles should report the latest events in health sciences and medical research from around the world. News should not exceed 500 words in length.

Letters should present considered opinions in response to articles published in Drug Discoveries & Therapeutics in the last 6 months or issues of general interest. Letters should not exceed 800 words in length and may contain a maximum of 10 references.

3. Editorial Policies

Ethics: Drug Discoveries & Therapeutics requires that authors of reports of investigations in humans or animals indicate that those studies were formally approved by a relevant ethics committee or review board.

Conflict of Interest: All authors are required to disclose any actual or potential conflict of interest including financial interests or relationships with other people or organizations that might raise questions of bias in the work reported. If no conflict of interest exists for each author, please state "There is no conflict of interest to disclose".

Submission Declaration: When a manuscript is considered for submission to Drug Discoveries & Therapeutics, the authors should confirm that 1) no part of this manuscript is currently under consideration for publication elsewhere; 2) this manuscript does not contain the same information in whole or in part as manuscripts that have been published, accepted, or are under review elsewhere, except in the form of an abstract, a letter to the editor, or part of a published lecture or academic thesis; 3) authorization for publication has been obtained from the authors' employer or institution; and 4) all contributing authors have agreed to submit this manuscript.

Cover Letter: The manuscript must be accompanied by a cover letter signed by the corresponding author on behalf of all authors. The letter should indicate the basic findings of the work and their significance. The letter should also include a statement affirming that all authors concur with the submission and that the material submitted for publication has not been published previously or is not under consideration for publication elsewhere. The cover letter should be submitted in PDF format. For example of Cover Letter, please visit http://www.ddtjournal.com/downcentre.php (Download Centre).

Copyright: A signed JOURNAL PUBLISHING AGREEMENT (JPA) must be provided by post, fax, or as a scanned file before acceptance of the article. Only forms with a hand-written signature are accepted. This copyright will ensure the widest possible dissemination of information. A form facilitating transfer of copyright can be downloaded by clicking the appropriate link and can be returned to the e-mail address or fax number noted on the form (Please visit Download Centre). Please note that your manuscript will not proceed to the next step in publication until the JPA form is received. In addition, if excerpts from other copyrighted works are included, the author(s) must obtain written permission from the copyright owners and credit the source(s) in the article.

Suggested Reviewers: A list of up to 3 reviewers who are qualified to assess the scientific merit of the study is welcomed. Reviewer information including names, affiliations, addresses, and e-mail should be provided at the same time the manuscript is submitted online. Please do not suggest reviewers with known conflicts of interest, including participants or anyone with a stake in the proposed research; anyone from the same institution; former students, advisors, or research collaborators (within the last three years); or close personal contacts. Please note that the Editor-in-Chief may accept one or more of the proposed reviewers or may request a review by other qualified persons.

Language Editing: Manuscripts prepared by authors whose native language is not English should have their work proofread by a native English speaker before submission. If not, this might delay the publication of your manuscript in Drug Discoveries & Therapeutics.

The Editing Support Organization can provide English proofreading, Japanese-English translation, and Chinese-English translation services to authors who want to publish in Drug Discoveries & Therapeutics and need assistance before submitting a manuscript. Authors can visit this organization directly at http://www.iacmhr.com/iac-eso/support.php?lang=en. IAC-ESO was established to facilitate manuscript preparation by researchers whose native language is not English and to help edit works intended for international academic journals.

4. Manuscript Preparation

Manuscripts should be written in clear, grammatically correct English and submitted as a Microsoft Word file in a single-column format. Manuscripts must be paginated and typed in 12-point Times New Roman font with 24-point line spacing. Please do not embed figures in the text. Abbreviations should be used as little as possible and should be explained at first mention unless the term is a well-known abbreviation (*e.g.* DNA). Single words should not be abbreviated.

Title page: The title page must include 1) the title of the paper (Please note the title should be short, informative, and contain the major key words); 2) full name(s) and affiliation(s) of the author(s), 3) abbreviated names of the author(s), 4) full name, mailing address, telephone/fax numbers, and e-mail address of the corresponding author; and 5) conflicts of interest (if you have an actual or potential conflict of interest to disclose, it must be included as a footnote on the title page of the manuscript; if no conflict of interest exists for each author, please state "There is no conflict of interest to disclose"). Please visit Download Centre and refer to the title page of the manuscript sample.

Abstract: The abstract should briefly state the purpose of the study, methods, main findings, and conclusions. For article types including Original Article, Brief Report, Review, Policy Forum, and Case Report, a one-paragraph abstract consisting of no more than 250 words must be included in the manuscript. For News and Letters, a brief summary of main content in 150 words or fewer should be included in the manuscript. Abbreviations must be kept to a minimum and non-standard abbreviations explained in brackets at first mention. References should be avoided in the abstract. Key words or phrases that do not occur in the title should be included in the Abstract page.

Introduction: The introduction should be a concise statement of the basis for the study and its scientific context.

Materials and Methods: The description should be brief but with sufficient detail to enable others to reproduce the experiments. Procedures that have been published previously should not be described in detail but appropriate references should simply be cited. Only new and significant modifications of previously published procedures require complete description. Names of products and manufacturers with their locations (city and state/country) should be given and sources of animals and cell lines should always be indicated. All clinical investigations must have been conducted in accordance with Declaration of Helsinki principles. All human and animal studies must have been approved by the appropriate institutional review board(s) and a specific declaration of approval must be made within this section.

Results: The description of the experimental results should be succinct but in sufficient detail to allow the experiments to be analyzed and interpreted by an independent reader. If necessary, subheadings may be used for an orderly presentation. All figures and tables must be referred to in the text.

Discussion: The data should be interpreted concisely without repeating material already presented in the Results section. Speculation is permissible, but it must be well-founded, and discussion of the wider implications of the findings is encouraged. Conclusions derived from the study should be included in this section.

Acknowledgments: All funding sources should be credited in the Acknowledgments section. In addition, people who contributed to the work but who do not meet the criteria for authors should be listed along with their contributions.

References: References should be numbered in the order in which they appear in the text. Citing of unpublished results, personal communications, conference abstracts, and theses in the reference list is not recommended but these sources may be mentioned in the text. In the reference list, cite the names of all authors when there are fifteen or fewer authors; if there are sixteen or more authors, list the first three followed by *et al*. Names of journals should be abbreviated in the style used in PubMed. Authors are responsible for the accuracy of the references. Examples are given below:

Example 1 (Sample journal reference):
Nakata M, Tang W. Japan-China Joint Medical Workshop on Drug Discoveries and Therapeutics 2008: The need of Asian pharmaceutical researchers' cooperation. Drug Discov Ther. 2008; 2:262-263.

Example 2 (Sample journal reference with more than 15 authors):
Darby S, Hill D, Auvinen A, *et al*. Radon in homes and risk of lung cancer: Collaborative analysis of individual data from 13 European case-control studies. BMJ. 2005; 330:223.

Example 3 (Sample book reference):
Shalev AY. Post-traumatic stress disorder: Diagnosis, history and life course. In: Post-traumatic Stress Disorder, Diagnosis, Management and Treatment (Nutt DJ, Davidson JR, Zohar J, eds.). Martin Dunitz, London, UK, 2000; pp. 1-15.

Example 4 (Sample web page reference):
World Health Organization. The World Health Report 2008 – primary health care: Now more than ever. *http://www.who.int/whr/2008/whr08_en.pdf* (accessed September 23, 2010).

Tables: All tables should be prepared in Microsoft Word or Excel and should be arranged at the end of the manuscript after the References section. Please note that tables should not in image format. All tables should have a concise title and should be numbered consecutively with Arabic numerals. If necessary, additional information should be given below the table.

Figure Legend: The figure legend should be typed on a separate page of the main manuscript and should include a short title and explanation. The legend should be concise but comprehensive and should be understood without referring to the text. Symbols used in figures must be explained.

Figure Preparation: All figures should be clear and cited in numerical order in the text. Figures must fit a one- or two-column format on the journal page: 8.3 cm (3.3 in.) wide for a single column, 17.3 cm (6.8 in.) wide for a double column; maximum height: 24.0 cm (9.5 in.). Please make sure that artwork files are in an acceptable format (TIFF or JPEG) at minimum resolution (600 dpi for illustrations, graphs, and annotated artwork, and 300 dpi for micrographs and photographs). Please provide all figures as separate files. Please note that low-resolution images are one of the leading causes of article resubmission and schedule delays. All color figures will be reproduced in full color in the online edition of the journal at no cost to authors.

Units and Symbols: Units and symbols conforming to the International System of Units (SI) should be used for physicochemical quantities. Solidus notation (*e.g.* mg/kg, mg/mL, mol/mm^2/min) should be used. Please refer to the SI Guide www.bipm.org/en/si/ for standard units.

Supplemental data: Supplemental data might be useful for supporting and enhancing your scientific research and Drug Discoveries & Therapeutics accepts the submission of these materials which will be only published online alongside the electronic version of your article. Supplemental files (figures, tables, and other text materials) should be prepared according to the above guidelines, numbered in Arabic numerals (*e.g.*, Figure S1, Figure S2, and Table S1, Table S2) and referred to in the text. All figures and tables should have titles and legends. All figure legends, tables and supplemental text materials should be placed at the end of the paper. Please note all of these supplemental data should be provided at the time of initial submission and note that the editors reserve the right to limit the size and length of Supplemental Data.

5. Submission Checklist

The Submission Checklist will be useful during the final checking of a manuscript prior to sending it to Drug Discoveries & Therapeutics for review. Please visit Download Centre and download the Submission Checklist file.

6. Online submission

Manuscripts should be submitted to Drug Discoveries & Therapeutics online at http://www.ddtjournal.com. The manuscript file should be smaller than 5 MB in size. If for any reason you are unable to submit a file online, please contact the Editorial Office by e-mail at office@ddtjournal.com

7. Accepted manuscripts

Proofs: Galley proofs in PDF format will be sent to the corresponding author *via* e-mail. Corrections must be returned to the editor (proof-editing@ddtjournal.com) within 3 working days.

Offprints: Authors will be provided with electronic offprints of their article. Paper offprints can be ordered at prices quoted on the order form that accompanies the proofs.

Page Charge: A page charge of $140 will be assessed for each printed page of an accepted manuscript. The charge for printing color figures is $340 for each page. Under exceptional circumstances, the author(s) may apply to the editorial office for a waiver of the publication charges at the time of submission.

(Revised February 2013)

Editorial and Head Office:

Pearl City Koishikawa 603
2-4-5 Kasuga, Bunkyo-ku
Tokyo 112-0003
Japan
Tel: +81-3-5840-9697
Fax: +81-3-5840-9698
E-mail: office@ddtjournal.com

DD&T
Drug Discoveries & Therapeutics

JOURNAL PUBLISHING AGREEMENT (JPA)

Manuscript No.:

Title:

Corresponding author:

The International Advancement Center for Medicine & Health Research Co., Ltd. (IACMHR Co., Ltd.) is pleased to accept the above article for publication in Drug Discoveries & Therapeutics. The International Research and Cooperation Association for Bio & Socio-Sciences Advancement (IRCA-BSSA) reserves all rights to the published article. Your written acceptance of this JOURNAL PUBLISHING AGREEMENT is required before the article can be published. Please read this form carefully and sign it if you agree to its terms. The signed JOURNAL PUBLISHING AGREEMENT should be sent to the Drug Discoveries & Therapeutics office (Pearl City Koishikawa 603, 2-4-5 Kasuga, Bunkyo-ku, Tokyo 112-0003, Japan; E-mail: office@ddtjournal.com; Tel: +81-3-5840-9697; Fax: +81-3-5840-9698).

1. Authorship Criteria

As the corresponding author, I certify on behalf of all of the authors that:

1) The article is an original work and does not involve fraud, fabrication, or plagiarism.
2) The article has not been published previously and is not currently under consideration for publication elsewhere. If accepted by Drug Discoveries & Therapeutics, the article will not be submitted for publication to any other journal.
3) The article contains no libelous or other unlawful statements and does not contain any materials that infringes upon individual privacy or proprietary rights or any statutory copyright.
4) I have obtained written permission from copyright owners for any excerpts from copyrighted works that are included and have credited the sources in my article.
5) All authors have made significant contributions to the study including the conception and design of this work, the analysis of the data, and the writing of the manuscript.
6) All authors have reviewed this manuscript and take responsibility for its content and approve its publication.
7) I have informed all of the authors of the terms of this publishing agreement and I am signing on their behalf as their agent.

2. Copyright Transfer Agreement

I hereby assign and transfer to IACMHR Co., Ltd. all exclusive rights of copyright ownership to the above work in the journal Drug Discoveries & Therapeutics, including but not limited to the right 1) to publish, republish, derivate, distribute, transmit, sell, and otherwise use the work and other related material worldwide, in whole or in part, in all languages, in electronic, printed, or any other forms of media now known or hereafter developed and the right 2) to authorize or license third parties to do any of the above.

I understand that these exclusive rights will become the property of IACMHR Co., Ltd., from the date the article is accepted for publication in the journal Drug Discoveries & Therapeutics. I also understand that IACMHR Co., Ltd. as a copyright owner has sole authority to license and permit reproductions of the article.

I understand that except for copyright, other proprietary rights related to the Work (*e.g.* patent or other rights to any process or procedure) shall be retained by the authors. To reproduce any text, figures, tables, or illustrations from this Work in future works of their own, the authors must obtain written permission from IACMHR Co., Ltd.; such permission cannot be unreasonably withheld by IACMHR Co., Ltd.

3. Conflict of Interest Disclosure

I confirm that all funding sources supporting the work and all institutions or people who contributed to the work but who do not meet the criteria for authors are acknowledged. I also confirm that all commercial affiliations, stock ownership, equity interests, or patent-licensing arrangements that could be considered to pose a financial conflict of interest in connection with the article have been disclosed.

Corresponding Author's Name (Signature):

Date: